NASA TECHNICAL MEMORANDUM

NASA TM X- 64609

SKYLAB THREE-AXIS MOTION PLATFORM TEST RESULTS

By Michael T. Borelli
Astrionics Laboratory

Jack Templeton
Sperry Rand Corporation

June 25, 1971

NASA

George C. Marshall Space Flight Center
Marshall Space Flight Center, Alabama

TECHNICAL REPORT STANDARD TITLE PAGE

1. REPORT NO.	2. GOVERNMENT ACCESSION NO.	3. RECIPIENT'S CATALOG NO.
TM X-64609		

4. TITLE AND SUBTITLE	5. REPORT DATE
Skylab Three-Axis Motion Platform Test Results	June 25, 1971
	6. PERFORMING ORGANIZATION CODE
7. AUTHOR(S) Michael T. Borelli (MSFC) and Jack Templeton (Sperry Rand Corporation)	8. PERFORMING ORGANIZATION REPORT #
9. PERFORMING ORGANIZATION NAME AND ADDRESS George C. Marshall Space Flight Center Marshall Space Flight Center, Alabama 35812	10. WORK UNIT NO. 11. CONTRACT OR GRANT NO.
12. SPONSORING AGENCY NAME AND ADDRESS National Aeronautics and Space Administration Washington, D. C. 20546	13. TYPE OF REPORT & PERIOD COVERED Technical memorandum 14. SPONSORING AGENCY CODE

15. SUPPLEMENTARY NOTES

Prepared by Astrionics Laboratory, Science and Engineering

16. ABSTRACT

The results of a series of tests conducted on the Skylab three-axis motion platform (STAMP) to establish its performance capabilities are presented. Included in the test series are frequency response, transient response, servosystem stiffness, dynamic position and rate accuracy, friction and stiction, and parameter sensitivity tests. The results pinpoint some of the system's deficiencies and document the nonlinear characteristics of the system. Investigators utilizing the STAMP will find these test results helpful in planning their experiments. The results of these tests will also be used in the development of a nonlinear mathematical model of the STAMP's servocontrol system.

17. KEY WORDS	18. DISTRIBUTION STATEMENT
Motion simulator Skylab Gimbaled platform	Unclassified - Unlimited Michael T. Borelli

19. SECURITY CLASSIF. (of this report)	20. SECURITY CLASSIF. (of this page)	21. NO. OF PAGES	22. PRICE
Unclassified	Unclassified	96	$3.00

MSFC - Form 3292 (May 1969)

TABLE OF CONTENTS

	Page
SUMMARY	1
INTRODUCTION	1
SYSTEM DESCRIPTION	5
PERFORMANCE REQUIREMENTS	7
TEST RESULTS	10
Frequency Response Test	10
Transient Response Test	22
Dynamic Position and Rate Accuracies	38
Stiffness Test	41
Gimbal Friction	59
Parameter Sensitivity Test	60
DISCUSSION	61
RECOMMENDATIONS	65
APPENDIX A: PHYSICAL CHARACTERISTICS OF THE STAMP	67
APPENDIX B: FREQUENCY RESPONSES FOR THE ROLL AND SIDEREAL AXIS	69
REFERENCES	81

LIST OF ILLUSTRATIONS

Figure	Title	Page
1a.	Top view of the STAMP's load platform with CMG's mounted in the torque measuring fixtures (TMF's)	3
1b.	Bottom view of the STAMP with steel plates mounted on the load platform	4
2.	Block diagram for a single axis of the STAMP	6
3.	Block diagram for a single axis of the STAMP in the digital mode of operation	6
4.	Flow curves of roll-axis servovalves	8
5.	Roll-axis frequency response for 0.03 deg/s input signal, analog-position mode, for original and replacement servovalves	8
6.	Configuration for frequency response test in the digital mode	11
7.	Sidereal-axis tachometer response, analog-position mode, CMG case	11
8.	Yaw-axis frequency response for 0.002 deg/s input signal, analog-position mode, steel plate case	12
9.	Yaw-axis frequency response for 0.005 deg/s input signal, analog-position mode, steel plate case	12
10.	Yaw-axis frequency response for 0.01 deg/s input signal, analog-position mode, steel plate case	13
11.	Yaw-axis frequency response for 0.03 deg/s input signal, analog-position mode, steel plate case	13
12.	Yaw-axis frequency response for 0.1 deg/s input signal, analog-position mode, steel plate case	14

LIST OF ILLUSTRATIONS (Continued)

Figure	Title	Page
13.	Yaw-axis frequency response for 0.5 deg/s input signal, analog-position mode, steel plate case	14
14.	Yaw-axis frequency response for 1.0 deg/s input signal, analog-position mode, steel plate case	15
15.	Yaw-axis frequency response for 0.005 deg/s input signal, analog-position mode, CMG case	15
16.	Yaw-axis frequency response for 0.01 deg/s input signal, analog-position mode, CMG case	16
17.	Yaw-axis frequency response for 0.05 deg/s input signal, analog-position mode, CMG case	16
18.	Yaw-axis frequency response for 0.10 deg/s input signal, analog-position mode, CMG case	17
19.	Yaw-axis frequency response for 0.5 deg/s input signal, analog-position mode, CMG case	17
20.	Yaw-axis frequency response for 0.005 deg/s input signal, digital mode, CMG case	18
21.	Yaw-axis frequency response for 0.01 deg/s input signal, digital mode, CMG case	18
22.	Yaw-axis frequency response for 0.1 deg/s input signal, digital mode, CMG case	19
23.	Yaw-axis frequency response for 0.5 deg/s input signal, digital mode, CMG case	19
24.	Sidereal-yaw-axis coupling amplitude frequency response for 0.5 deg/s input signal, analog-position mode, CMG case	21
25.	Transient responses for the STAMP's three modes of operation	23

LIST OF ILLUSTRATIONS (Continued)

Figure	Title	Page
26.	Definition of the transient response parameters	24
27.	Roll-axis position response to low-level signal inputs, digital mode, steel plate case	31
28.	Yaw-axis position response to low-level signal inputs, digital mode, steel plate case	32
29.	Sidereal-axis position response to low-level signal inputs, digital mode, steel plate case	33
30.	Roll-axis position response to low-level signal inputs, digital mode, CMG case	34
31.	Yaw-axis position response to low-level signal inputs, digital mode, CMG case	35
32.	Sidereal-axis position response to low-level signal inputs, digital mode, CMG case	36
33.	STAMP's gimbal responses to zero-signal input, digital mode, CMG case	37
34.	Sidereal-axis position responses at zero deg, analog-position mode, steel plate case	39
35.	Sidereal-axis position response at 1.8 deg, analog-position mode, steel plate case	40
36.	Yaw-axis position responses at zero deg, analog-position mode, steel plate case	42
37.	Roll-axis position responses at zero deg, analog-position mode, steel plate case	43
38.	Measurement of rate smoothness	45
39.	Roll-axis rate response, analog-position mode, steel plate case	45

LIST OF ILLUSTRATIONS (Continued)

Figure	Title	Page
40.	Roll-axis rate response, analog-position mode, CMG case	46
41.	Yaw-axis rate response, analog-position mode, steel plate case	47
42.	Yaw-axis rate response, analog-position mode, CMG case	48
43.	Sidereal-axis rate response, analog-position mode, steel plate case	49
44.	Sidereal-axis rate response, analog-position mode, steel plate case	50
45.	Sidereal-axis rate response, analog-position mode, CMG case	51
46.	Sidereal-axis rate response, analog-position mode, CMG case	52
47.	Coordinates for the STAMP and CMG's mounted on the load platform	54
48.	A single-axis block diagram of the STAMP's linearized equations of motion	62
49.	A simulation of nonlinear responses of the STAMP's tachometers and potentiometers	66
B-1.	Roll-axis frequency response for 0.03 deg/s input signal, analog-position mode, steel plate case	70
B-2.	Roll-axis frequency response for 0.1 deg/s input signal, analog-position mode, steel plate case	70
B-3.	Roll-axis frequency response for 0.5 deg/s input signal, analog-position mode, steel plate case	71

LIST OF ILLUSTRATIONS (Continued)

Figure	Title	Page
B-4.	Roll-axis frequency response for 0.01 deg/s input signal, analog-position mode, CMG case	71
B-5.	Roll-axis frequency response for 0.1 deg/s input signal, analog-position mode, CMG case	72
B-6.	Roll-axis frequency response for 0.5 deg/s input signal, analog-position mode, CMG case	72
B-7.	Roll-yaw-axis coupling amplitude frequency response for 0.5 deg/s input signal, analog-position mode, CMG case	73
B-8.	Roll-axis frequency response for 0.01 deg/s input signal, digital mode, CMG case	73
B-9.	Roll-axis frequency response for 0.1 deg/s input signal, digital mode, CMG case	74
B-10.	Roll-axis frequency response for 0.5 deg/s input signal, digital mode, CMG case	74
B-11.	Sidereal-axis frequency response for 0.01 deg/s input signal, analog-position mode, steel plate case	75
B-12.	Sidereal-axis frequency response for 0.05 deg/s input signal, analog-position mode, steel plate case	75
B-13.	Sidereal-axis frequency response for 0.1 deg/s input signal, analog-position mode, steel plate case	76
B-14.	Sidereal-axis frequency response for 0.5 deg/s input signal, analog-position mode, steel plate case	76
B-15.	Sidereal-axis frequency response for 1.0 deg/s input signal, analog-position mode, steel plate case	77

LIST OF ILLUSTRATIONS (Concluded)

Figure	Title	Page
B-16.	Sidereal-axis frequency response for 0.05 deg/s input signal, analog-position mode, CMG case	77
B-17.	Sidereal-axis frequency response for 0.1 deg/s input signal, analog-position mode, CMG case	78
B-18.	Sidereal-axis frequency response for 0.5 deg/s input signal, analog-position mode, CMG case	78
B-19.	Sidereal-axis frequency response for 0.05 deg/s input signal, digital mode, CMG case	79
B-20.	Sidereal-axis frequency response for 0.1 deg/s input signal, digital mode, CMG case	79
B-21.	Sidereal-axis frequency response for 0.5 deg/s input signal, digital mode, CMG case	80

LIST OF TABLES

Table	Title	Page
1.	Qualitative Summary of the STAMP's Performance	2
2.	Step Response Characteristics for Analog-Position Mode, Steel Plate Case	25
3.	Step Response Characteristics for Analog-Position Mode, CMG Case	26
4.	Step Response Characteristics for Digital Mode, CMG Case	28
5.	Transient Characteristics of Step Responses with STAMP in Digital Mode, Steel Plate Case	29
6.	Transient Characteristics of Step Response with STAMP in Digital Mode, CMG Case	30
7.	Dynamic Position Accuracy for STAMP's Potentiometers and Inductosyns	44
8.	Dynamic Rate Accuracy for STAMP's Tachometers	44
9.	Measurements of the STAMP's Servosystem Stiffness — The STAMP and CMG Responses to Step Rate Commands Applied to the CMG Servos. Input Signal Amplitudes are 3.5, 1.5, and 0.75 deg/s	55
10.	Measurements of the STAMP's Servosystem Stiffness — The STAMP and CMG Responses to Sinusoidal Rate Commands Applied to the CMG Servos. Input Signal Frequency is 1 Hz	56
11.	Measurements of the STAMP's Servosystem Stiffness — The STAMP and CMG Responses to Sinusoidal Rate Commands Applied to the CMG Servos. Input Signal Amplitude of 3.5 deg/s Peak at 1, 0.1, and 0.01 Hz	57

LIST OF TABLES (Concluded)

Table	Title	Page
12.	Measurements of the STAMP's Servosystem Stiffness — The STAMP and CMG Responses to Sinusoidal Rate Command Applied to the CMG Servos. Input Signal Frequency is 3.5 Hz	58
13.	Parameter Sensitivities	63

DEFINITION OF SYMBOLS

Symbol	Definition
D_m	Actuator displacement
D_q	Linear valve flow constant (gain)
i	Index
J_m	Actuator inertia
J_L	Load inertia
K_A	Pressure feedback gain
K_P	Position feedback gain
K_R	Rate feedback gain
K_i	Control system gains
K_s	Gimbal torsional stiffness
K_{sa}	Gimbal torsional damping
L_D	Actuator leakage
M_P	Resonant peak amplitude of frequency response
P_D	Actuator driving pressure
P_s	Supply pressure
P_Q	Linear valve flow constant
T_d	Torque disturbance
$2\beta/V$	Actuator constant
θ_c	Input position command

DEFINITION OF SYMBOLS (Concluded)

Symbol	Definition
$\dot{\theta}_c$	Input rate command
θ_R	Output position response
$\dot{\theta}_R$	Output rate response
τ_i	Control system time constants
ω_d	Frequency of the resonant peak of frequency response

TECHNICAL MEMORANDUM X-64609

SKYLAB THREE-AXIS MOTION PLATFORM TEST RESULTS

SUMMARY

This report presents the results of a series of tests conducted on the Skylab three-axis motion platform (STAMP) to establish its performance capabilities. Included in the test series are frequency response, transient response, servosystem stiffness, dynamic position and rate accuracy, friction and stiction, and parameter sensitivity tests. The results pinpoint some of the system's deficiencies and document the nonlinear characteristics of the system. Investigators utilizing the STAMP will find these test results helpful in planning their experiments. A qualitative summary of the STAMP's performance is given in Table 1. The data supporting this table are in the body of the report. The results of these tests will also be used in the development of a nonlinear mathematical model of the STAMP's servocontrol system.

INTRODUCTION

The STAMP is a large, computer-controlled, three-degree-of-freedom dynamic simulator that was built to check out prototype hardware, computer software, and attitude control systems that utilize control moment gyros (CMG's). A series of tests were conducted on the STAMP to establish its performance capabilities. Appendix A briefly describes the physical characteristics and the maneuvering capabilities of the STAMP. Two views of the STAMP are shown in Figures 1a and 1b.

The STAMP was designed to check out the Apollo Telescope Mount (ATM) system. The specific objectives were to design a system with a relatively wide dynamic range of operation and also one that was highly responsive to small command signals. To determine the precise operational capabilities of the STAMP to a broad variety of conditions and to establish its adequacy for the Skylab project, a comprehensive test program was initiated. The test program consisted essentially of six different tests that will be

TABLE 1. QUALITATIVE SUMMARY OF THE STAMP'S PERFORMANCE

Test or Requirement		Test Results and Evaluation		
		Roll Axis	Yaw Axis	Sidereal Axis
Frequency Response Digital Mode:	Bandwidth - Expected - Measured - Rating	> 5 Hz for 0.01 to 3.5 deg/s 1 Hz at 0.1 deg/s FAIR	>5 Hz for 0.01 to 3.5 deg/s 0.7 Hz at 0.1 deg/s FAIR	> 5 Hz for 0.01 to 3.5 deg/s 0.66 Hz at 0.1 deg/s FAIR
	Phase Shift - Expected - Measured - Rating	< 45 deg from 0 to 5 Hz for 0.01 to 3.5 deg/s 45 deg at 1 Hz and 0.1 deg/s FAIR	< 45 deg from 0 to 5 Hz for 0.01 to 3.5 deg/s 45 deg at 1.9 Hz and 0.1 deg/s FAIR	< 45 deg from 0 to 5 Hz for 0.01 to 3.5 deg/s 45 deg at 6.5 Hz and 0.1 deg/s GOOD
Transient Response Digital Mode:	Damping Ratio - Expected - Measured - Rating	< 0.5 at 0.01 to 3.5 deg/s 0.5 at 0.016 deg/s GOOD	< 0.5 at 0.01 to 3.5 deg/s 0.0 at 0.016 deg/s GOOD	< 0.5 at 0.01 to 3.5 deg/s 0.0 at 0.016 deg/s EXCELLENT
	Rise Time - Expected - Measured - Rating	< 0.05 s at 0.01 to 3.5 deg/s 1 s at 0.016 deg/s FAIR	< 0.05 s at 0.01 to 3.5 deg/s 2 s at 0.016 deg/s FAIR	< 0.05 s at 0.01 to 3.5 deg/s 2 s at 0.016 deg/s FAIR
Servosystem Stiffness	- Expected - Measured - Rating	6.77×10^4 N-m/deg $> 6.77 \times 10^4$ N-m/deg EXCELLENT	6.77×10^4 N-m/deg $< 2.5 \times 10^3$ N-m/deg POOR	6.77×10^4 N-m/deg $> 6.77 \times 10^4$ N-m/deg EXCELLENT
Dynamic Position and Rate Accuracy	Position - Expected (Inductosyn) - Measured - Rating	< 0.005 deg at 0.01 to 0.1 deg/s 0.0044 deg at 0.1 deg EXCELLENT	< 0.005 deg at 0.01 to 0.1 deg/s 0.0044 deg at 0.1 deg/s EXCELLENT	< 0.005 deg at 0.01 to 0.1 deg/s 0.0065 deg at 0.1 deg/s GOOD
	Rate - Expected (Tachometer) - Measured - Rating	< 0.02 deg/s at 0.15 deg/s 0.04 deg/s at 0.15 deg/s POOR	< 0.02 deg/s at 0.3 deg/s 0.05 deg/s at 0.3 deg/s POOR	< 0.02 deg/s at 0.3 deg/s 0.06 deg/s at 0.3 deg/s POOR

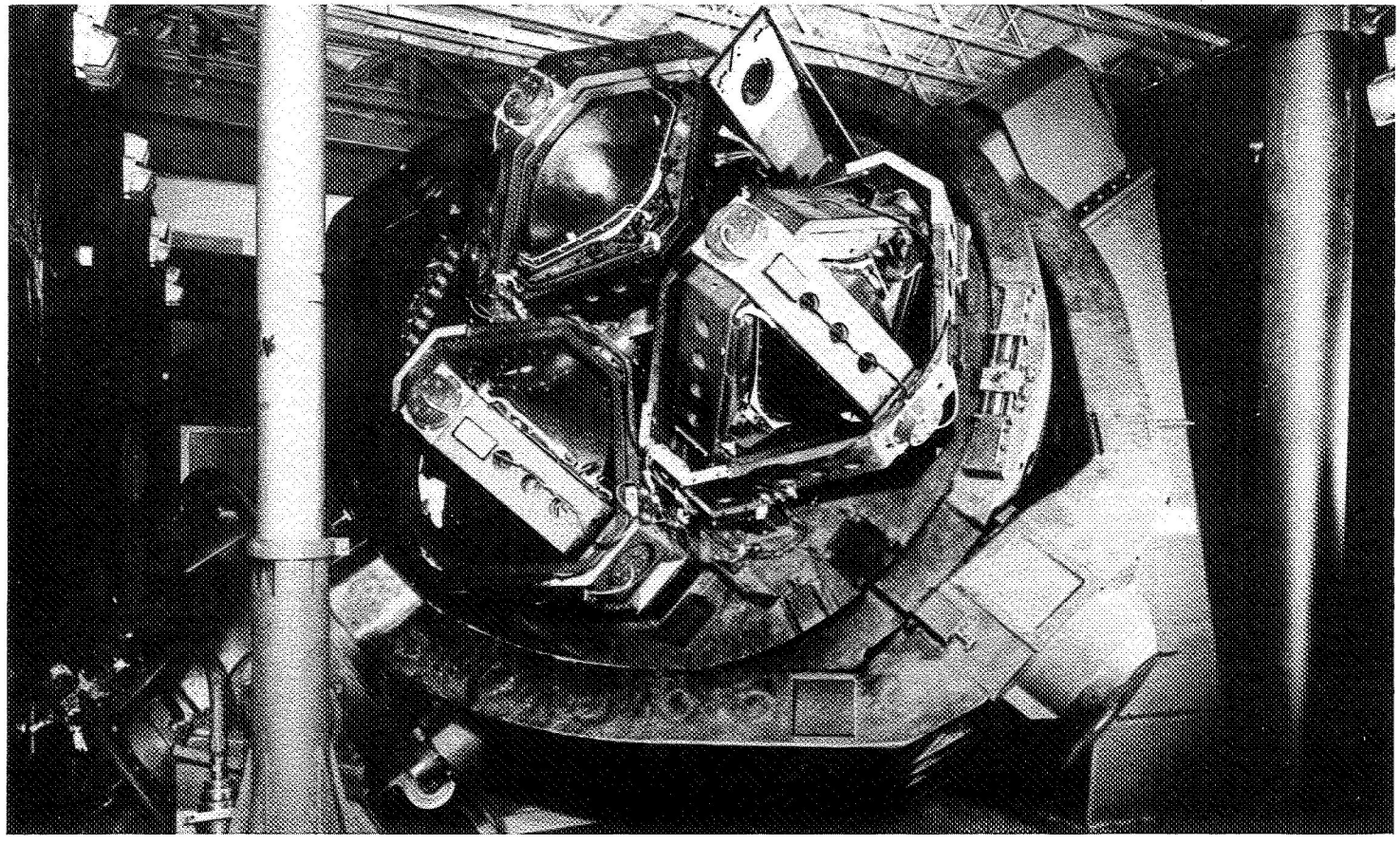

Figure 1a. Top view of the STAMP's load platform with CMG's mounted in the torque measuring fixtures (TMF's).

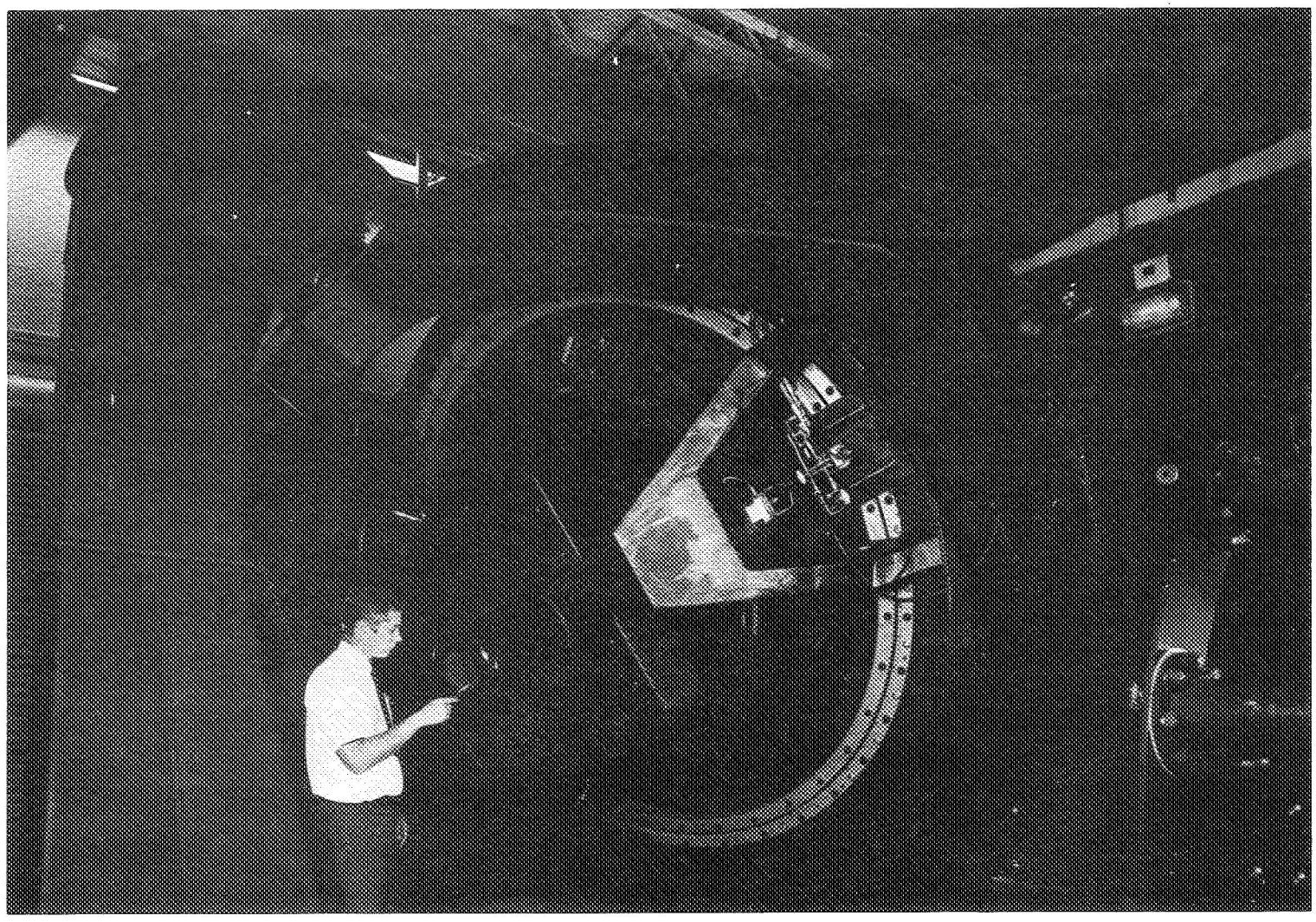

Figure 1b. Bottom view of the STAMP with steel plates mounted on the load platform.

described and discussed in subsequent sections. A secondary objective of the test program was to obtain data to define the nonlinear characteristics of the STAMP and thereby complete the derivation of a mathematical model of the Skylab simulation laboratory CMG attitude control system. The data necessary to meet these objectives required the operation of the simulation laboratory's equipment in several different modes. These modes of operation and the equipment used in the test program, plus some of the difficulties encountered in its operation, are described.

SYSTEM DESCRIPTION

The STAMP has two primary modes of operation — analog and digital; however, the analog mode can be further configured into a position or rate mode of operation. The analog-rate, analog-position, and digital modes have parallel inputs of a rate and a position signal as shown in the simplified block diagram of Figure 2. The configuration of Figure 2, with the three additional amplifiers and a signal generator, was used for testing in the analog mode of operation. In the analog-rate mode, the position-error amplifier inputs are grounded and the capacitor is paralleled with a resistor to remove any residual charge. Normally, the STAMP will be operated in the digital mode.

When referring to the STAMP, the following equipment is considered as part of the system: the three-axis gimbaled platform, electrohydraulic servovalves, hydraulic actuators, tachometers, potentiometers, inductosyns, differential pressure transducers, and control electronics that complete the position, rate, and pressure feedback loops. In the simplified block diagram of Figure 2, the filters or shaping networks used to suppress certain system resonances are omitted. The additional equipment necessary to operate the STAMP in the digital mode is shown in the block diagram of Figure 3.

The hydraulic actuators for the three gimbals consist of a double-vane actuator for the outer gimbal or sidereal axis, a single-vane type for the middle gimbal or yaw axis, and a pair of hydraulic motors for the inner gimbal or roll axis. The sidereal- and yaw-axis actuators are connected directly to those gimbals through flexible couplings, but the roll-axis hydraulic motors are connected by gears to the roll gimbal. Each hydraulic motor is preloaded to eliminate backlash and arranged so that one motor drives the roll gimbal clockwise and the other motor drives the gimbal counterclockwise.

The electrohydraulic servovalves used for each gimbal are the same type but have different capacities. The roll and yaw axes have servovalves

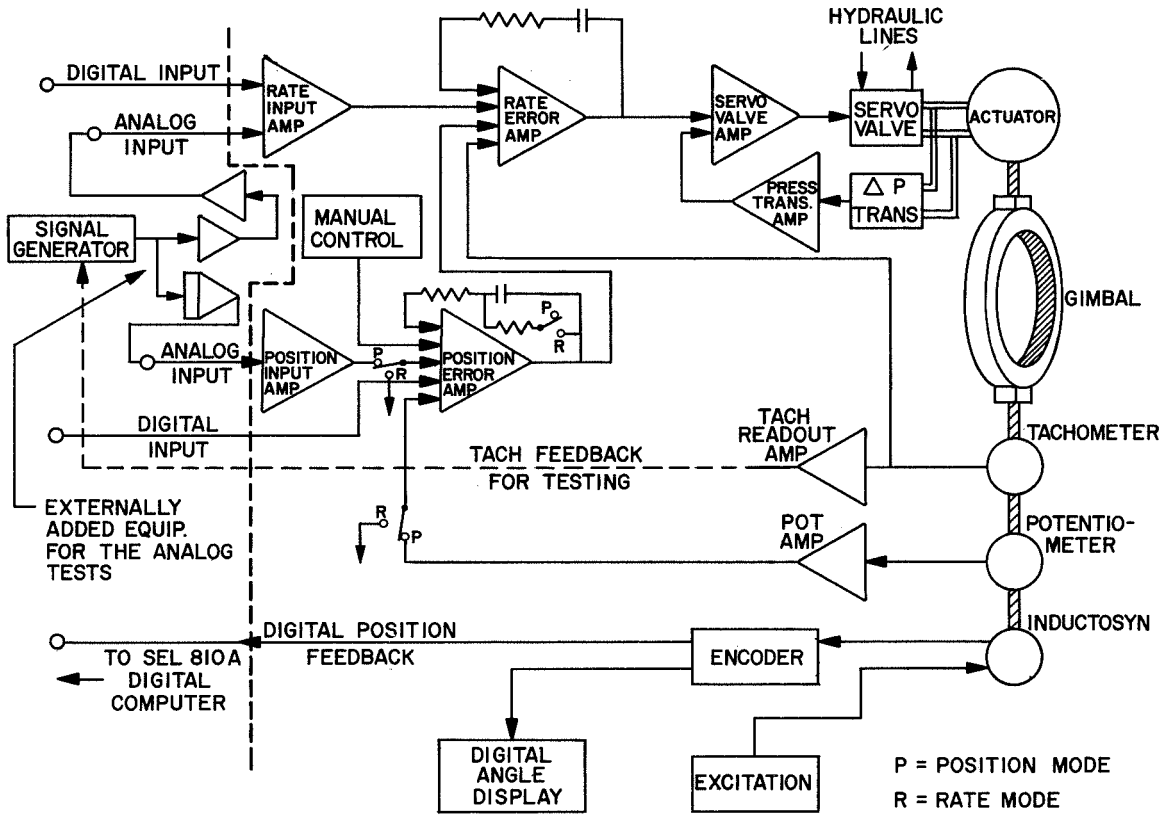

Figure 2. Block diagram for a single axis of the STAMP.

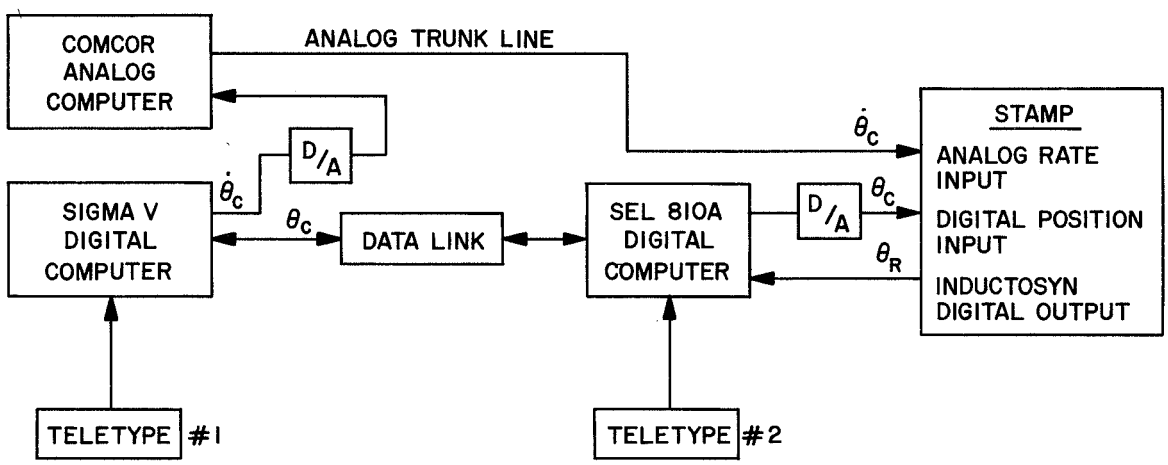

Figure 3. Block diagram for a single axis of the STAMP in the digital mode of operation.

with a 9.48×10^2 cm^3/s rating and the sidereal servovalve has a 2.53×10^3 cm^3/s rating. The sidereal axis uses two 2.53×10^3 cm^3/s servovalves in parallel operation to handle its large flow requirements. When the originally supplied servovalves were tested, they were found to have considerable leakage. Higher quality valves were obtained with less leakage as shown in Figure 4. Initial testing of the STAMP with the replacement valves indicated improved performance; however, more recent tests with both the replacement and the original valves indicate no significant difference in the dynamic performance as expressed with a frequency response plot as shown in Figure 5.

Of the number of difficulties encountered while testing the STAMP, only four interruptions can be attributed to the STAMP equipment. One shutdown occurred when the yaw-axis servovalve spool stuck because of silt; it was repaired by removing it and flushing it out. The other three shutdowns occurred because of the electronics associated with the inductosyn's digital encoders. The printed circuit (PC) boards on which these circuits are located have the appearance of a breadboard rather than a finished project. These PC boards need to be reworked or replaced if this source of difficulty is to be eliminated.

Seven other interruptions were caused by difficulties associated with the Sigma-V digital computer or the data link. Four of these shutdowns resulted from component failures in the data link and one required an adjustment of the timing. One of the two interruptions attributed to the Sigma-V was caused by moisture in the unit and the other was caused by an equipment modification that was incorrect. The potential sources of trouble for the total system appear to be the data link and the digital encoders.

PERFORMANCE REQUIREMENTS

A realistic set of performance requirements for the STAMP should be based on the expected performance of the Skylab flight vehicle. However, many of the variables and parameters for the Skylab are not known precisely or are subject to modification as additional information becomes available; therefore, there is a tendency to over specify the performance requirements of the STAMP to provide a margin of safety which, unfortunately, often exceeds the capability of the equipment. The nonlinear characteristics of the STAMP further add to the complexity of defining a good set of performance requirements.

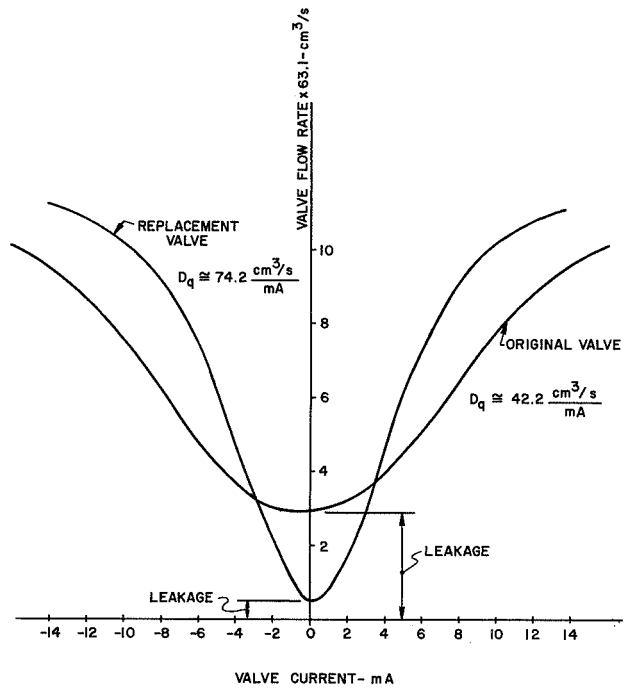

Figure 4. Flow curves of roll-axis servovalves.

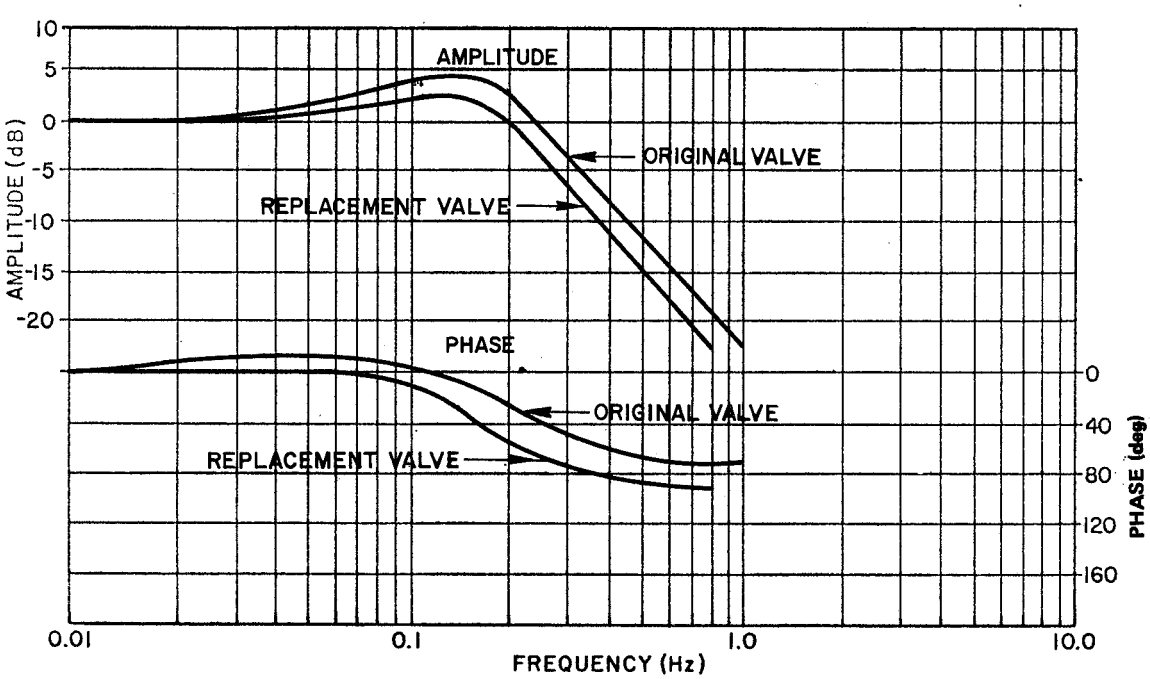

Figure 5. Roll-axis frequency response for 0.03 deg/s input signal, analog-position mode, for original and replacement servovalves.

The performance requirements presented here are a composite of requirements taken from two documents: the NASA acceptance test report for the STAMP [1] and the Skylab integration test plan [2]. The performance requirements are presented here without further comment. An analysis of the test results and a comparison with these requirements are presented in a later section.

1. Frequency response — For rate sinusoidal input signal levels from 0.01 to 3.5 deg/s, the following results are expected:

   a. Bandwidth - 0 to 5 Hz < 3 dB down at 5 Hz.

   b. Phase shift - < 45 deg from 0 to 5 Hz.

   c. Noise level - Jitter < 0.001 deg/s at 5 Hz.

2. Transient response — For rate step input levels from 0.01 to 3.5 deg/s, the following results are expected:

   a. Stability — Damping ratio < 0.5.

   b. Linearity — ± 20 percent at rates from 0.01 to 1 deg/s.

   c. Rise and fall times — < 0.05 s.

3. Servosystem stiffness — This test is described as a static or steady state test [1] but was not actually performed at MSFC. The required stiffness is given as 6.77×10^4 N-m/deg or higher. In the STAMP test program, this test was performed dynamically.

4. Dynamic position and rate accuracy.

   a. The dynamic position accuracy will be checked to be 0.005 deg or better.

   b. The dynamic rate accuracy will be checked to be 0.02 deg/s or better for sinusoidal motions of 2 deg peak to peak to 0.637 Hz.

5. Friction and stiction of the gimbals — Design values of friction and stiction are numerically the same; for each axis they are:

   a. Sidereal axis - 2710 N-m.

   b. Yaw axis - 1355 N-m.

   c. Roll axis - 8130 N-m.

TEST RESULTS

Frequency Response Test

Frequency response data were taken on the STAMP to obtain an indication of its dynamic range and to help characterize its nonlinearities. Each of the three axes was tested separately in both the analog-position mode (Fig. 2) and in the digital mode (Fig. 6). For both configurations, a Boonshaft frequency analyzer was used to supply the excitation rate signal and to analyze the response from the gimbal tachometers. Although the input signal is a smooth sine wave, the response as measured by the tachometer is not, as shown in Figure 7 for the sidereal tachometer. The Boonshaft analyzer uses only the fundamental frequency component of the tachometer output signal to compute the amplitude and phase responses; therefore, the results are frequency responses only in a describing function sense. It should be understood that all responses presented in this section are closed-loop responses to sine wave inputs and that for different types of inputs, such as square waves, a different response would likely result.

The magnitude of the input signal was varied from 0.002 to 1 deg/s. At the low signal levels, the tachometer output signal was boosted by a gain of 100 to increase the accuracy of the Boonshaft analysis. For signal levels below 0.002 deg/s, the Boonshaft did not give consistent results because of the low voltage of the signals and the noise content in the response signal. When the CMG's were running, the noise level in the output signals increased and the lowest input signal to give consistent results was 0.005 deg/s. Frequency responses with the input signal larger than 1 deg/s were not run because the responses at 0.5 and 1 deg/s appeared to be adequate; i.e., the bandwidth was approximately 5 Hz; thus testing was concentrated at the lower signal levels.

In the analog-position mode (Fig. 2), the STAMP was tested for two different cases: the first used steel plates mounted on the STAMP's load plate to simulate the weight of the CMG's which were not available at that time. The second case had the CMG's mounted in the torque measuring fixtures (TMF's) on the load plate and running at nominal speed (7800 rpm). The responses for the analog-position mode for the steel plate case of the yaw axis are shown in Figures 8 through 14, and the responses for the analog-position mode for the CMG case of the yaw axis are shown in Figures 15 through 19. In the digital mode (Fig. 7), the CMG's were mounted in the TMF's and running at nominal speed. The responses for the digital mode of the yaw axis are shown in Figures 20 through 23.

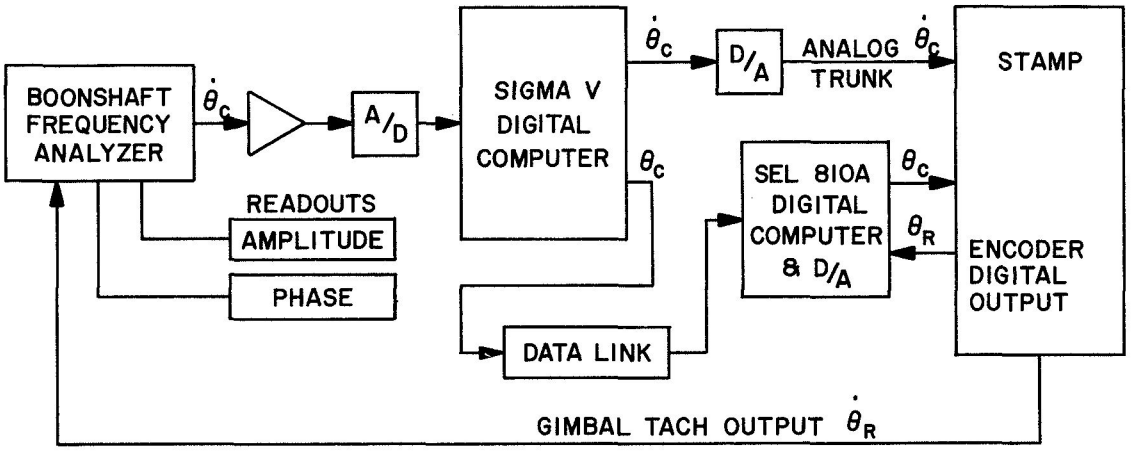

Figure 6. Configuration for frequency response test in the digital mode.

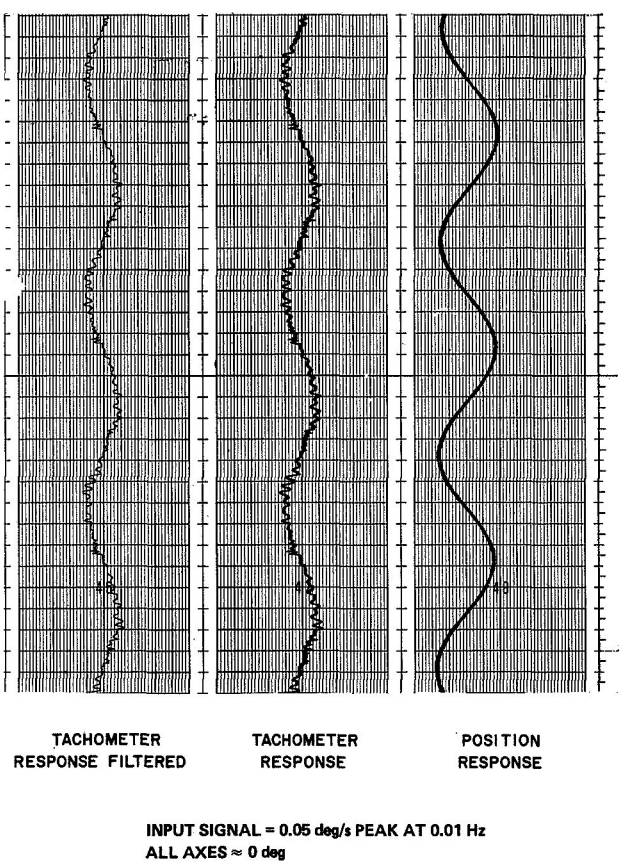

Figure 7. Sidereal-axis tachometer response, analog-position mode, CMG case.

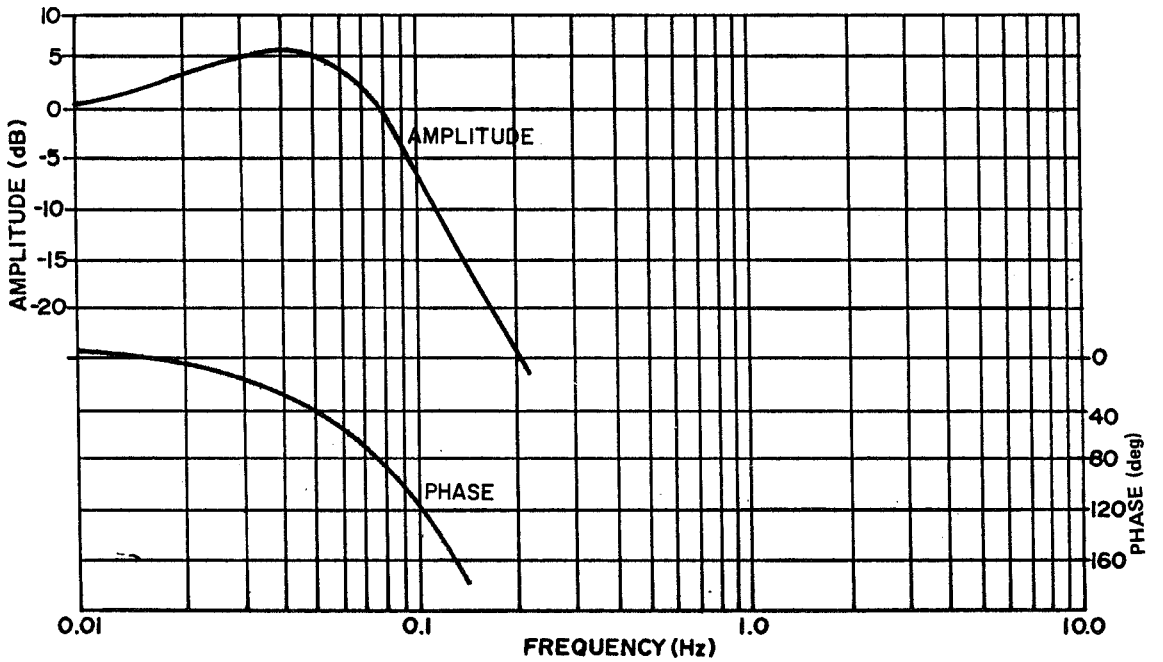

Figure 8. Yaw-axis frequency response for 0. 002 deg/s input signal, analog-position mode, steel plate case.

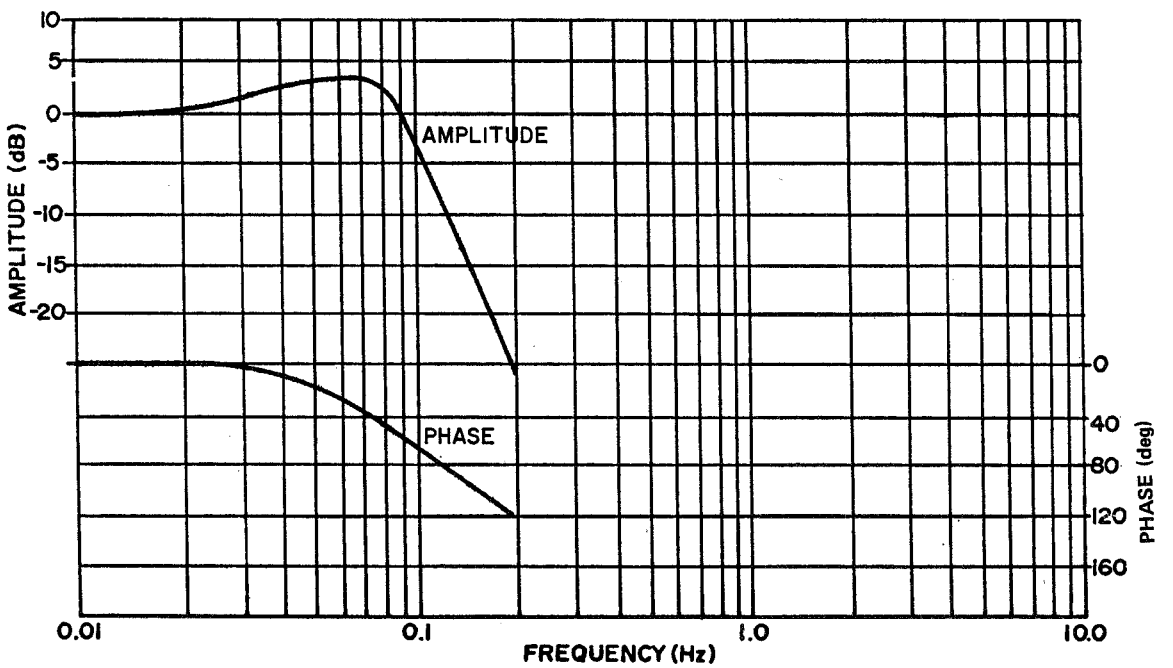

Figure 9. Yaw-axis frequency response for 0. 005 deg/s input signal, analog-position mode, steel plate case.

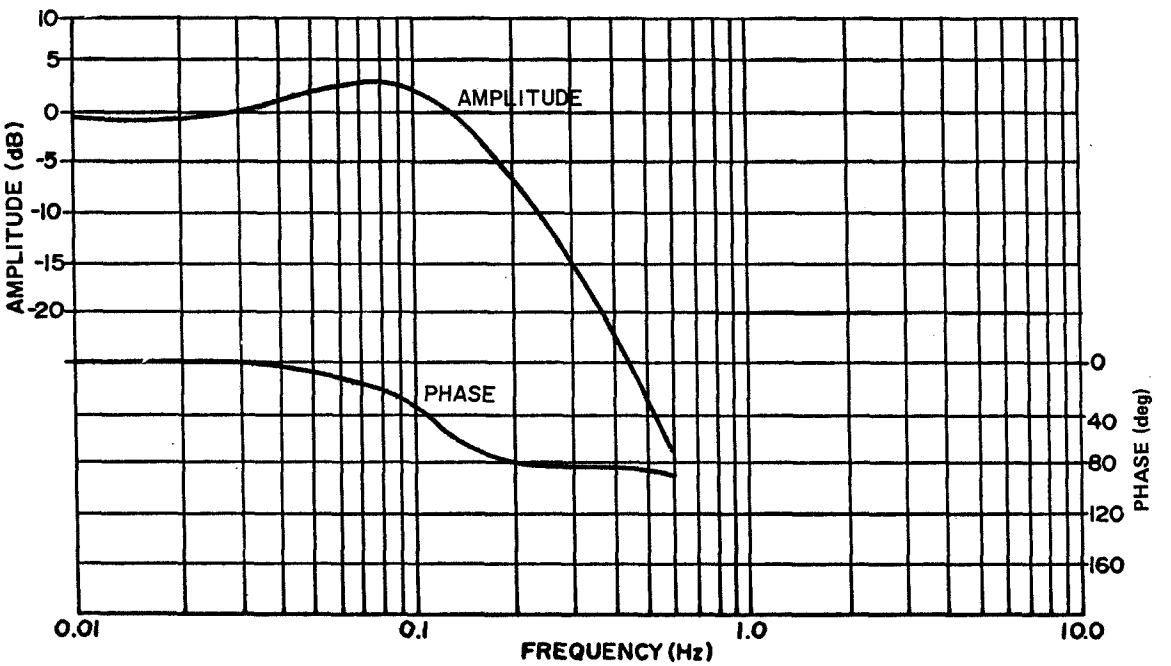

Figure 10. Yaw-axis frequency response for 0.01 deg/s input signal, analog-position mode, steel plate case.

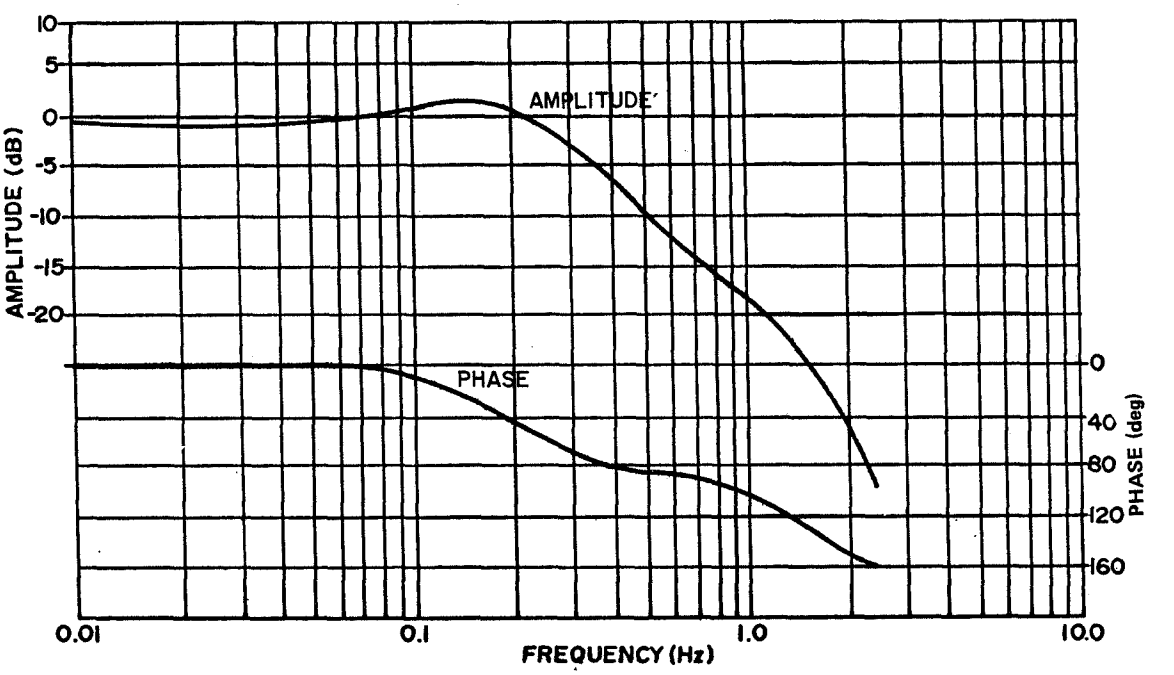

Figure 11. Yaw-axis frequency response for 0.03 deg/s input signal, analog-position mode, steel plate case.

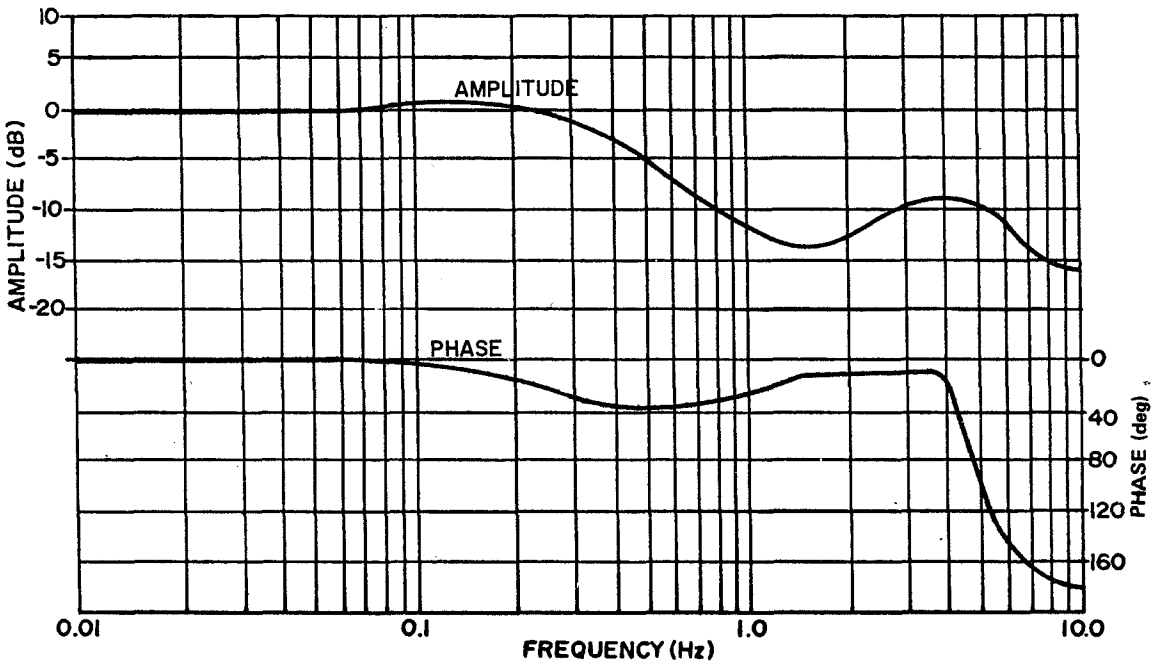

Figure 12. Yaw-axis frequency response for 0.1 deg/s input signal, analog-position mode, steel plate case.

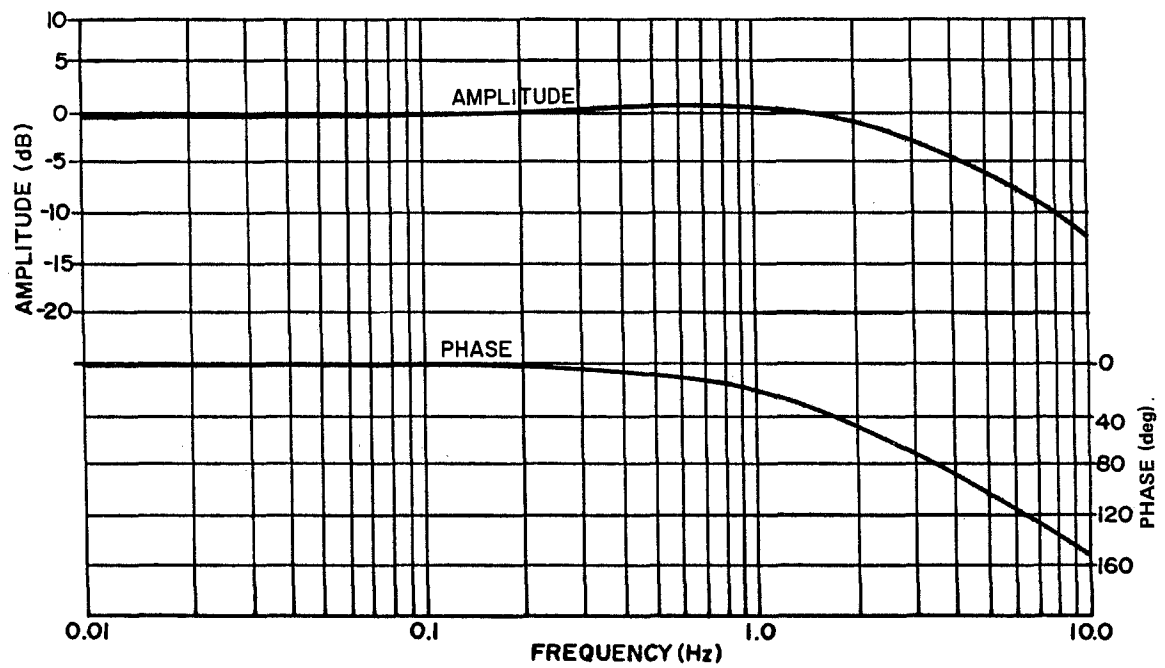

Figure 13. Yaw-axis frequency response for 0.5 deg/s input signal, analog-position mode, steel plate case.

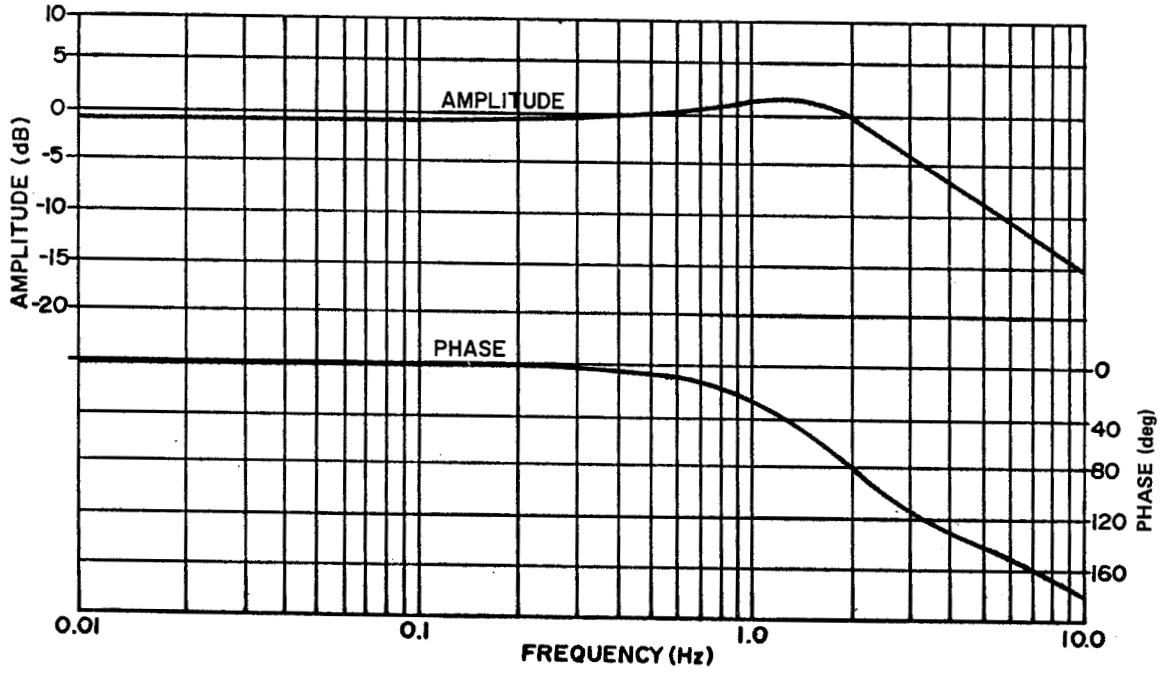

Figure 14. Yaw-axis frequency response for 1.0 deg/s input signal, analog-position mode, steel plate case.

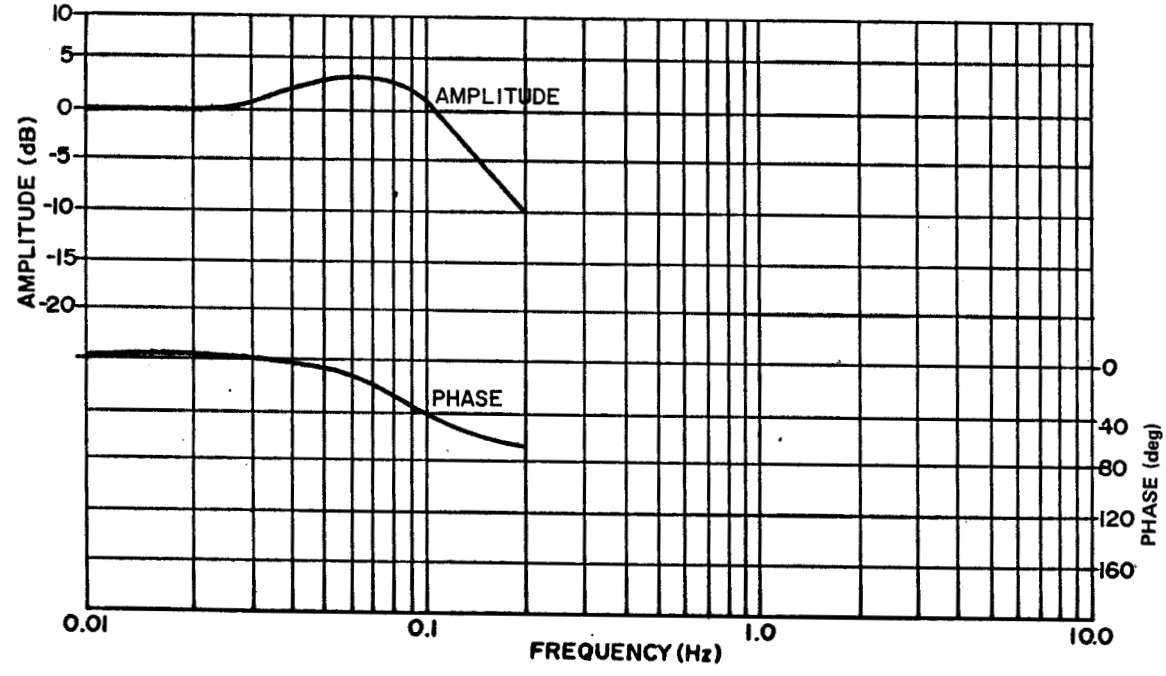

Figure 15. Yaw-axis frequency response for 0.005 deg/s input signal, analog-position mode, CMG case.

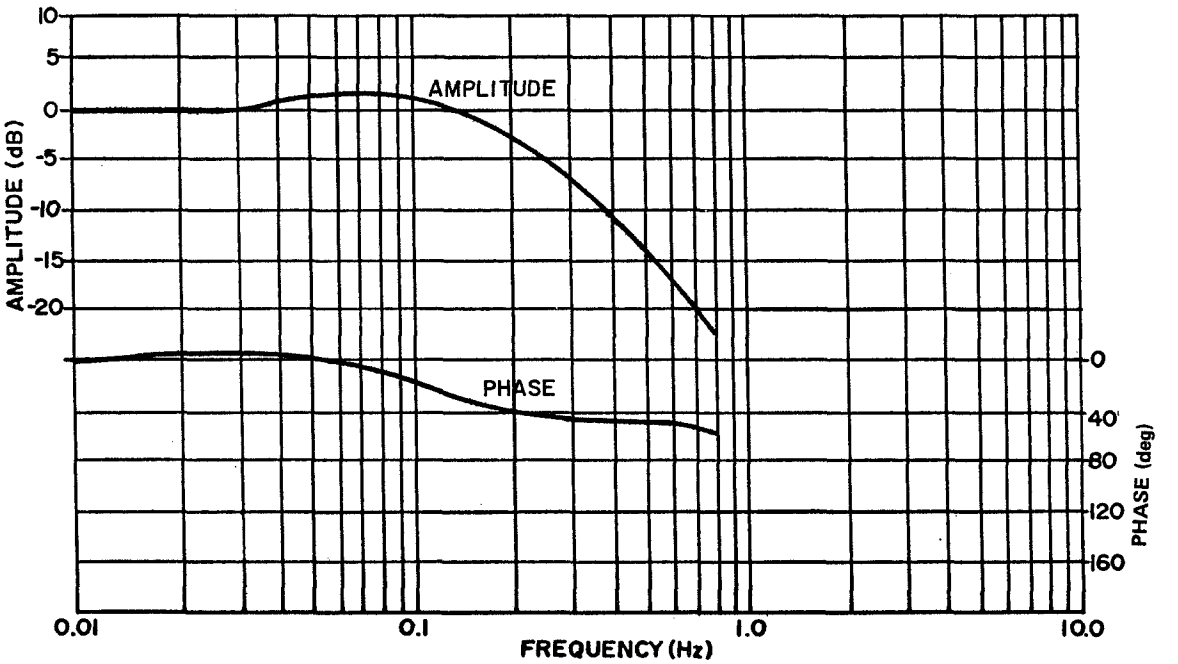

Figure 16. Yaw-axis frequency response for 0.01 deg/s input signal, analog-position mode, CMG case.

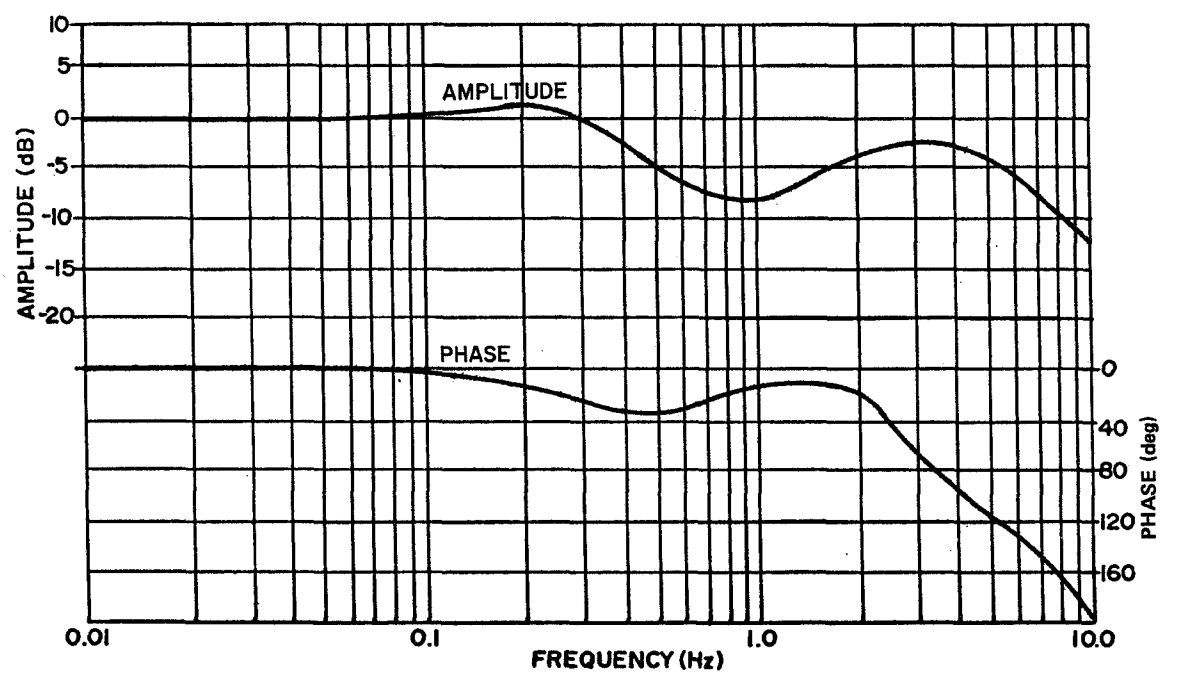

Figure 17. Yaw-axis frequency response for 0.05 deg/s input signal, analog-position mode, CMG case.

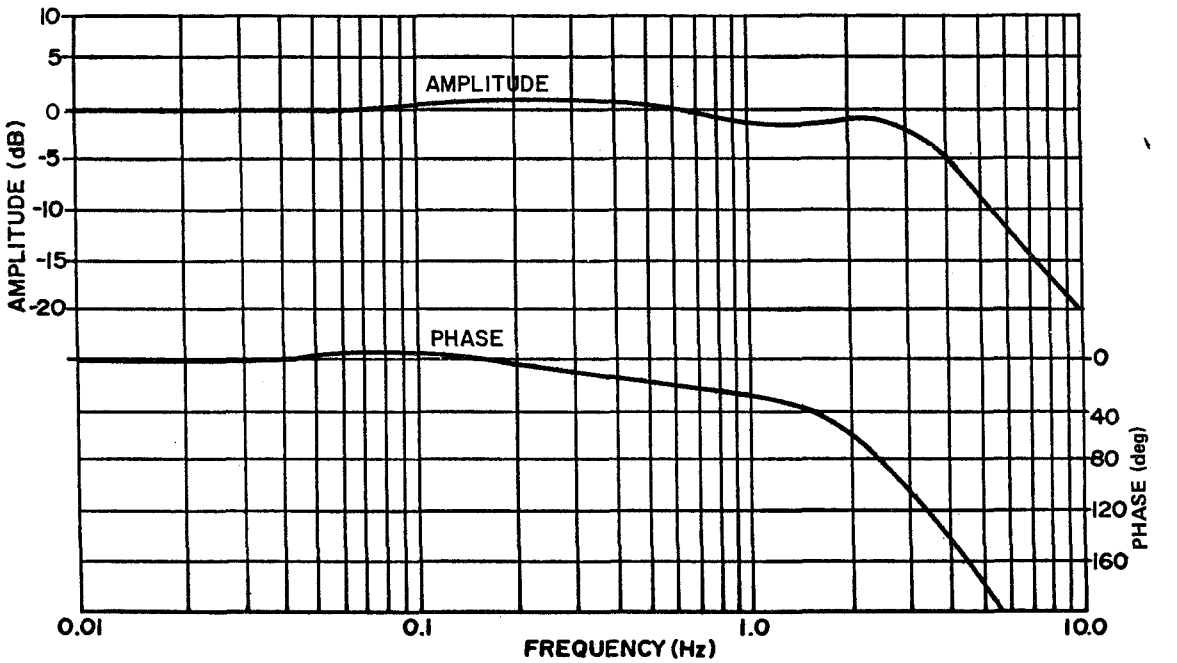

Figure 18. Yaw-axis frequency response for 0.10 deg/s input signal, analog-position mode, CMG case.

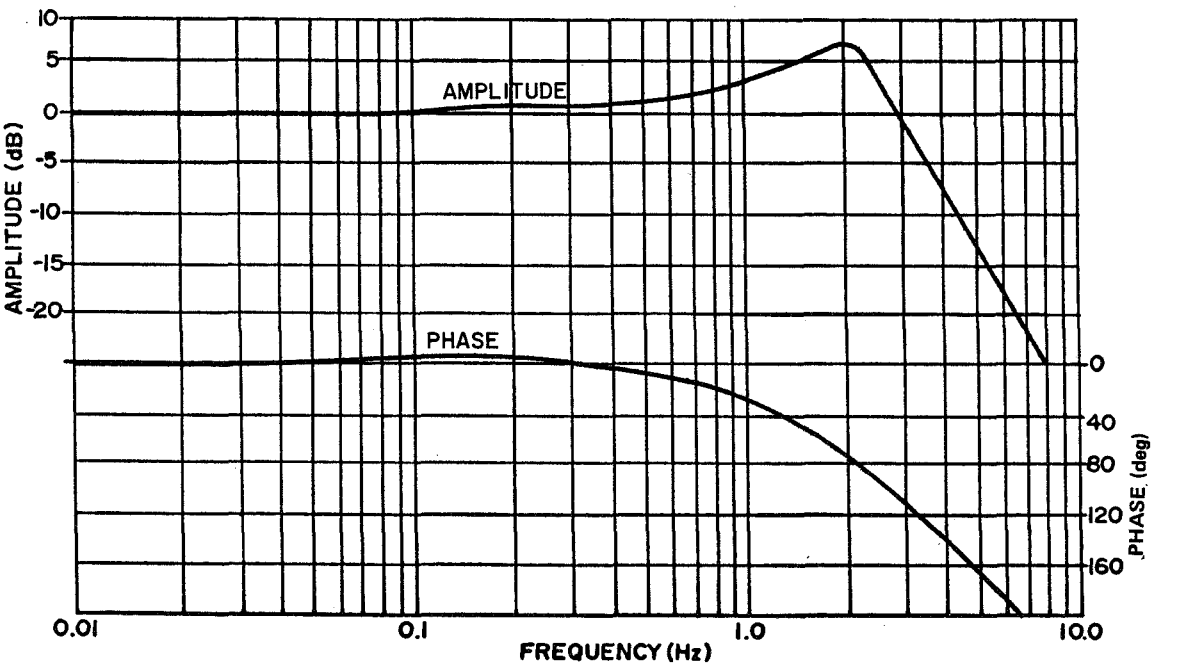

Figure 19. Yaw-axis frequency response for 0.5 deg/s input signal, analog-position mode, CMG case.

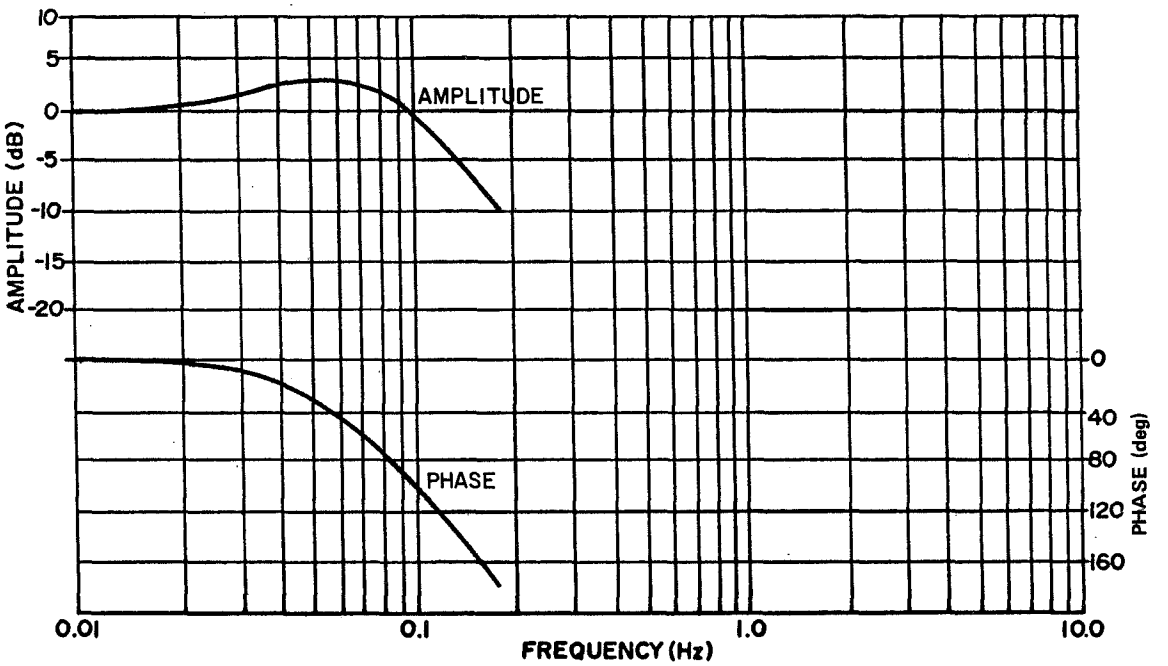

Figure 20. Yaw-axis frequency response for 0.005 deg/s input signal, digital mode, CMG case.

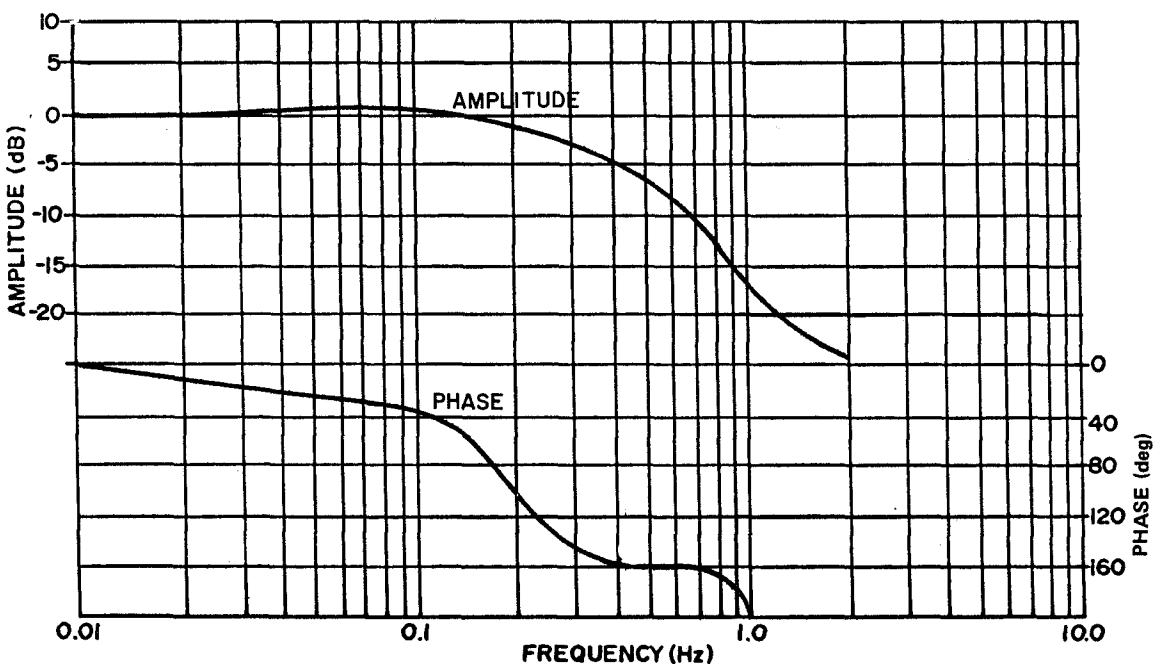

Figure 21. Yaw-axis frequency response for 0.01 deg/s input signal, digital mode, CMG case.

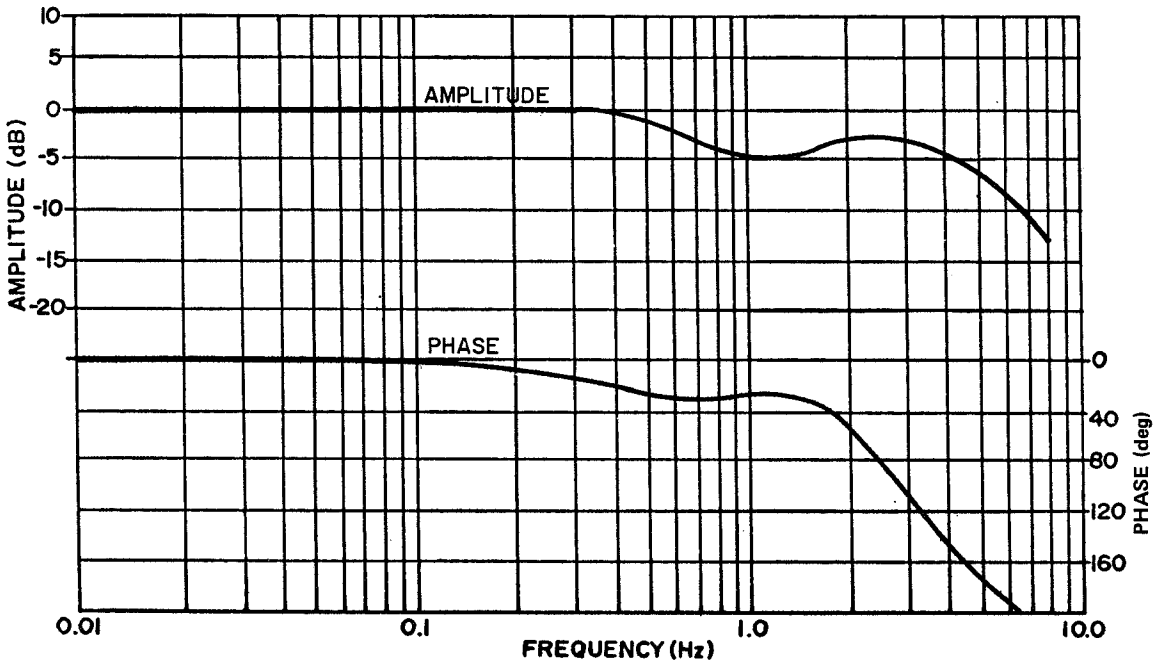

Figure 22. Yaw-axis frequency response for 0.1 deg/s input signal, digital mode, CMG case.

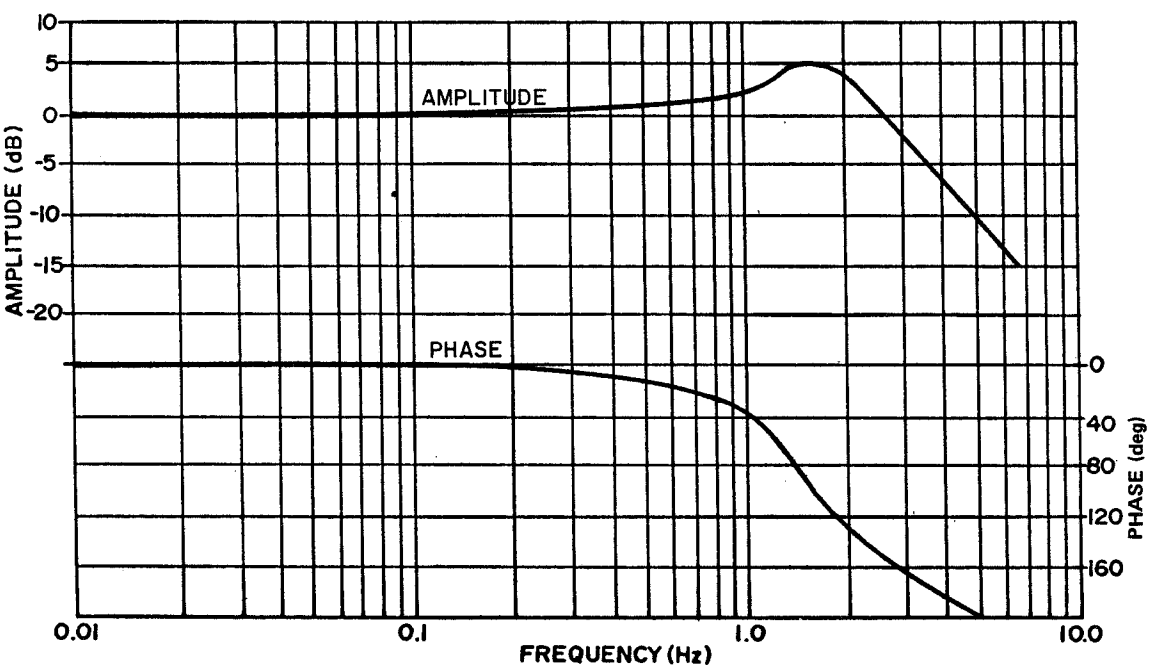

Figure 23. Yaw-axis frequency response for 0.5 deg/s input signal, digital mode, CMG case.

Examination of the frequency response plots of the yaw axis (Figs. 8 through 23) establishes the STAMP as a complex nonlinear system. This is manifested by the system's dependency on the level of the input signal amplitude as reflected by the corresponding variations in the system's bandwidth, order, and damping, as well as a variation in the system's responses. Variations in all four of these characteristics are present in all three sets of data and for all three of the STAMP's axes. The nonlinear complexity of the system is compounded by the coupling of the dynamics of the running CMG-TMF combination with the dynamics of the STAMP. The effect and full extent of this coupling have not been determined.

The Skylab integration test plan [2] calls for a bandwidth of 5 Hz for input signal levels from 0.01 to 3.5 deg/s. Figures 8 through 23 for the yaw axis and the figures in Appendix B for the roll and sidereal axes show that these specifications apparently are not met. The 5-Hz bandwidth is attained only from signal levels of 1 deg/s or greater for the roll and yaw axes and 0.5 deg/s or greater for the sidereal axis. The bandwidth for a signal level of 0.1 deg/s in the digital mode (Fig. 21) is only 0.31 Hz, which is not an insignificant deficiency. Its practical aspects mean the STAMP may be incapable of coping with low-level, short-duration disturbances, such as those expected from astronaut movements within the Skylab.

The complex nonlinearity of the STAMP should make one cautious about making precise interpretations of such experimental data as presented in this section; however, some overall observations appear to be in order. The correspondence between the load plate, analog, and digital responses for each axis appears to be good, considering the data were accumulated over a period of 6 months. In general, the responses with the CMG's running, both analog and digital, have slightly broader bandwidths than the steel plate responses. This is attributed to the additional noise in the tachometer signals which apparently acts as a dither signal to the hydraulic servocontrol loop.

A similar type of nonlinearity appears to be present in the yaw and sidereal axes, but the roll axis responses do not exhibit an extra high frequency (2 to 6 Hz) resonant peak. The data for the sidereal and yaw axes were taken with all the gimbals at 0 deg, but the data for the roll axis were taken with the yaw axis at approximately 34 deg or with the load platform level with respect to the ground. With the gimbals at the zero position, a check was made of the cross-coupling between the gimbals; in all cases it was extremely small. Figure 24 shows the sidereal and yaw axes coupling with a resonant peak of -17.5 dB occurring at 4 Hz. This was the maximum amount of cross-coupling recorded. Theoretically, the coupling between the sidereal axis and the roll axis will be a maximum for a yaw-gimbal angle of 90 deg [3].

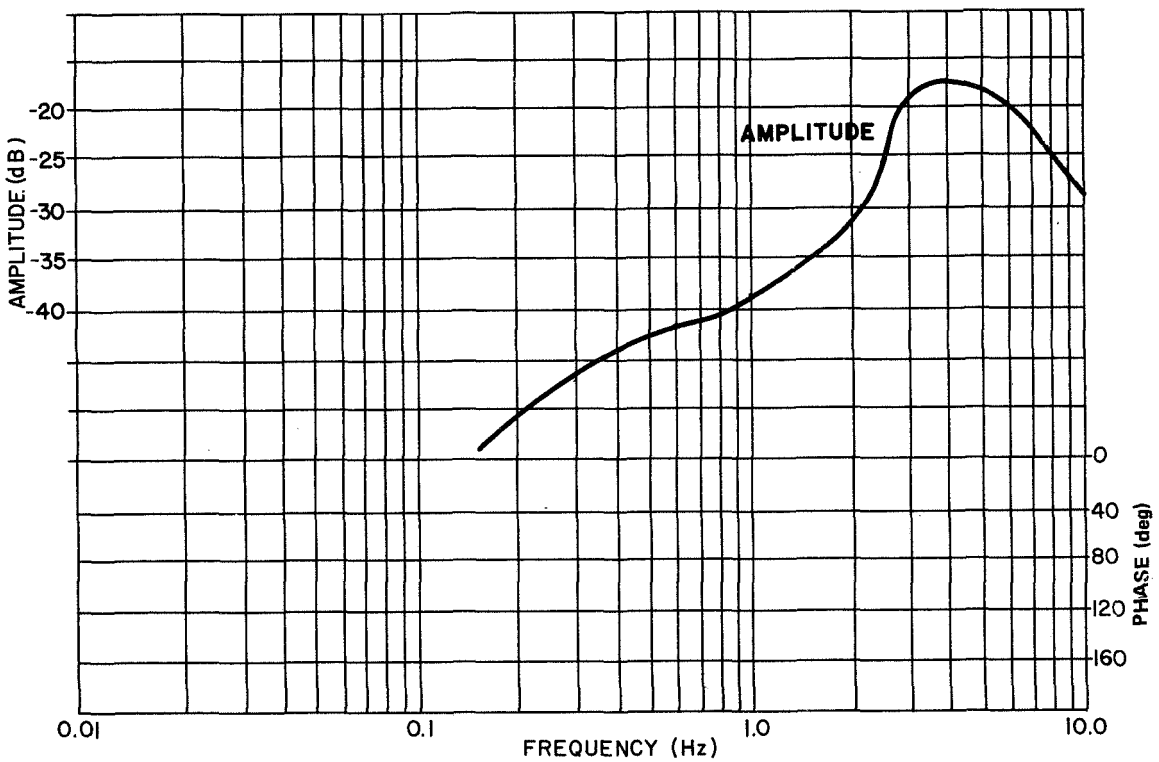

Figure 24. Sidereal-yaw-axis coupling amplitude frequency response for 0.5 deg/s input signal, analog-position mode, CMG case.

Transient Response Test

The transient response of a complex nonlinear system, such as the STAMP, to a step input depends on the amplitude of the step command. The response of a nonlinear system to a particular step function input gives information pertaining to that specific input and usually nothing more. However, as with the frequency response test, obtaining the transient response characteristics for a set of step function inputs of different magnitudes provides the spread that these characteristics will assume in the proposed operating range of the STAMP. The transient response data will be of particular importance in developing the nonlinear mathematical model of the STAMP for computer simulation.

The STAMP was tested in all three modes of operation with steel plates or CMG's mounted on the load platform. A response for each of the three modes of operation is shown in Figure 25. All the response data were reduced to tabular form by calculating the rise time, overshoot, and settling time. The standard definitions of these transient response characteristics [4] are illustrated in Figure 26.

For the analog-rate mode of operation, with the CMG's mounted and running at nominal speed, the transient response characteristics were: a rise time of less than 0.5 s, an overshoot of 0, and a settling time of less than 2 s. These parameters were relatively constant over the range of step inputs from 0.01 to 2 deg/s. The data were taken primarily to check against the nonlinear mathematical model of the STAMP under current development.

Transient responses with the STAMP in the analog-position mode were taken with either steel plates or CMG's mounted on the load platform. Table 2 shows the response characteristics for the steel plate case for the roll and yaw axes. The CMG's were mounted on the load platform before the test could be completed, so that data for the sidereal axis with steel plates were not obtained. The results show that for this mode of operation, the STAMP has a rise time of 1 to 2 s, no overshoot, and a settling time of 2 to 3 s for step inputs of 0.01 to 2 deg. Table 3 gives the results of the STAMP in the analog-position mode but with the CMG's mounted and running. A comparison of the results in Tables 2 and 3 indicates that the addition of the CMG's to the system tends to destabilize the system. All the axes in Table 3 exhibit some overshoot; in fact, 80 percent of the responses result in overshoot. Also, the settling times are longer than those for the same test signals in Table 2 (at least for 35 percent of the cases). The rise times in Table 3 appear to be slightly shorter than those in Table 2. The changes in the transient response characteristics caused by the CMG operation are not unexpected.

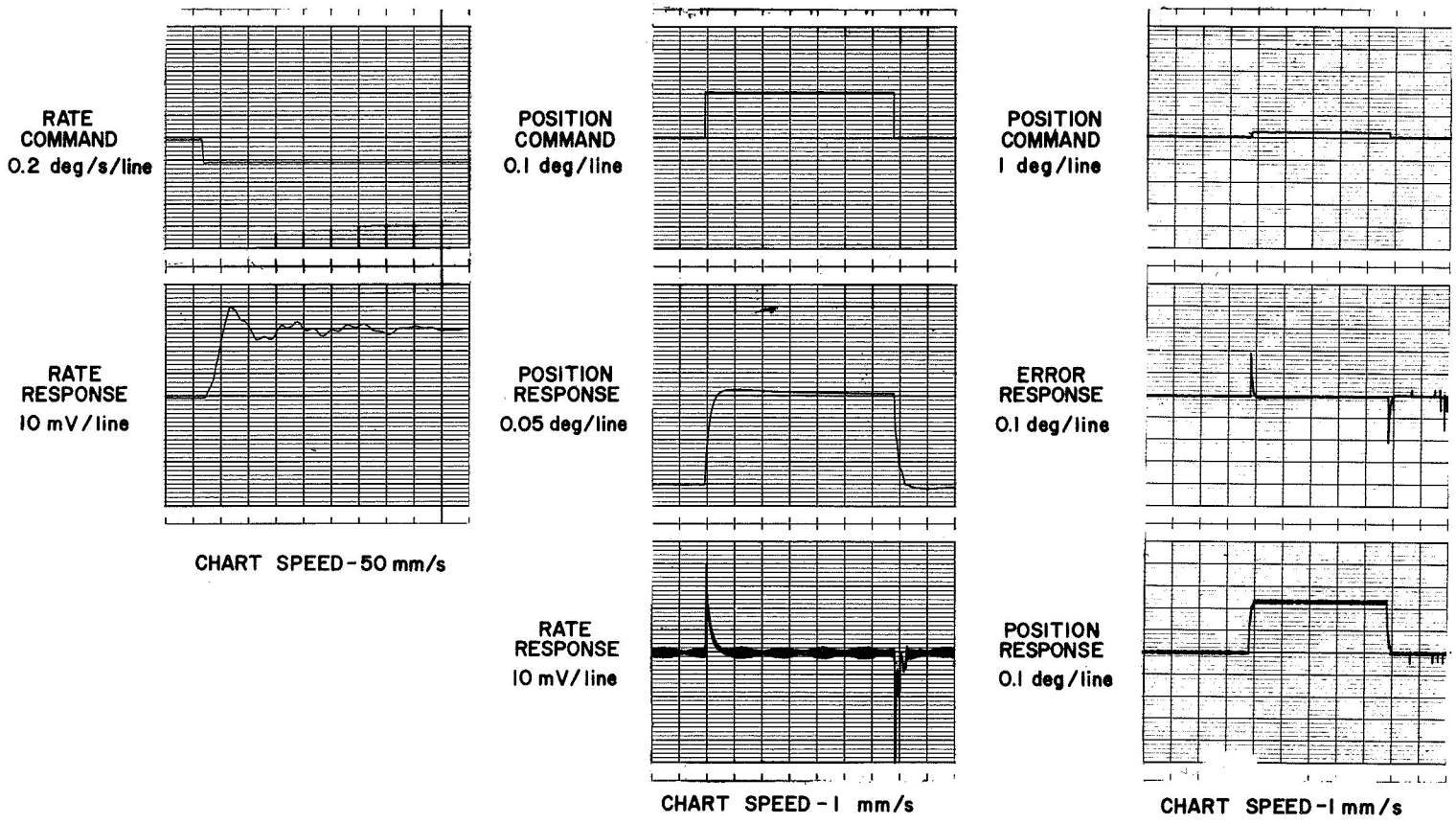

Figure 25. Transient responses for the STAMP's three modes of operation.

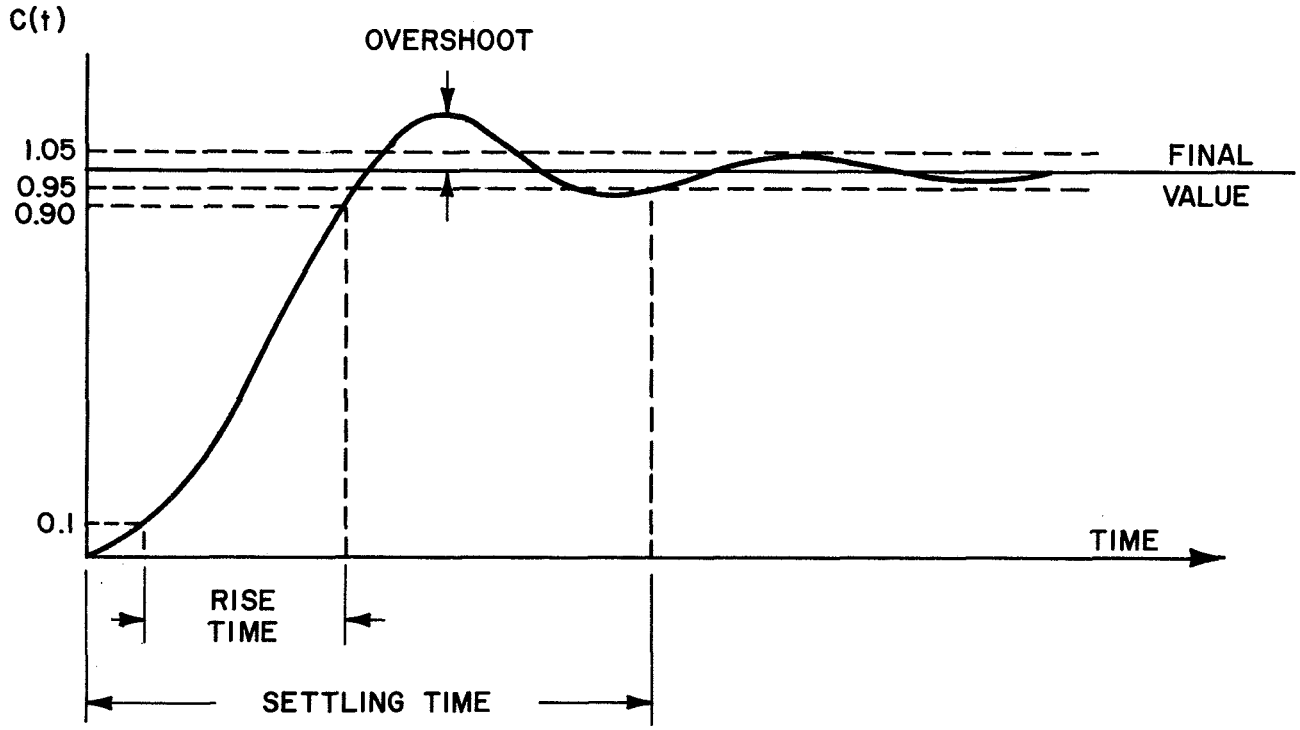

Figure 26. Definition of the transient response parameters.

TABLE 2. STEP RESPONSE CHARACTERISTICS FOR ANALOG-POSITION MODE, STEEL PLATE CASE

Position Command (deg)	Roll Axis			Yaw Axis		
	Rise Time (s)	Overshoot (%)	Settle Time (s)	Rise Time (s)	Overshoot (%)	Settle Time (s)
2	1.15	0	1.4	1.7	0	2.32
1	1.4	0	2	1.7	0	2.2
0.5	1.4	0	2	1.4	0	1.75
0.1	1.25	0	1.6	1.78	0	2.2
0.05	2.4	0	3.3	2	0	2.6
0.01	2.05	0	3.1	2.4	0	3.5

TABLE 3. STEP RESPONSE CHARACTERISTICS FOR ANALOG-POSITION MODE, CMG CASE

Position Command (deg)	Roll Axis			Yaw Axis			Sidereal Axis		
	Rise Time (s)	Overshoot (%)	Settle Time (s)	Rise Time (s)	Overshoot (%)	Settle Time (s)	Rise Time (s)	Overshoot (%)	Settle Time (s)
2	1.5	0	2	1.5	5	2	1	2	1.5
1	1.5	0	2	2	5	2.5	1	4	1.5
0.5	1.5	3	2	1.5	4	2	1	0	1
0.1	1.5	5	2	1.5	4	2.5	1	6	8
0.05	2	15	8	1.5	8	8	1	30	22
0.01	1	10	16	2	10	17	1	80	27

The noise added to the system because of the CMG's running has the effect of adding a dither signal to the servocontrol system; hence, a more responsive system results.

Results from the digital mode of operation, with the CMG's mounted and running, are given in Table 4. There does not appear to be any consistent improvement in the characteristics of Table 4 over those of Table 3. The settling times of the roll and sidereal axes appear better in the digital mode, but the yaw-axis settling time is about the same for both modes of operation. A close correspondence of the data for analog and digital modes of operation was also observed in the frequency response data.

In addition to the foregoing transient response tests, another series of low-level step signal responses were run in the digital mode for the 1 arc s to 1 arc min range. The primary objective of these tests was to determine the accuracy of the STAMP to low-level signal commands. The transient response data were reduced to the standard characteristics and are presented in Tables 5 and 6 for the steel plate and CMG cases, respectively. In the steel plate case (Table 5), the rise time is 1 to 3 s and the settling time is 2 to 4 s. The yaw and sidereal axes have practically no overshoot, while the overshoot in the roll axis varied considerably with the input signal amplitude.

The responses of the roll, yaw, and sidereal axes to commands of 1, 2, 3, and 5 arc s for the steel plate case are shown in Figures 27, 28, and 29, respectively. The error signal, rather than the command signal, is shown in these traces. When the Sigma-V digital computer executes a change in the command signal, a clamp mode, shown in all three figures, holds the recorder at the last instantaneous value at which the clamp was energized; therefore, the clamped value is not necessarily the average value of the gimbal position. The accuracy for all these low-level signals is less than 0.5 arc s for all three axes.

For the low-level responses in the CMG case (Table 6), the inductosyn outputs were filtered before they were analyzed because of some additional noise in the response, as shown in Figures 30, 31, and 32. The accuracy for all axes in this case was also less than 0.5 arc s after the transients disappeared. The slightly larger variations observed in the recording are caused by clamping an instantaneous value of the noise. In Figures 30 and 31 the command signals were 1, 2, 3, and 5 arc s, and in Figure 32 the commands were 2, 3, and 5 arc s. Sporadically, a limit cycle would occur in the sidereal axis response. The limit cycle had a period of 40 to 60 s and a peak amplitude of approximately 38 arc s as shown in Figure 33. It was observed that when the STAMP was commanded to zero position from teletype No. 2

TABLE 4. STEP RESPONSE CHARACTERISTICS FOR DIGITAL MODE, CMG CASE

Position Command (deg)	Roll Axis			Yaw Axis			Sidereal Axis		
	Rise Time (s)	Overshoot (%)	Settle Time (s)	Rise Time (s)	Overshoot (%)	Settle Time (s)	Rise Time (s)	Overshoot (%)	Settle Time (s)
2	1	0	1	2	0	2	1	0	1
1	1	0	1	1	0	1	1	0	1
0.5	1	0	1	2	0	2	1	0	1
0.1	1	0	1	1	6	7	1.5	6	5
0.05	1	0	1	3	30	8	2	6	8
0.01	1	25	6	6	30	15	3	0	3

TABLE 5. TRANSIENT CHARACTERISTICS OF STEP RESPONSES WITH STAMP IN DIGITAL MODE, STEEL PLATE CASE

Position Command (arc s)	Roll Axis			Yaw Axis			Sidereal Axis		
	Rise Time (s)	Overshoot (%)	Settle Time (s)	Rise Time (s)	Overshoot (%)	Settle Time (s)	Rise Time (s)	Overshoot (%)	Settle Time (s)
1	0.5	20	3.5	1	0	1	1	0	1.5
2	1	15	6	1	0	1	1	25	4
3	1	10	2	1.6	0	1.8	1.5	20	2
5	2	80	4	3	0	5	1	0	2
10	1	80	5	3	5	7	1.5	20	4.5
30	0.2	70	4	1	0	2	1.5	5	2
60	0.8	8	1	2	0	3	0.5	5	1

TABLE 6. TRANSIENT CHARACTERISTICS OF STEP RESPONSE WITH STAMP IN DIGITAL MODE, CMG CASE

Position Command (arc s)	Roll Axis			Yaw Axis			Sidereal Axis		
	Rise Time (s)	Overshoot (%)	Settle Time (s)	Rise Time (s)	Overshoot (%)	Settle Time (s)	Rise Time[a] (s)	Overshoot[a] (%)	Settle Time[a] (s)
1	2	0	3	5	0	8	--	--	--
2	2	10	6	4	0	11	1	0	4
3	2	15	6	4	60	12	1	0	2
5	2	60	7	2	5	3	1	0	1
10	1	50	14	2	0	3	2	0	3
30	1	50	17	2	8	3	2	0	3
60	1	20	25	2	0	3	2	0	3

a. Sidereal data taken with its bypass valve closed (normally kept open 1 turn).

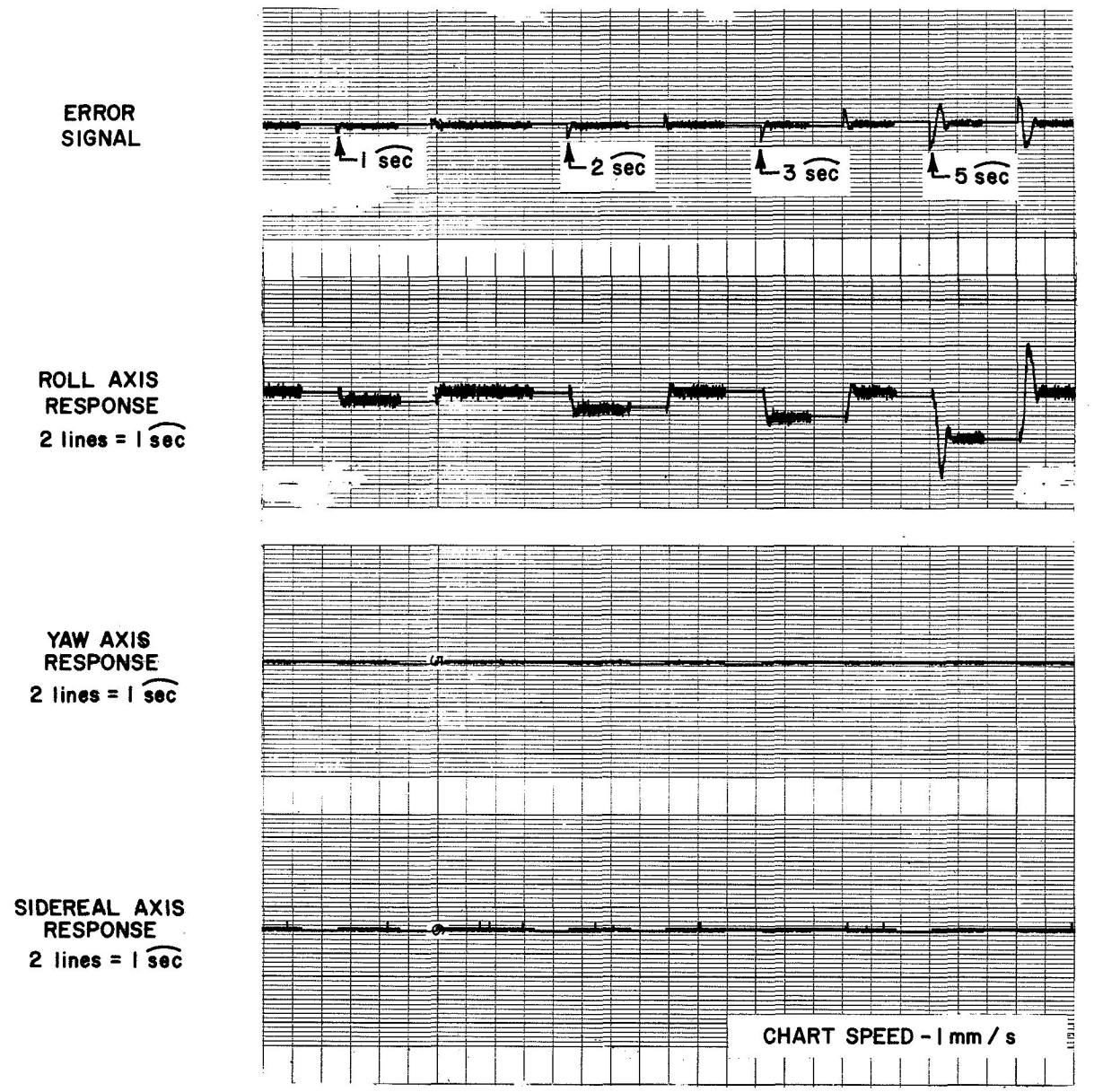

Figure 27. Roll-axis position response to low-level signal inputs, digital mode, steel plate case.

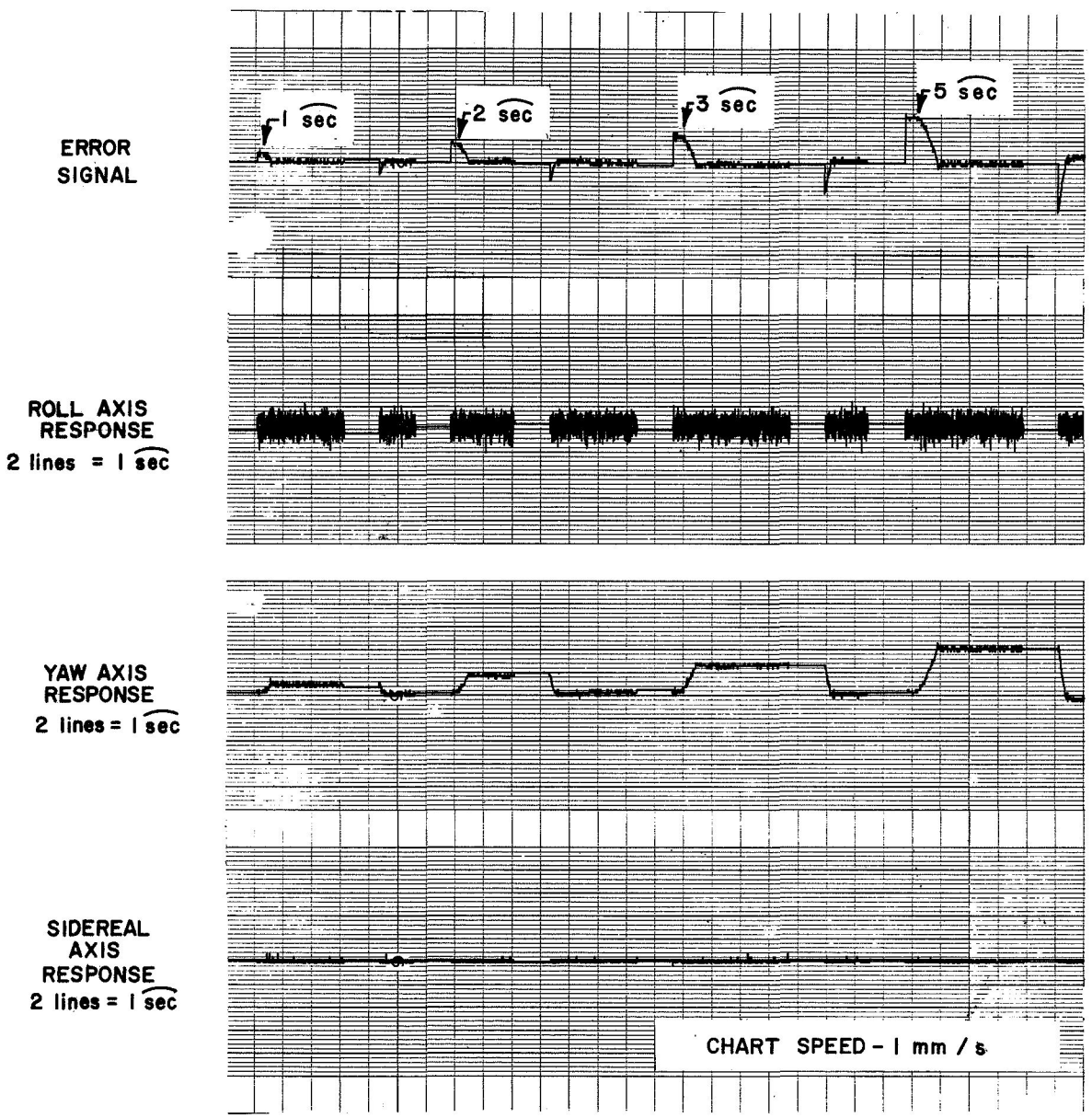

Figure 28. Yaw-axis position response to low-level signal inputs, digital mode, steel plate case.

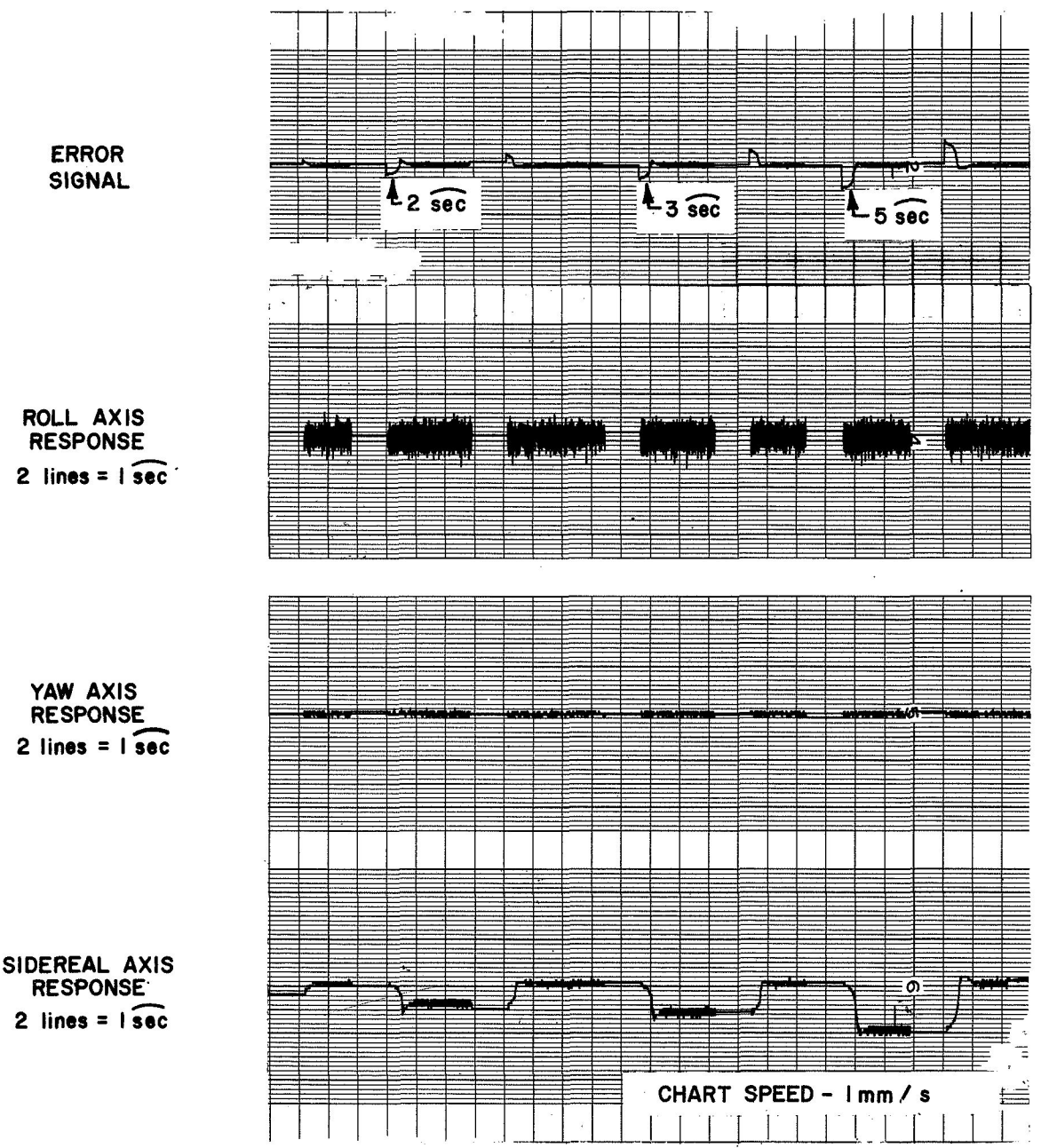

Figure 29. Sidereal-axis position response to low-level signal inputs, digital mode, steel plate case.

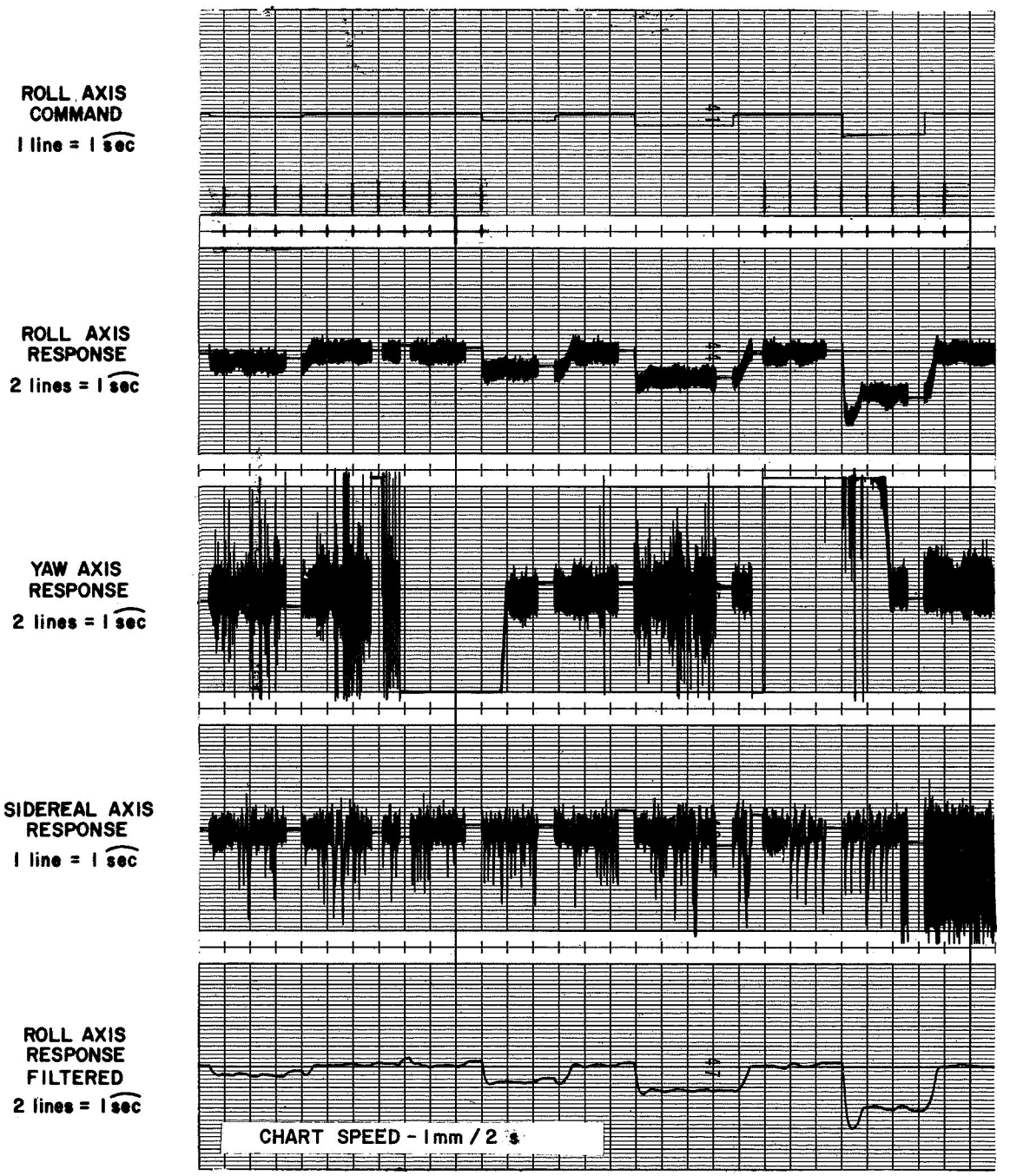

Figure 30. Roll-axis position response to low-level signal inputs, digital mode, CMG case.

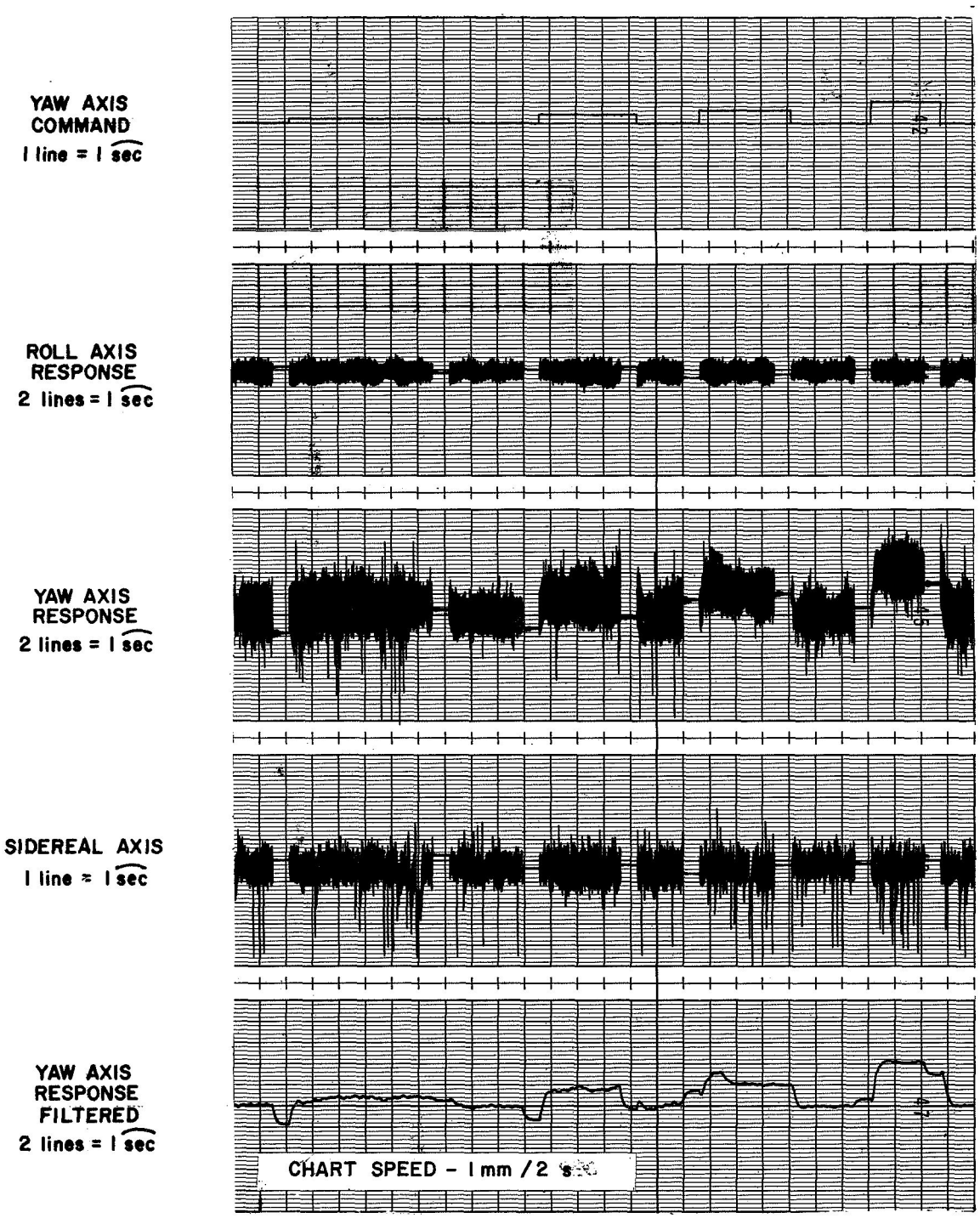

Figure 31. Yaw-axis position response to low-level signal inputs, digital mode, CMG case.

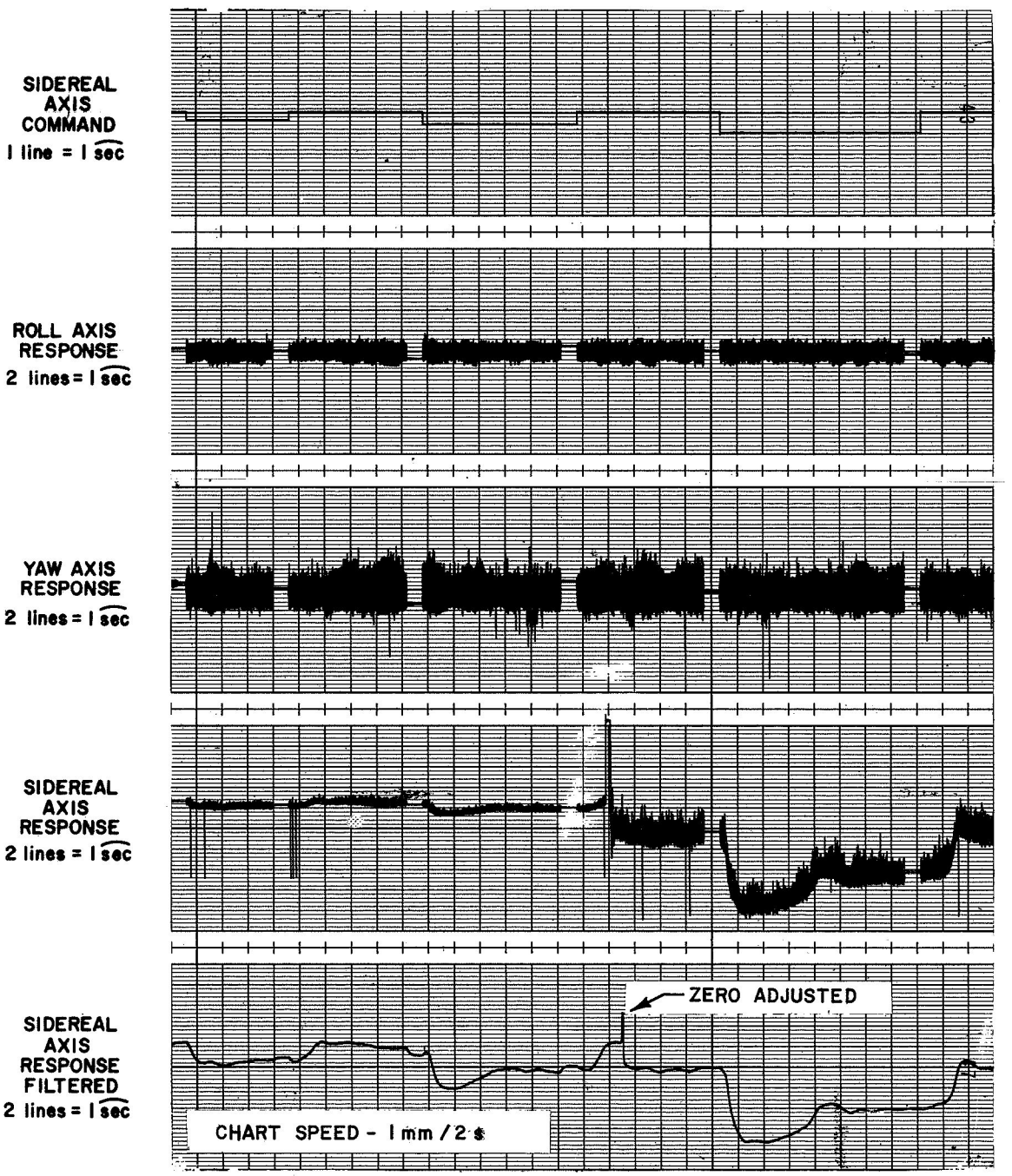

Figure 32. Sidereal-axis position response to low-level signal inputs, digital mode, CMG case.

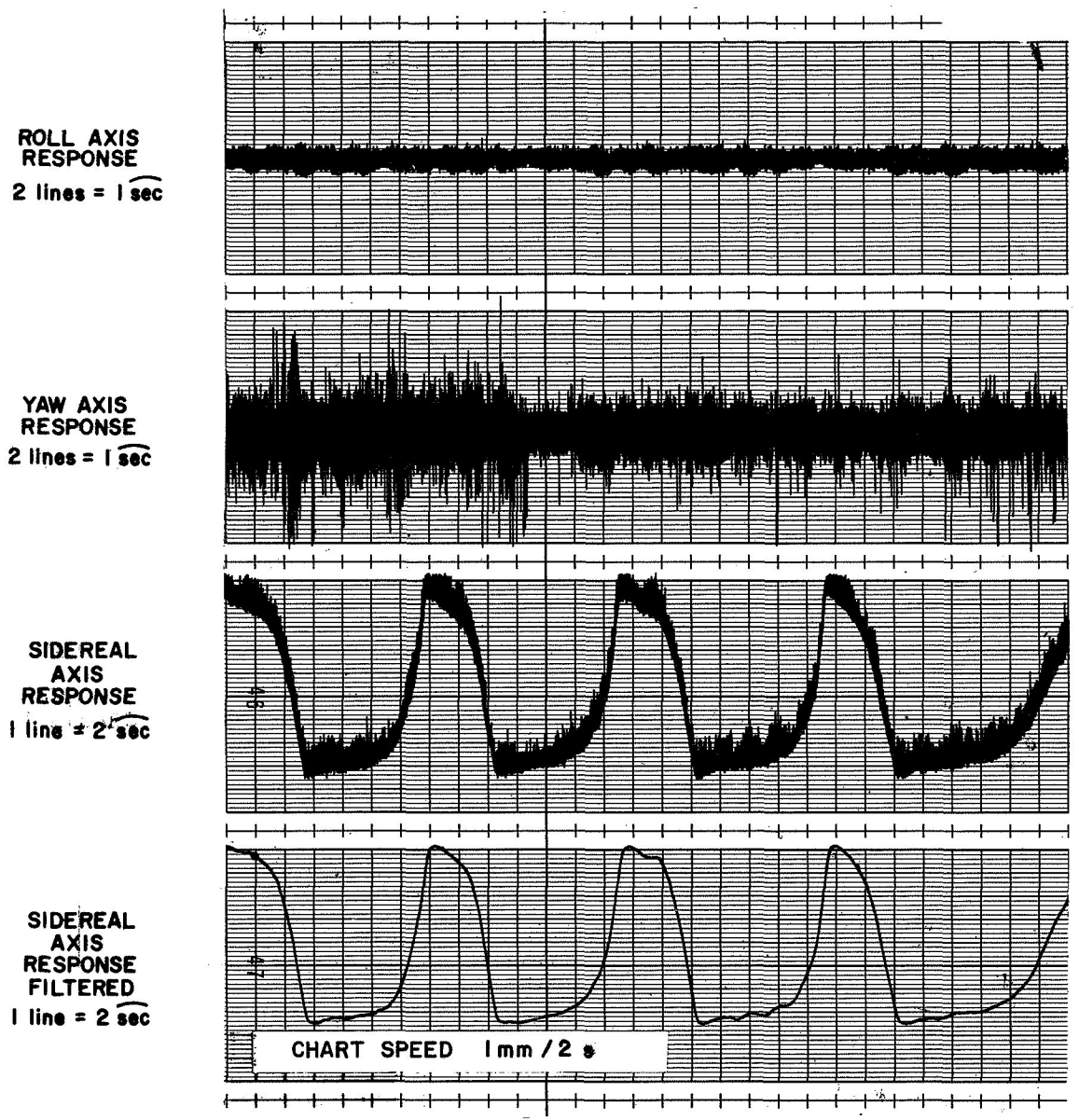

Figure 33. STAMP's gimbal responses to zero-signal input, digital mode, CMG case.

(Fig. 3), rather than teletype No. 1, the limit cycle did not occur. This indicates that the cause of the limit cycle originates in the Sigma-V data link combination.

When the results from all the foregoing tests are compared to Test No. 111 [2], the STAMP overshoot meets the expected results in 15 out of 18 tests and the actual rise time is 20 to 40 times greater than expected. The expected linearity of the response was achieved for all test cases.

Dynamic Position and Rate Accuracies

The objective of the STAMP's servoactuator system is to move or position the load platform so as to faithfully represent the motion of the Skylab spacecraft. An indication of this motion is obtained from the gimbal tachometers, potentiometers, and inductosyns. The tachometers provide rate information while the potentiometers and inductosyns provide analog and digital position information, respectively. Data were obtained on these instruments with and without the CMG's running.

The dynamic position accuracy is specified as 0.005 deg or better. For the sidereal axis potentiometer, this specification at or close to 0-deg gimbal position is not met. The test configuration was as shown in Figure 2 with a sinusoidal rate input signal of 0.10-deg/s peak at 0.01 Hz and a resulting position command signal of 0.288-deg peak. Figure 34 shows the potentiometer and inductosyn responses for the sidereal axis at 0-deg nominal, and Figure 35 shows the input signal and the potentiometer response with the sidereal axis at 1.8 deg. In Figure 34, the potentiometer response does not meet the specification but the inductosyn does; the error measured for the given conditions is 0.0065 deg for the inductosyn and 0.161 deg for the potentiometer. For the sidereal axis commanded about the 1.8-deg position, the potentiometer output (Fig. 35) has an error of 0.026 deg. If the response of the inductosyn of Figure 34 is compared with the response of the potentiometer of Figure 35, a common irregularity will be observed immediately after the peaks on the right side occur. This indicates the irregularity is caused by the gimbal system (bearings, actuator, etc.) rather than the individual instruments. The irregular response of the sidereal potentiometer could adversely affect the performance of the earth-rate drive at 0 deg. In the normal mode of operation, however, the position feedback signals utilized for control of all the STAMP's gimbals will be provided by the inductosyns.

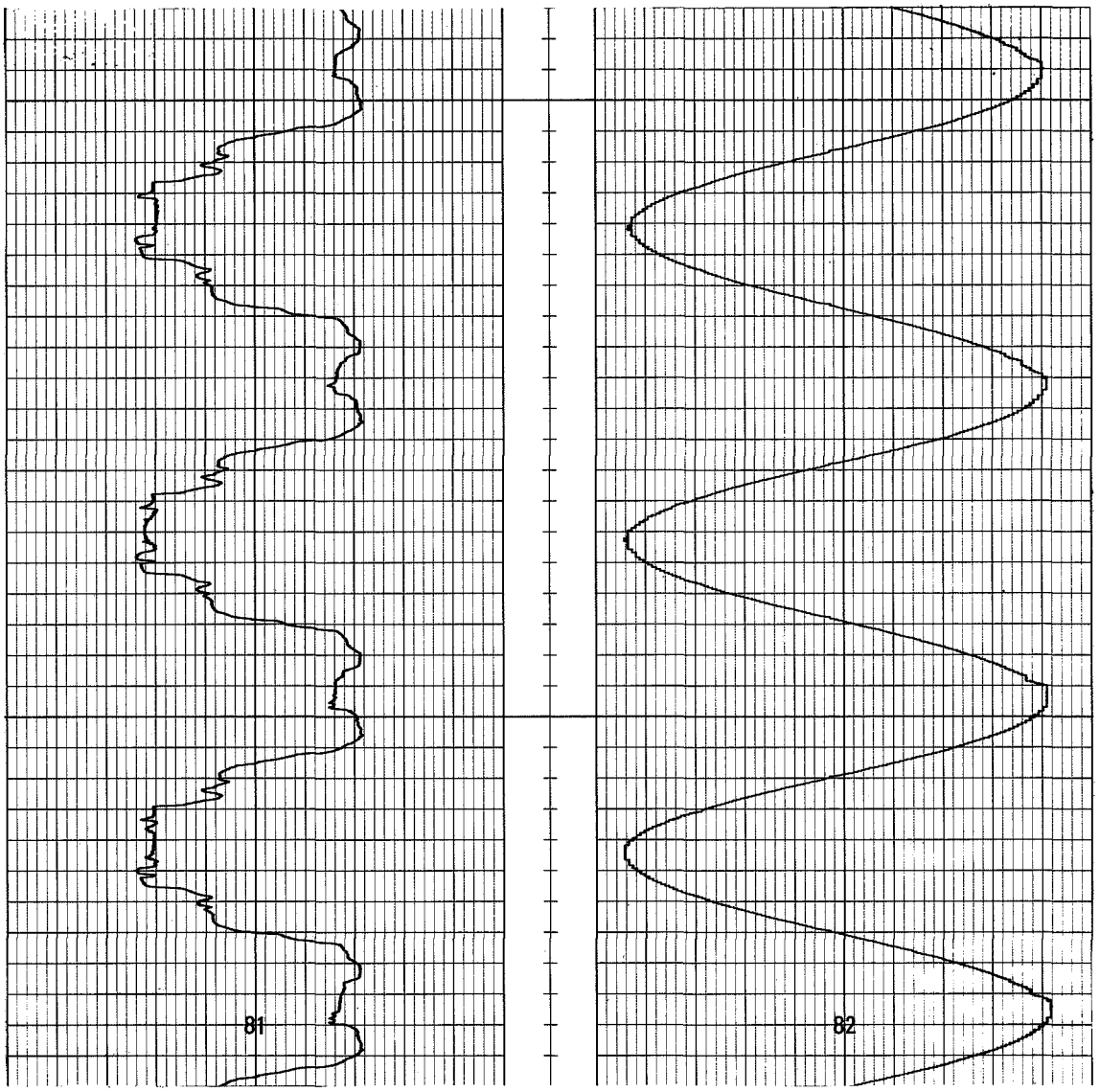

Figure 34. Sidereal-axis position responses at zero deg, analog-position mode, steel plate case.

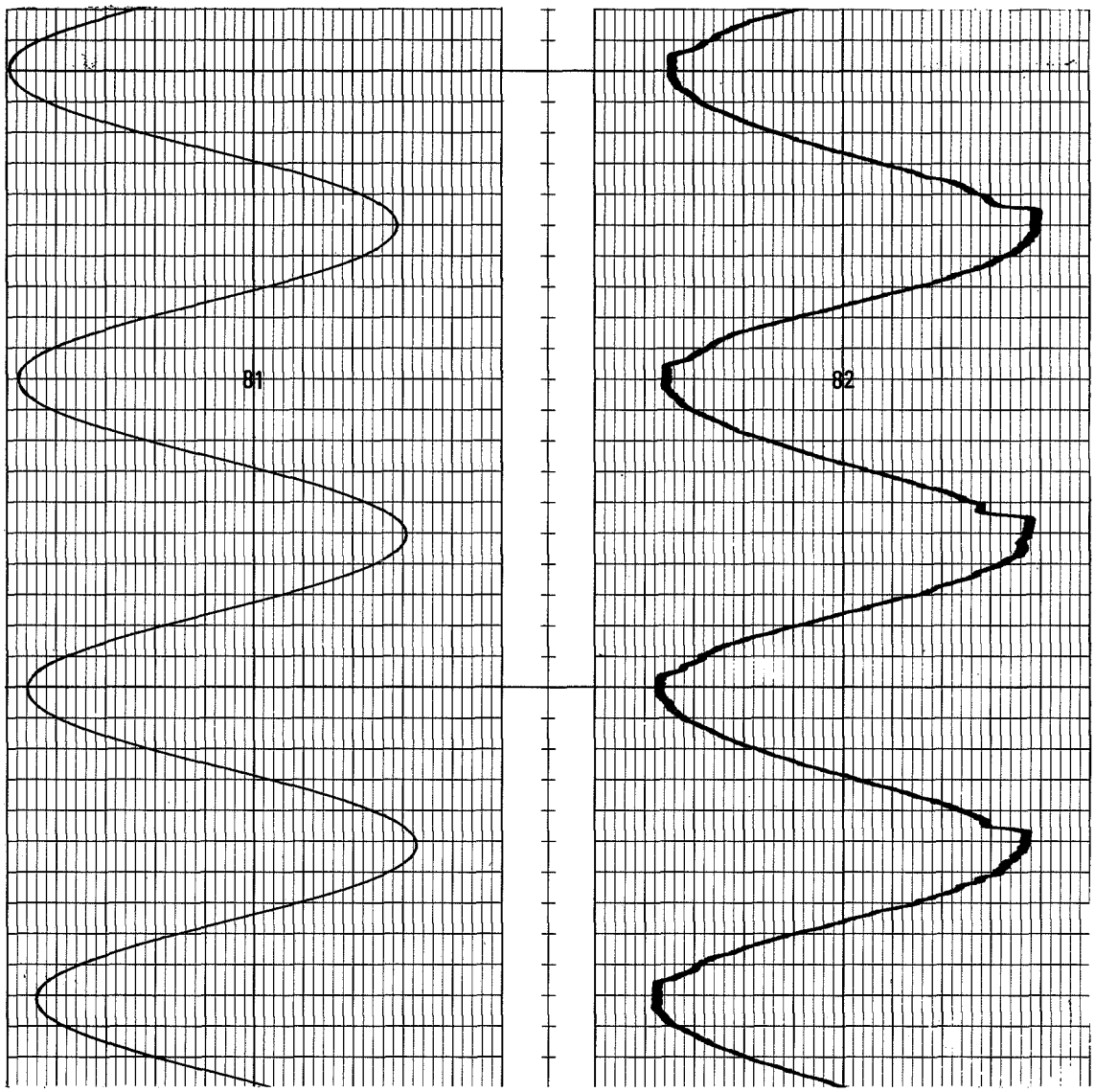

Figure 35. Sidereal-axis position response at 1.8 deg, analog-position mode, steel plate case.

The potentiometer and inductosyn responses for the yaw and roll axes are shown in Figures 36 and 37, respectively. The error in the inductosyn and potentiometer responses for both gimbals is less than 0.005 deg; a summary of the potentiometer and inductosyn errors is given in Table 7. All the position responses have a slight flattening on the peaks; this is the effect of the dead-zone nonlinearity of the STAMP system and is not attributed to the instrumentation.

At least two sets of data were taken on the tachometer for each axis; one set shows the tachometer response with the CMG's running and the other with the CMG's shut down. Rate smoothness or rate error is measured as shown in Figure 38.

The rate responses for the roll axis are shown in Figures 39 and 40, for the yaw axis in Figures 41 and 42, and for the sidereal axis in Figures 43, 44, 45, and 46. The maximum rate errors are given in Table 8 and it is evident that only the yaw gimbal tachometer without the CMG's running meets the required specification of 0.02 deg/s. The errors given in Table 8 are larger than the corresponding values given in Reference 1. One reason for these larger errors is that the contractor filtered the tachometer output signal with a second-order 12-Hz filter before recording the responses; this could easily account for the difference in the rate errors. All the rate responses exhibit a flat spot at the zero crossover point, which is characteristic of a dead-zone nonlinear system response.

In summary, the roll and yaw axes potentiometers and inductosyns meet the specifications while the sidereal axis potentiometer does not meet the specifications. The sidereal axis inductosyn came very close to meeting the specification and will probably be satisfactory. The yaw axis tachometer meets the specification without the CMG's running but does not with the CMG's running. The roll and sidereal tachometer errors exceed the specification by a considerable amount and the maximum errors are due to the dead-zone nonlinear characteristic of the STAMP. No special effort was made to obtain worst-case results in any of these tests.

Stiffness Test

A position servosystem's stiffness is a measure of the system's capability to resist movement resulting from disturbance torques. The STAMP's specifications call for a servosystem stiffness of 6.77×10^4 N-m/deg or higher for each axis. The technique described in Reference 1 for measuring

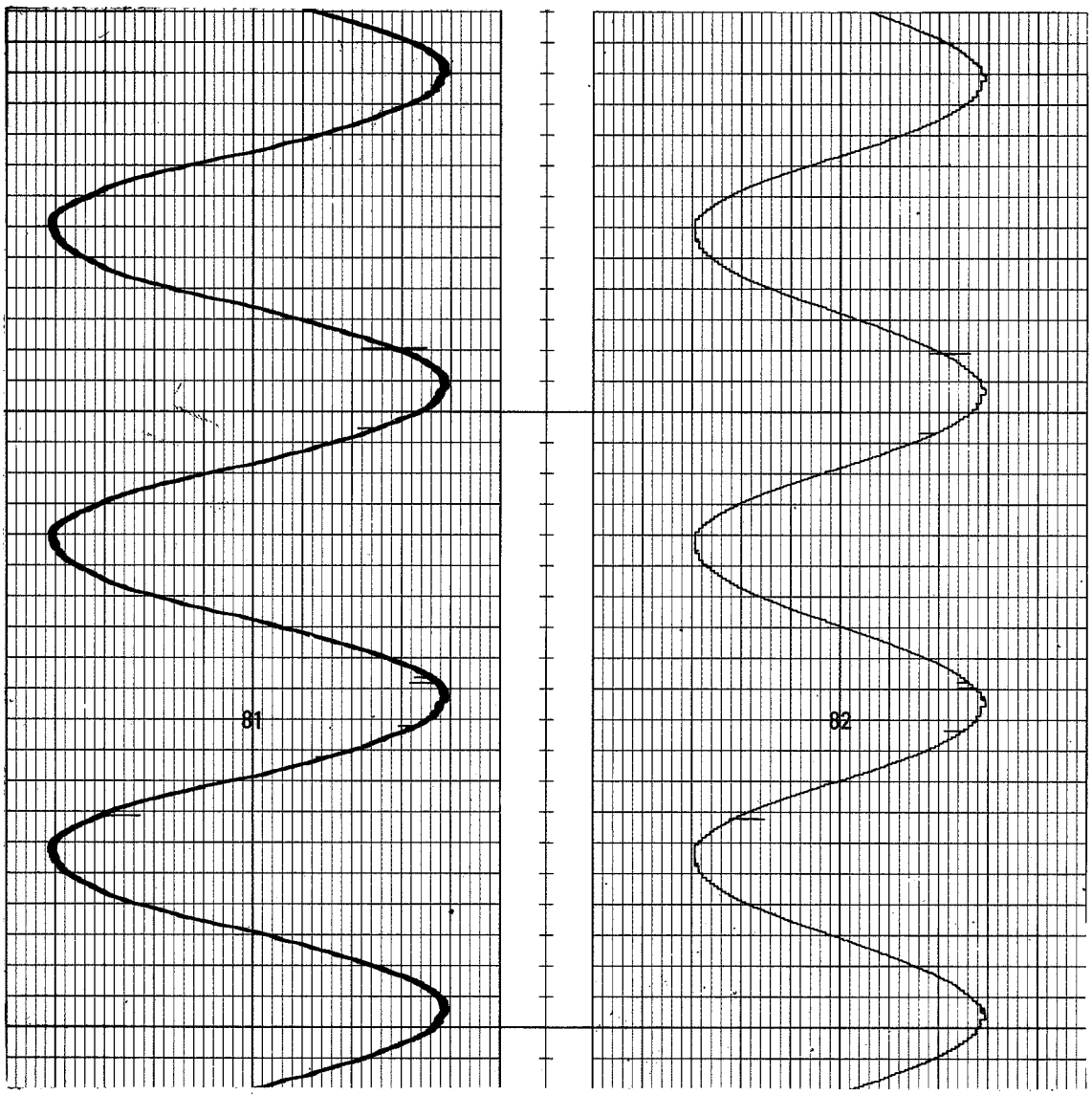

Figure 36. Yaw-axis position responses at zero deg, analog-position mode, steel plate case.

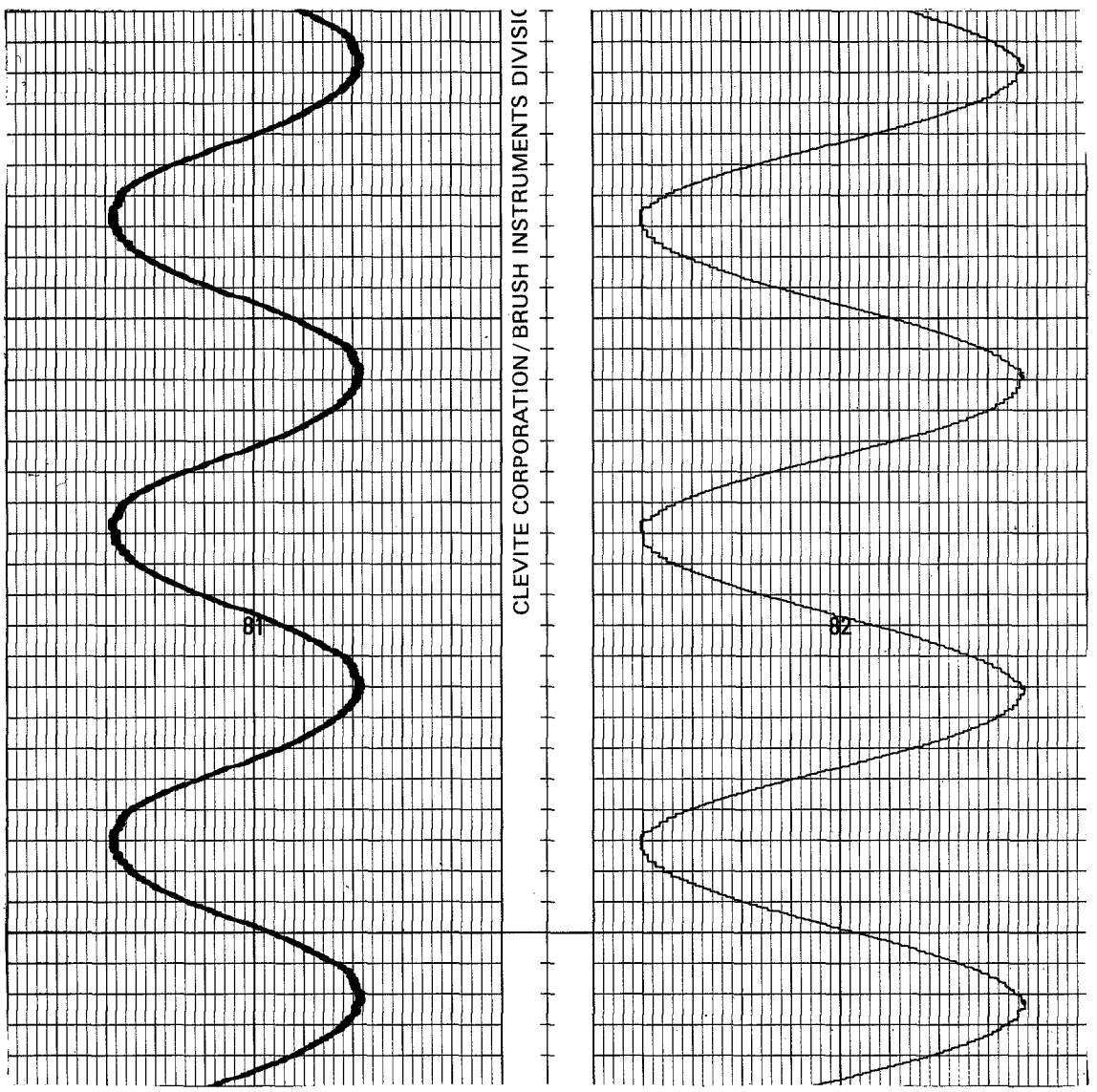

Figure 37. Roll-axis position responses at zero deg, analog-position mode, steel plate case.

TABLE 7. DYNAMIC POSITION ACCURACY FOR STAMP'S POTENTIOMETERS AND INDUCTOSYNS[a]

Axis (deg)	Sinusoidal Command at 0.01 Hz (deg/s-peak)	Response Error (deg)	
		Potentiometer	Inductosyn
Roll -0	0.10	0.005	0.0044
Yaw -0	0.10	0.005	0.0044
Sidereal -0	0.10	0.161	0.0065
-1.8	0.10	0.026	0.0065

a. Specification < 0.005 deg

TABLE 8. DYNAMIC RATE ACCURACY FOR STAMP'S TACHOMETERS[a]

Axis	Sinusoidal Command at 0.1 Hz (deg/s-peak to peak)	Maximum Rate Perturbation (deg/s-peak)	
		CMG's Not Running	CMG's Running
Roll	0.15	0.075	0.04
Yaw	0.30	0.016	0.05
Sidereal	0.30	0.06	0.06
	0.60	0.11	0.25

a. Specification < 0.02 deg/s

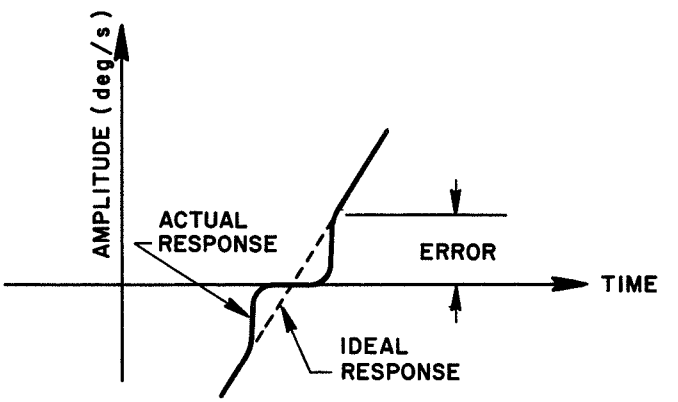

Figure 38. Measurement of rate smoothness.

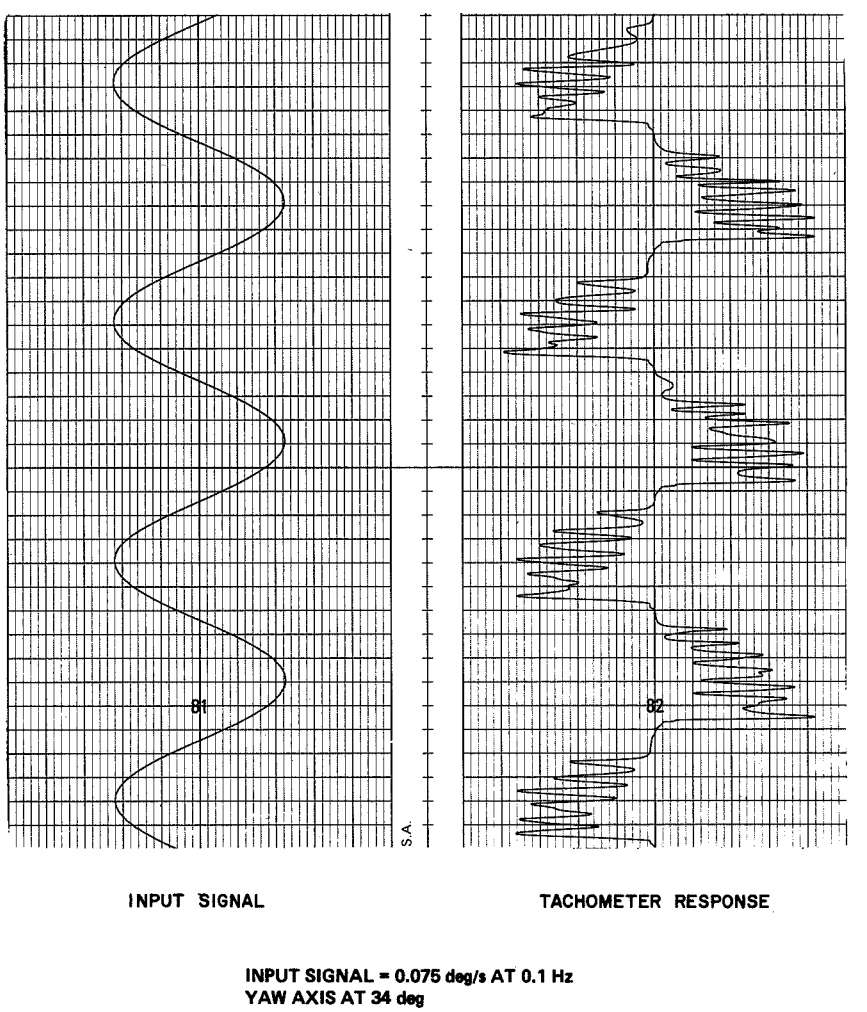

Figure 39. Roll-axis rate response, analog-position mode, steel plate case.

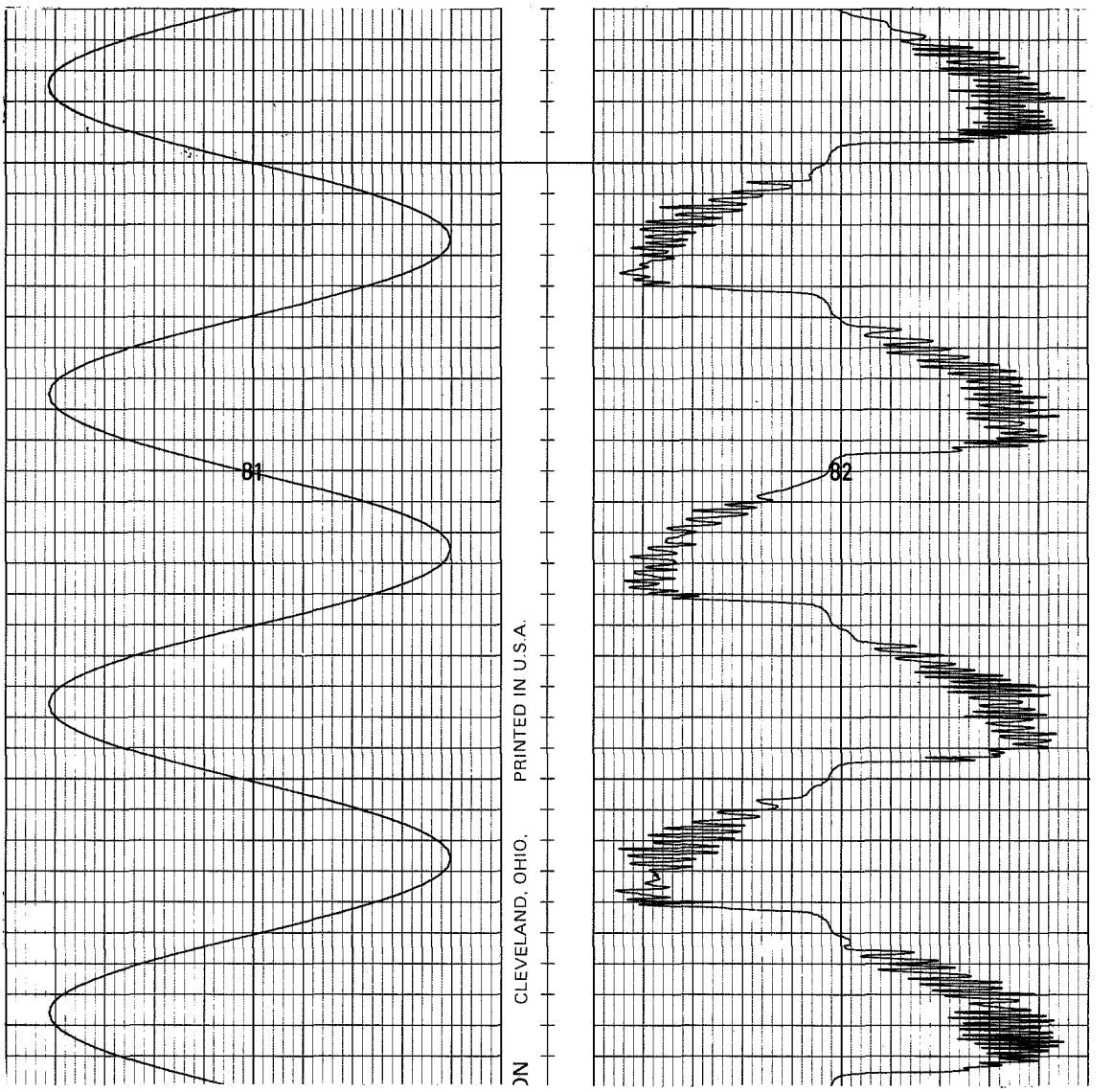

Figure 40. Roll-axis rate response, analog-position mode, CMG case.

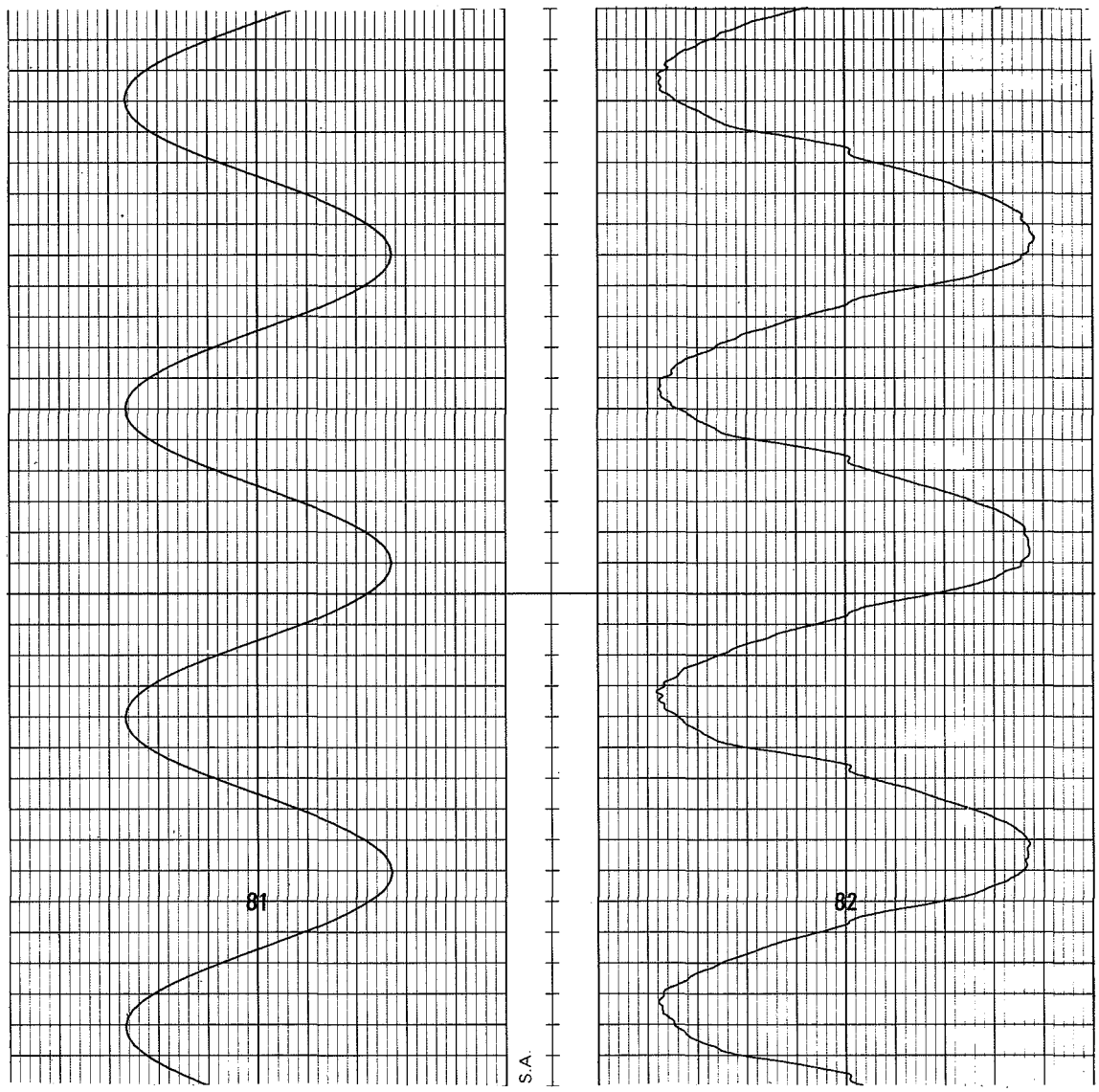

Figure 41. Yaw-axis rate response, analog-position mode, steel plate case.

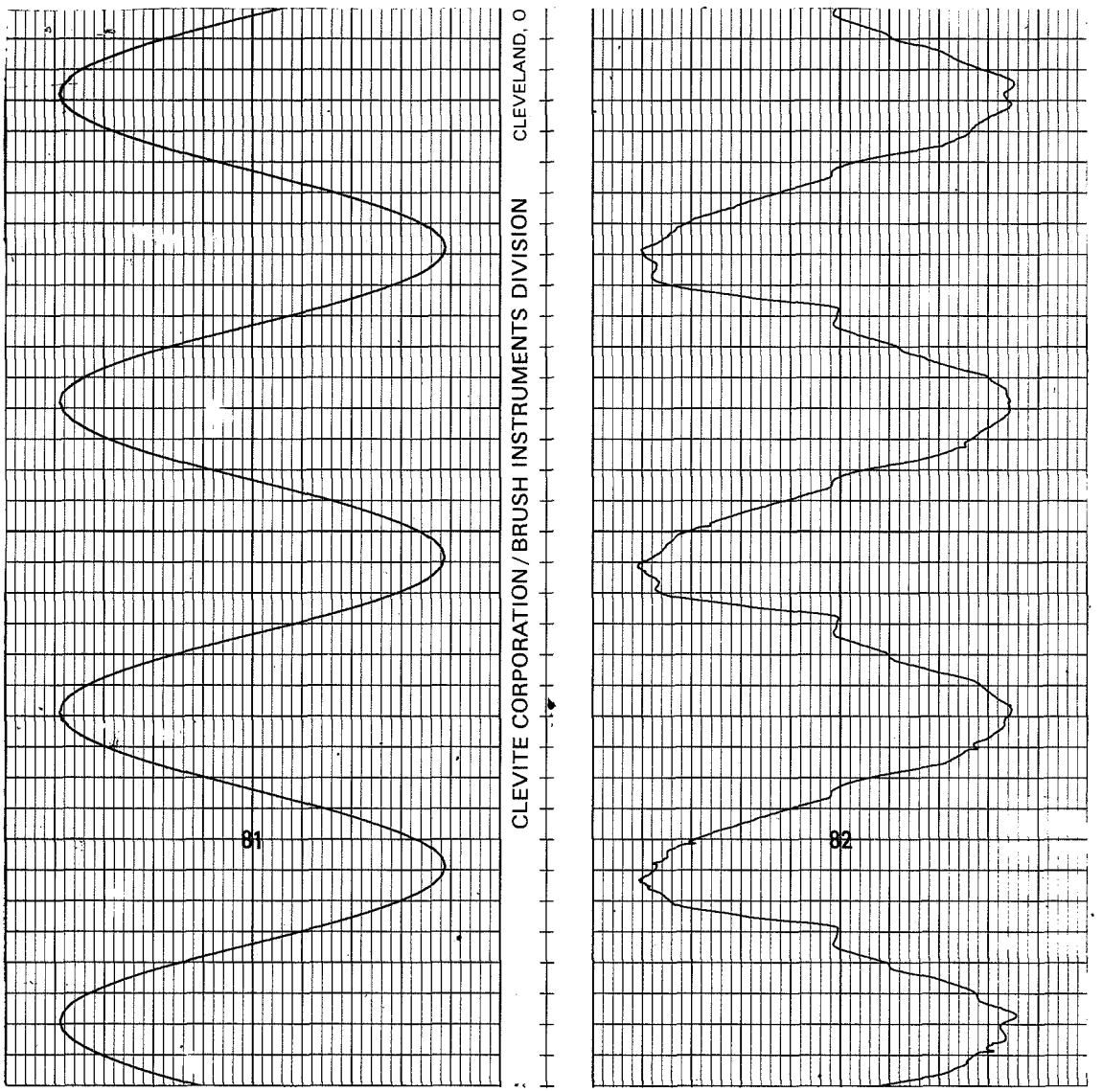

Figure 42. Yaw-axis rate response, analog-position mode, CMG case.

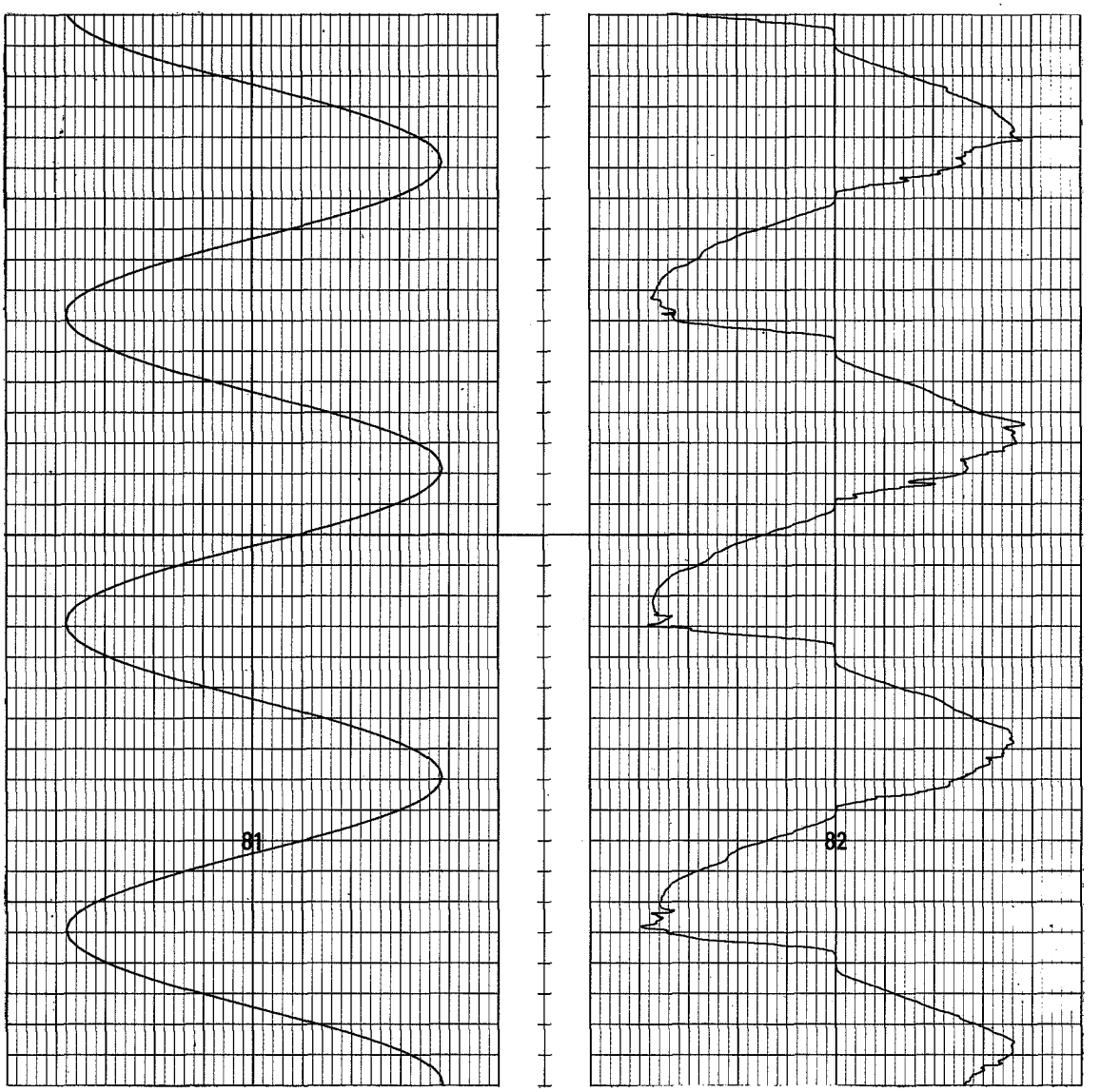

Figure 43. Sidereal-axis rate response, analog-position mode, steel plate case.

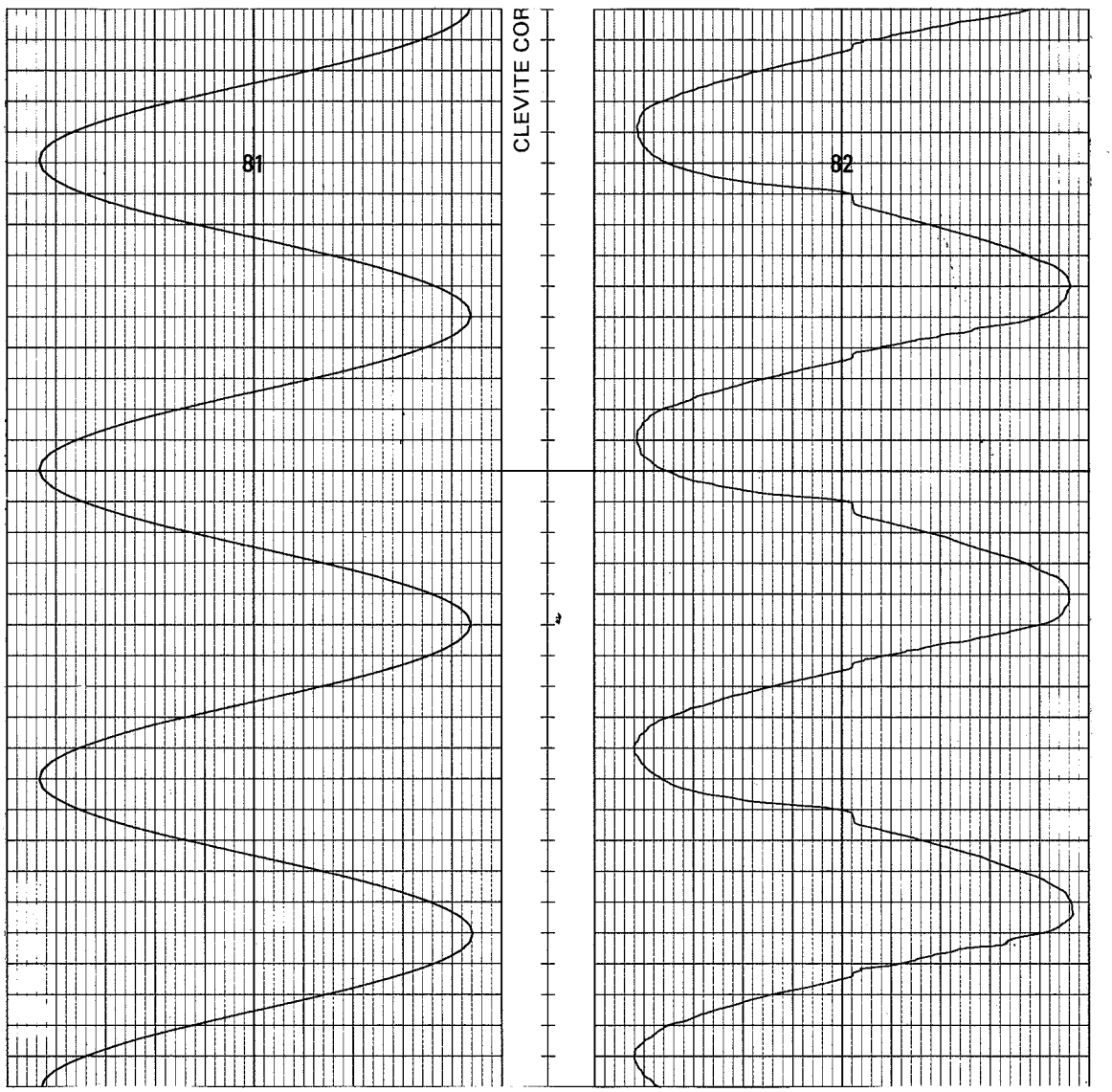

Figure 44. Sidereal-axis rate response, analog-position mode, steel plate case.

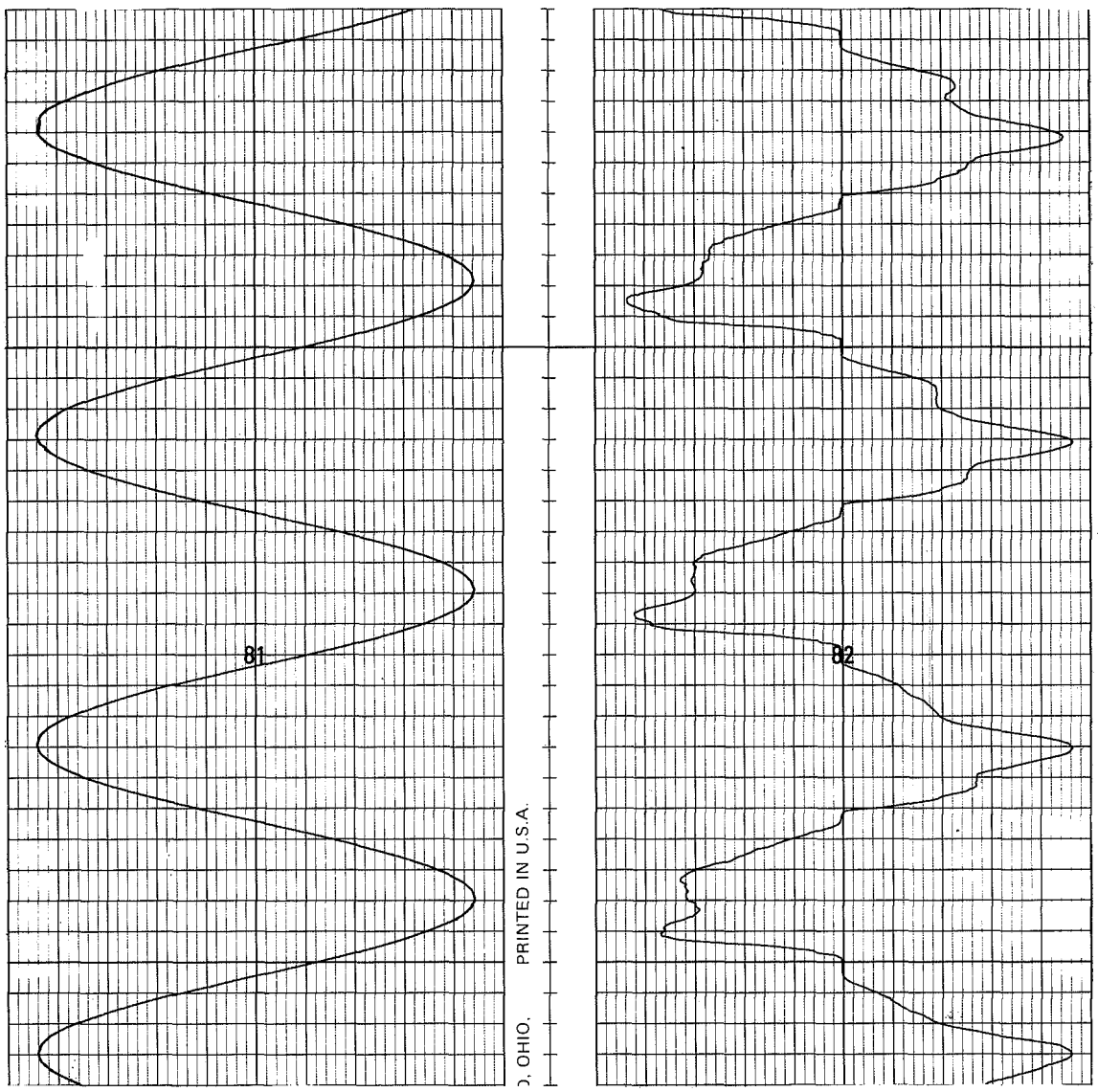

Figure 45. Sidereal-axis rate response, analog-position mode, CMG case.

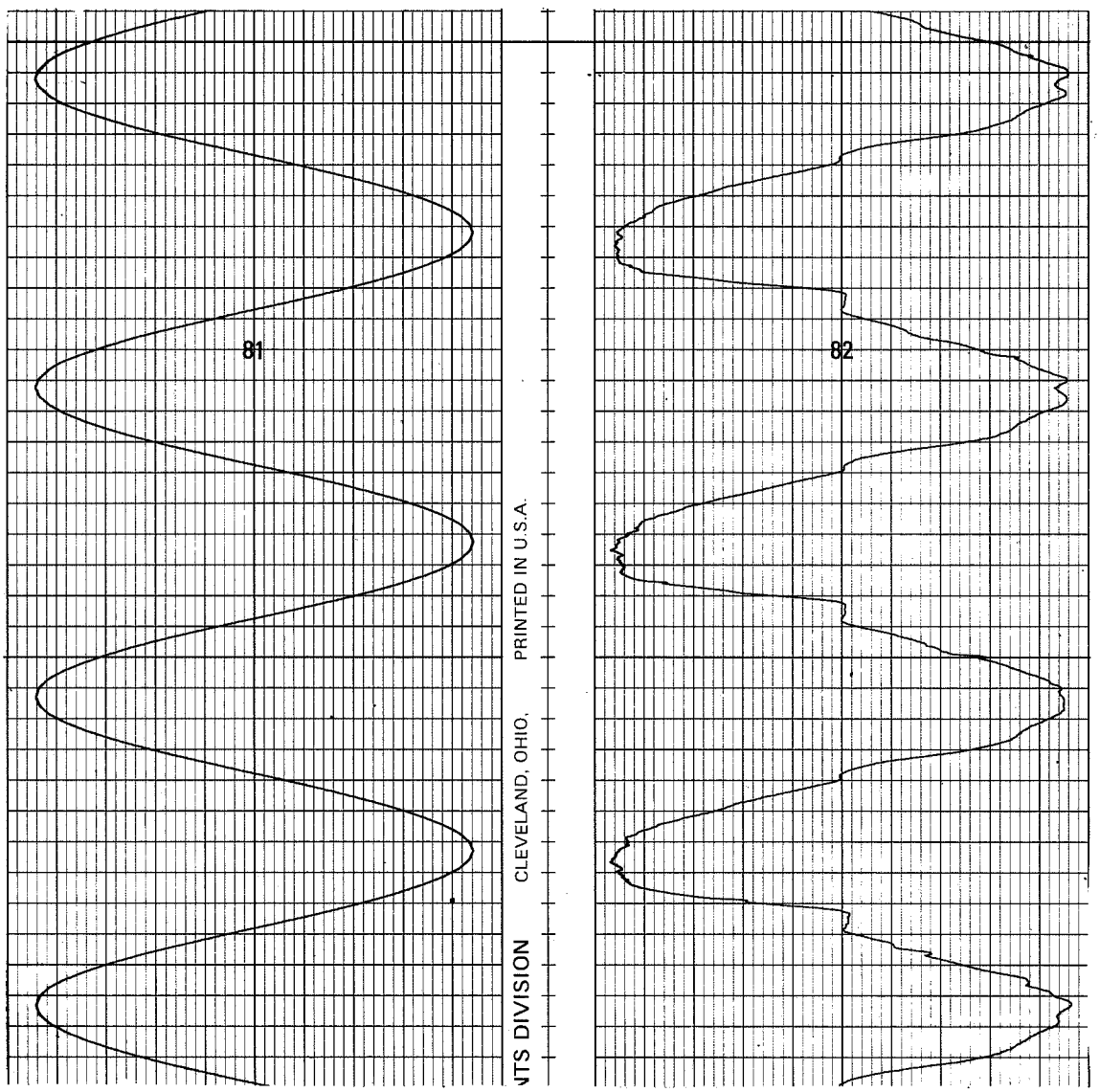

Figure 46. Sidereal-axis rate response, analog-position mode, CMG case.

the servosystem's stiffness results in a steady state value of stiffness; however, at MSFC, the stiffness tests were made dynamically.

Dynamic stiffness tests were conducted by applying both step and sinusoidal signals of various magnitudes and frequencies to individual gimbals of the CMG's mounted on the STAMP's platform or load plate. Since the reaction torques of the CMG's are known for specific inputs, as well as the CMG's orientation with respect to the STAMP's axes, the disturbance torques applied to a particular STAMP axis were also known or could be calculated. The orientation of the CMG's gimbals and the STAMP's axes is shown in Figure 47. With all the CMG and STAMP gimbals at nominally zero positions, a rate command to a given CMG gimbal results primarily in a torque about a specific STAMP gimbal. The relationships between the CMG and STAMP gimbals as determined from Figure 47 and the cross-product law are:

CMG Gimbal	STAMP Gimbal
X inner	Roll
X outer	Yaw
Y inner	Sidereal
Y outer	Roll
Z inner	Yaw
Z outer	Sidereal

The results of the stiffness tests are given in Tables 9, 10, 11, and 12. The shaded boxes are the input signals given in either magnitudes or frequencies; the other boxes are the measured responses. The rate response signals for the CMG's and STAMP's gimbals were impulses or spikes and not sustained rate errors. The deflection responses for the STAMP's gimbal were both trapezoidal- and triangular-shaped pulses of 1- to 5-s duration. The values given in the tables are the peak values for the maximum responses; i. e., the triangular-shaped responses. The trapezoidal-shaped responses resulted from the initial step disturbance and the triangular-shaped responses resulted from the return to zero step. The input step commands were 10- to 20-s duration or of sufficient time to allow the gimbal to return to its commanded zero position.

From the data of Tables 9, 10, 11, and 12, only the yaw-axis gimbal experienced any measurable deflection to either the step or sinusoidal disturbances. Note that the deflections are not proportional to the disturbance signals; the larger disturbance signals result in relatively large deflections. From Table 11 it is apparent that the deflections are also frequency dependent.

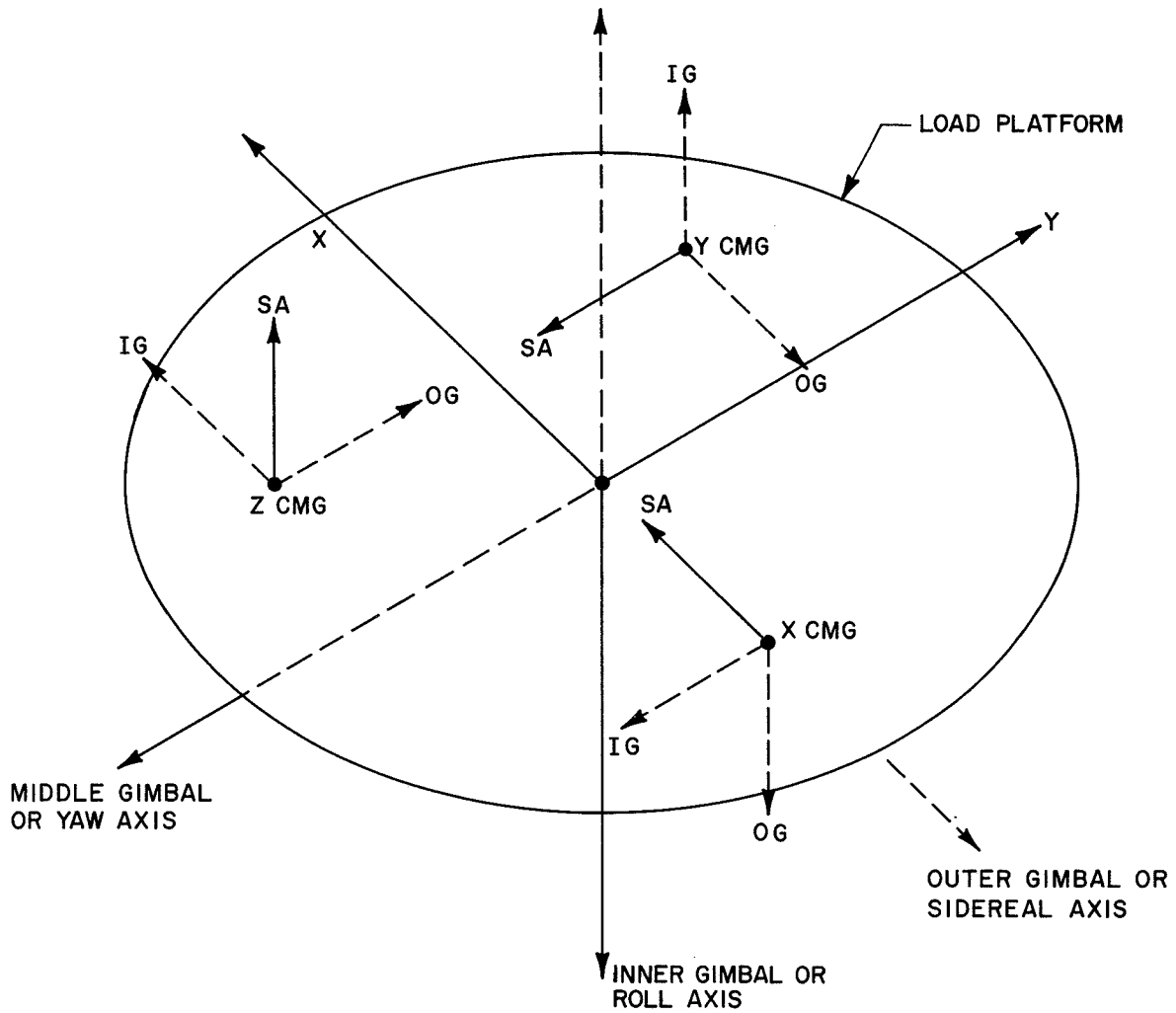

IG(j) SA(j) OG(j) CMG COORDINATE SYSTEM

IG - INNER GIMBAL AXIS
OG - OUTER GIMBAL AXIS
SA - SPIN AXIS

Figure 47. Coordinates for the STAMP and CMG's mounted on the load platform.

TABLE 9. MEASUREMENTS OF THE STAMP'S SERVOSYSTEM STIFFNESS — THE STAMP AND CMG RESPONSES TO STEP RATE COMMANDS APPLIED TO THE CMG SERVOS. INPUT SIGNAL AMPLITUDES ARE 3.5, 1.5, and 0.75 deg/s

CMG Gimbal Rate Response						STAMP Gimbal Response					
						Roll Axis		Yaw Axis		Sidereal Axis	
INPUT → X_{IG} (deg/s)	X_{OG} (deg/s)	Y_{IG} (deg/s)	Y_{OG} (deg/s)	Z_{IG} (deg/s)	Z_{OG} (deg/s)	Position (arc s)	Rate (deg/s)	Position (arc s)	Rate (deg/s)	Position (arc s)	Rate (deg/s)
3.5	0.8	0.002	0.002	0.02	0.024	–	–	10	0.1	–	–
1.5	0.3	–	–	0.01	0.008	–	–	–	–	–	–
0.75	0.2	–	–	0.002	0.003	–	–	–	–	–	–
1.1	**3.5**	–	–	0.008	0.004	–	–	90	0.16	–	–
0.5	**1.5**	–	–	0.001	–	–	–	12	0.066	–	–
0.25	**0.75**	–	–	–	–	–	–	–	0.033	–	–
–	0.002	**3.5**	0.85	0.002	0.002	–	0.009	–	–	–	0.022
–	–	**1.5**	0.25	–	–	–	0.003	–	0.013	–	0.01
–	–	**0.75**	0.12	–	–	–	0.007	–	0.01	–	0.01
–	–	1.1	**3.5**	0.002	0.001	–	0.0066	–	–	–	0.022
–	–	0.4	**1.5**	0.0005	–	–	0.004	–	–	–	0.01
–	–	0.15	**0.75**	–	–	–	–	–	–	–	0.006
–	0.01	–	–	**3.5**	1	–	–	72	0.165	–	0.01
–	–	–	–	**1.5**	0.4	–	–	18	0.03	–	–
–	–	–	–	**0.75**	0.2	–	–	–	0.01	–	–
0.01	0.02	0.002	0.001	1	**3.5**	–	–	–	0.066	–	0.01
0.002	0.008	–	–	0.4	**1.5**	–	–	–	0.03	–	–
–	0.002	–	–	0.2	**0.75**	–	–	–	–	–	–

TABLE 10. MEASUREMENTS OF THE STAMP'S SERVOSYSTEM STIFFNESS — THE STAMP AND CMG RESPONSES TO SINUSOIDAL RATE COMMANDS APPLIED TO THE CMG SERVOS. INPUT SIGNAL FREQUENCY IS 1 Hz.

INPUT ↓	CMG Gimbal Rate Response						STAMP Gimbal Response					
							Roll Axis		Yaw Axis		Sidereal Axis	
	X_{IG} (deg/s)	X_{OG} (deg/s)	Y_{IG} (deg/s)	Y_{OG} (deg/s)	Z_{IG} (deg/s)	Z_{OG} (deg/s)	Position (arc s)	Rate (deg/s)	Position (arc s)	Rate (deg/s)	Position (arc s)	Rate (deg/s)
	5.	1	–	–	0.085	0.02	–	–	220	0.266	–	–
	2.5	0.8	–	–	–	–	–	–	–	0.02	–	–
	1.45	0.2	–	–	–	–	–	–	–	–	–	–
	1.1	4.8	–	–	0.195	0.01	–	–	360	0.63	–	–
	0.4	2.5	–	–	0.095	0.085	–	–	250	0.40	–	–
	0.2	1.4	–	–	–	–	–	–	20	0.02	–	–
	–	–	5	1	–	–	–	0.003	–	0.01	–	0.03
	–	–	2.5	0.35	–	–	–	–	–	–	–	–
	–	–	1.5	0.15	–	–	–	–	–	–	–	–
	–	–	1	5	–	–	–	–	–	0.007	–	0.01
	–	–	0.4	2.5	–	–	–	–	–	0.007	–	0.003
	–	–	0.2	1.4	–	–	–	–	–	–	–	0.006
	0.09	0.21	–	–	5	1.2	–	–	360	0.66	–	0.006
	0.06	0.14	–	–	2.6	0.4	–	–	250	0.4	–	0.006
	–	0.004	–	–	1.5	0.2	–	–	10	0.03	–	–
	–	0.015	0.004	–	1.2	5	–	–	40	0.16	–	0.033
	–	0.004	–	–	0.4	2.6	–	–	18	0.02	–	–
	–	–	–	–	0.2	1.4	–	–	–	–	–	–

TABLE 11. MEASUREMENTS OF THE STAMP'S SERVOSYSTEM STIFFNESS — THE STAMP AND CMG RESPONSES TO SINUSOIDAL RATE COMMANDS APPLIED TO THE CMG SERVOS. INPUT SIGNAL AMPLITUDE OF 3.5 deg/s PEAK AT 1, 0.1, AND 0.01 Hz.

INPUT	CMG Gimbal Rate Response						STAMP Gimbal Response					
							Roll Axis		Yaw Axis		Sidereal Axis	
X_{IG}	X_{OG}	Y_{IG}	Y_{OG}	Z_{IG}	Z_{OG}	Position (arc s)	Rate (deg/s)	Position (arc s)	Rate (deg/s)	Position (arc s)	Rate (deg/s)
1.0 Hz 0.1 Hz 0.01 Hz	0.6 deg/s 0.05 deg/s 0.02 deg/s	– – –	– – –	– – –	– – –	– – –	– – –	– – –	– – –	– – –	0.01 – –
0.06 deg/s 0.06 deg/s 0.02 deg/s	1 Hz 0.1 Hz 0.01 Hz	– – –	– – –	0.01 deg/s 0.01 deg/s –	– – –	– – –	– – –	36 108 18	0.08 0.13 –	– – –	– – –
– – –	– – –	1 Hz 0.1 Hz 0.01 Hz	0.5 deg/s 0.04 deg/s 0.02 deg/s	– – –	– – –	– – –	– 0.007 –	– – 10	– – 0.01	– – –	– – –
– – –	– – 0.003 deg/s	0.6 deg/s 0.05 deg/s 0.02 deg/s	1 Hz 0.1 Hz 0.01 Hz	– – –	– – 0.004 deg/s	– – –	– – –	– – 18	– – 0.03	– – –	– – –
– – –	0.01 deg/s 0.026 deg/s 0.003 deg/s	– – –	– – 0.006 deg/s	1 Hz 0.1 Hz 0.01 Hz	0.5 deg/s 0.05 deg/s 0.02 deg/s	– – –	– – –	50 120 –	0.16 0.16 –	– – –	– – –
– – –	0.01 deg/s – 0.006 deg/s	– – –	– – 0.006 deg/s	0.6 deg/s 0.06 deg/s 0.02 deg/s	1 Hz 0.1 Hz 0.01 Hz	– – –	– – –	– – –	– – –	– – –	– – –

TABLE 12. MEASUREMENTS OF THE STAMP'S SERVOSYSTEM STIFFNESS — THE STAMP AND CMG RESPONSES TO SINUSOIDAL RATE COMMAND APPLIED TO THE CMG SERVOS. INPUT SIGNAL FREQUENCY IS 3.5 Hz.

CMG Gimbal Rate Response						STAMP Gimbal Response					
						Roll Axis		Yaw Axis		Sidereal Axis	
INPUT → X_{IG} (deg/s)	X_{OG} (deg/s)	Y_{IG} (deg/s)	Y_{OG} (deg/s)	Z_{IG} (deg/s)	Z_{OG} (deg/s)	Position (arc s)	Rate (deg/s)	Position (arc s)	Rate (deg/s)	Position (arc s)	Rate (deg/s)
3.8	1.4	-	-	0.11	0.075	-	-	18	0.173	-	-
1.8	1.1	-	-	0.1	0.065	-	-	18	0.16	-	-
1.1	0.6	-	-	0.022	0.003	-	-	10	0.113	-	-
2	3.2	-	-	0.115	0.09	-	-	25	0.2	-	-
1.5	1.7	-	-	0.1	0.04	-	-	22	0.165	-	-
0.78	1.1	-	-	0.03	0.013	-	-	18	0.105	-	-
-	0.002	3.4	1.6	-	0.004	-	-	-	0.01	-	0.06
-	-	1.2	1.2	-	0.004	-	-	-	0.007	-	0.01
-	-	0.8	0.6	-	0.002	-	-	-	0.007	-	0.01
-	0.003	2.0	2.6	-	0.006	-	-	-	0.02	-	0.03
-	-	1.4	1.15	-	0.002	-	-	-	0.01	-	0.02
-	-	0.7	0.50	-	0.002	-	-	-	0.007	-	0.01
0.055	0.12	0.004	-	3.2	1.6	-	-	30	0.2	-	0.023
0.04	0.13	0.002	0.002	1.6	1.3	-	-	30	0.165	-	0.01
0.02	0.07	-	-	1.1	0.6	-	-	18	0.133	-	0.006
0.05	0.125	-	-	1.6	3.2	-	-	40	0.2	-	0.01
0.05	0.105	-	-	1.5	1.6	-	-	18	0.2	-	0.01
0.02	0.070	-	-	0.75	1	-	-	18	0.13	-	0.006

The stiffness of the STAMP's yaw axis for a 3.5 deg/s step command to the X-CMG outer gimbal, which corresponds to 162 N-m of torque, is

$$\text{stiffness} = \frac{\text{applied torque}}{\text{deflection}}$$

$$= \frac{162 \text{ N-m}}{90 \text{ arc s}}$$

$$= 6500 \text{ N-m/deg.}$$

For a 5 deg/s sinusoidal command, at 1 Hz, applied to the inner gimbal of the Z-CMG, the STAMP's yaw gimbal has a stiffness of

$$\text{stiffness} = \frac{231 \text{ N-m}}{360 \text{ arc s}}$$

$$= 2310 \text{ N-m/deg.}$$

The specification of stiffness is 6.77×10^4 N-m/deg or more for each axis. The above results for the yaw axis are approximately 30 times below the specified value. This softness of the yaw axis is not a newly discovered deficiency; it has been observed since the equipment's initial operation. Since the sidereal- and roll-axis deflections were below the sensitivity of the instrumentation employed in this test, their stiffness is well above the required specification. The yaw-axis servosystem's softness may be due to more than a single deficient component. Additional testing will be required to identify the causes for this softness.

Gimbal Friction

The design values of running friction and breakaway friction or stiction as given in Reference 5 are:

Gimbal	Friction (N-m)	Stiction (N-m)
Roll	678	678
Yaw	112	112
Sidereal	226	226

Since friction and stiction are nonlinear phenomena and could, if excessive, detract from the desired performance of the STAMP, it was decided to check at least one gimbal to see how it compared to the design values. Because the roll gimbal has the largest values of friction and stiction, it was selected for verification. To determine the stiction or breakaway friction, the roll gimbal was put in the rate mode, the potentiometer and tachometer feedback loops were opened, and a signal of slowly increasing magnitude was applied to the input. This procedure was followed for about 30 runs with both positive and negative input voltages to determine the values for each direction of rotation of the gimbal. The resulting torques were calculated and averaged. To check the calculated values of friction and stiction, a dynometer was used to measure the two forces. Approximately 20 readings were taken for turning the gimbal in each direction and then the average of the readings was used to compute the friction and stiction. The readings obtained with the dynometer were taken with the hydraulic system off and with (1) the hydraulic fluid in the motors and (2) the hydraulic fluid pumped out of the motors. The results are summarized as follows:

Condition	Stiction (N-m)	Friction (N-m)
Design	± 678	± 678
Computed	+ 610, - 316	+ 665, - 640
Dynometer (1)	+ 309	+ 646
Dynometer (2)	+ 149, - 156	+ 610, - 644

The plus sign is for clockwise rotation of the gimbal as viewed from above and the minus sign is for counterclockwise rotation. The values of stiction vary considerably, but the values of the friction are very consistent and have good correspondence to the design values. In the STAMP operation, the importance of stiction is minimal because the noise in the hydraulic control system will act as a dither signal, effectively negating the stiction effect. In the mathematical model of the STAMP, the design values of friction will be used and stiction will not be included.

Parameter Sensitivity Test

The frequency response tests for low-amplitude input signals indicated that a broader bandwidth for the STAMP would be desirable. In a linear system, the closed-loop poles of a system can be varied by adjusting the open-loop gain and thereby changing the system's bandwidth. A linear root

locus analysis of the STAMP servocontrol system, such as the one presented in Reference 6 for the linearized system shown in Figure 48, could not be applied because the STAMP is a complex nonlinear system.

To determine the effect that parameters K_P, K_R, K_A, and L_D (Fig. 48) have on the system's dynamic range, a series of tests were run with different values of these parameters. Since there is a similarity in the nonlinearities in the STAMP's axes, it was decided to investigate only the yaw axis. The test results of an input sinusoidal command signal of 0.01 deg/s are given in Table 13 in terms of the amplitude of the resonant peak, M_P, and the frequency of the resonant peak, ω_d. The bandwidth for these cases would be slightly larger than the frequency, ω_d. As given in Table 13, the frequency of the resonant peak, ω_d, did not vary appreciably with a rather wide range of parameter values. In an experimental optimization procedure, smaller parameter values would have been incremented, but the objective in this investigation was to determine the range available by parameter adjustment. Larger variations occurred in the resonant peaks than in the bandwidths; however, the most significant conclusion that can be drawn from the results of Table 13 is that the sensitivity of the STAMP to parameter variations, i.e., component aging, etc., is low.

DISCUSSION

The test results presented here provide a good indication of the STAMP's capabilities. The frequency response plots give the dynamic characteristics of the system for a relatively wide range of input signal magnitudes, thereby permitting an experimenter to determine if the STAMP will be responsive to his expected input signals. As noted in the frequency response section, responses below 0.002 deg/s (7.2 arc s/s) input for the steel plate case and 0.005 deg/s (18 arc s/s) input for the CMG case were not run because the results from the Boonshaft analyzer were not consistent. This does not mean the STAMP response was inconsistent but that the command and response signals were too small (below 10 mV) for the Boonshaft to make an accurate analysis. As shown in the transient response data, the STAMP responds to much lower command signals. Frequency response data for command signals of 2.5 and 5 deg/s can be found in Reference 1. The operation of the STAMP has, therefore, been documented for command signals from 0.002 to 5 deg/s or for a 2500 to 1 operating range.

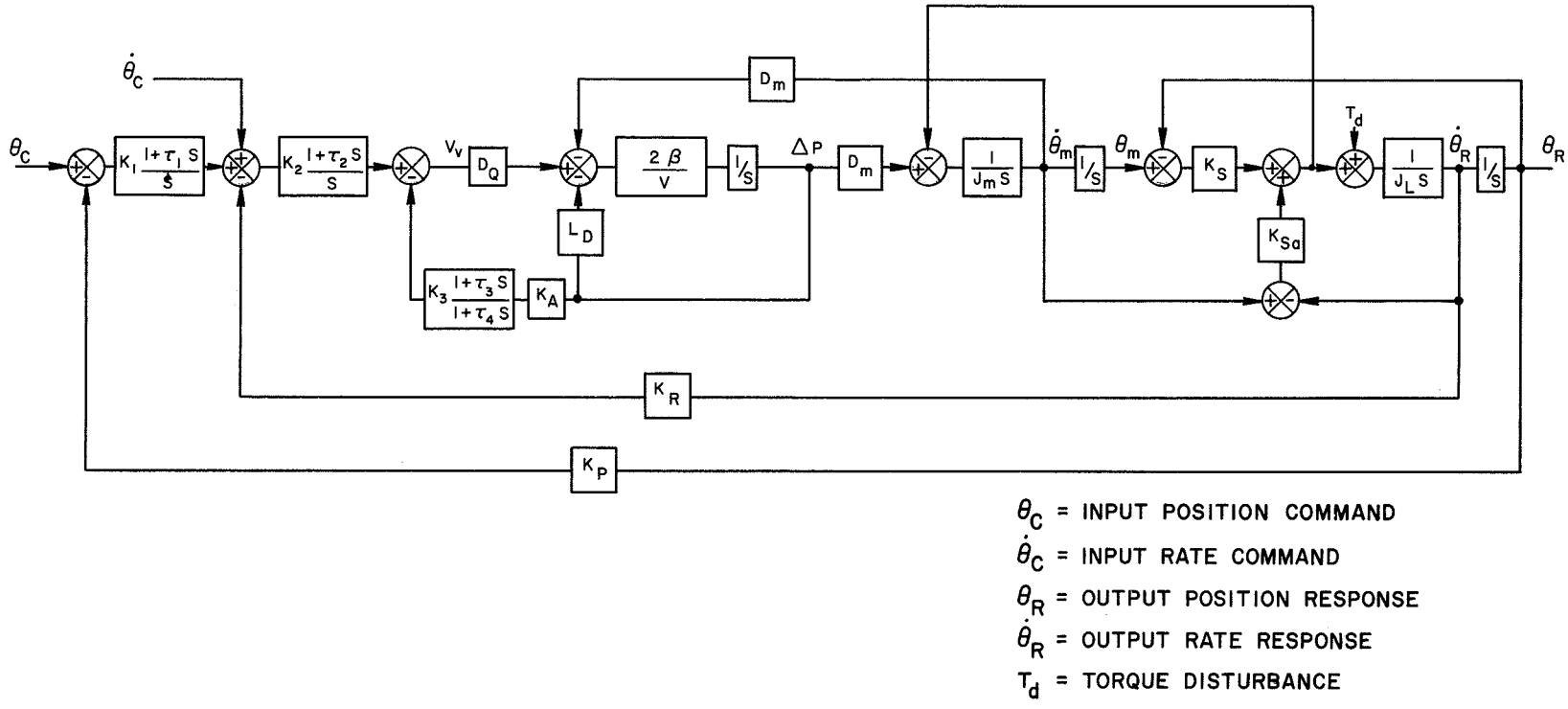

Figure 48. A single-axis block diagram of the STAMP's linearized equations of motion.

TABLE 13. PARAMETER SENSITIVITIES

Yaw-Axis Parameter	Gain	M_P (dB)	ω_d (Hz)
Position Feedback Gain - K_P	1.0	3.46	0.08
	0.5	1.52	0.10
Rate Feedback Gain - K_R	1.5	2.92	0.08
	1.0	3.46	0.08
	0.67	6.24	0.10
Δ Pressure Feedback Gain - K_A	2.0	2.68	0.08
	1.0	3.46	0.08
	0.5	5.26	0.08
Hydraulic Leakage[a] - L_D	0	3.46	0.08
	0.05	3.56	0.10
	0.5	3.36	0.08

a. Corresponds to turns of the bypass valve.

Several of the system's deficiencies are pinpointed, some of which may limit the uses to which the equipment can be applied; e.g., the system's limited bandwidth to small amplitude signals could restrict the investigation of the Skylab's CMG attitude control system responses to body bending and astronaut disturbances within the spacecraft. The foregoing conclusion is based on the results of these tests and the results of a zero-g aircraft crew-motion experiment.

The limit cycle that sporadically occurs in the sidereal axis (Fig. 33) could cause some difficulty when it is desired to maneuver the STAMP with low-level signals. The transient response data shown in Figures 27 through 32 and Tables 5 and 6 were taken during a period when the limit cycle was not present in the sidereal response. For large-angle maneuvers, such as 1 deg, the limit cycle would probably cause no difficulty.

The roll-axis tachometer gives an irregular response as shown in Figures 39 and 40. It may be possible to smooth the roll-axis response by installing hydraulic servomotors with integrally connected tachometers that provide a direct feedback signal to the servovalve. Reference 7 discusses a similar problem of irregular servosystem response and the solution to the problem using local tachometer feedback. This modification will present a design problem on selecting the proper tachometer signal to control the single servovalve. Figure 48 shows the present tachometer or rate signal closed around the entire servoloop, not just the servovalve; connecting tachometers to the individual servomotors will add another feedback loop.

The stiffness of the STAMP's yaw axis does not meet the design specifications but how will this affect the actual application of the system? In the limit cycle study [9], a step disturbance of 6.78 N-m, which is the expected peak gravity gradient torque, resulted in a periodic CMG torque output of 81 N-m peak in the vehicle Y axis. The resulting average vehicle deflection in the Y axis was 36 arc s, which is a worst-case situation. A disturbance torque of 81 N-m in the STAMP's yaw axis would result in a deflection of 15 to 20 arc s. However, in a more realistic situation where the gravity gradient torque is applied gradually, not as a large-step function, the resulting CMG torques and the yaw-axis deflection will be less. For a gravity gradient step disturbance of 0.678 N-m [8] in the vehicle X-axis, the resulting peak CMG torque was less than 10 N-m and the vehicle X-axis deflection was 20.6 arc s. In the STAMP's stiffness test, a torque of 10 N-m applied to the yaw axis did not result in any measurable deflection. Also, as mentioned earlier, the softness of the STAMP's yaw axis would not adversely affect studies involving wide-angle maneuvers. Therefore, the softness of the yaw axis, while certainly undesirable, does not appear to be a serious impediment to the utilization of the STAMP for many Skylab studies.

In summary, the STAMP's performance should be more than adequate for the Skylab's CMG attitude control system equipment checkout. It should also be capable of providing useful data for large-angle maneuvers, for verification of momentum desaturation schemes, and for studies involving relatively small-angle maneuvers. It will not be suitable for extremely small-angle maneuvers at relatively high frequencies because of its limited bandwidth for small command signals; but these will probably occur only in limited situations. Correction of the deficiencies mentioned in this report would improve the STAMP's performance, and some recommendations to achieve this objective are outlined.

One nonlinear characteristic of the STAMP has been identified and simulated. A simulation of the effect of the actuator dead zone on the gimbal velocity and position outputs is shown in Figure 49. The correspondence between the simulation and the actual equipment can be observed by comparing the tachometer response of Figure 49 with the tachometer response of Figure 41. A dead-zone nonlinearity is being incorporated into the analog computer simulation of the STAMP's servocontrol system.

RECOMMENDATIONS

The following actions can be taken to improve the performance of the STAMP:

1. Rework or replace the PC boards for the digital encoders for all axes.

2. Smooth the roll-axis tachometer response by installing hydraulic servomotors with integrally connected tachometers.

3. Eliminate the limit cycle that occurs sporadically in the sidereal position response. This will be difficult because of the intermittent nature of the disturbance. As indicated earlier, the source of the limit cycle appears to be in the data link and Sigma-V combination.

4. Stiffen the yaw axis to torque disturbances. This will be the most difficult action to accomplish. A suggestion has been made to counteract the disturbance torque by feeding forward into the hydraulic servosystem a signal, which is the measured value of the disturbance torque, taken from the TMF's. With a properly shaped TMF output signal, the hydraulic servosystem would receive a boost signal to maintain the desired platform orientation.

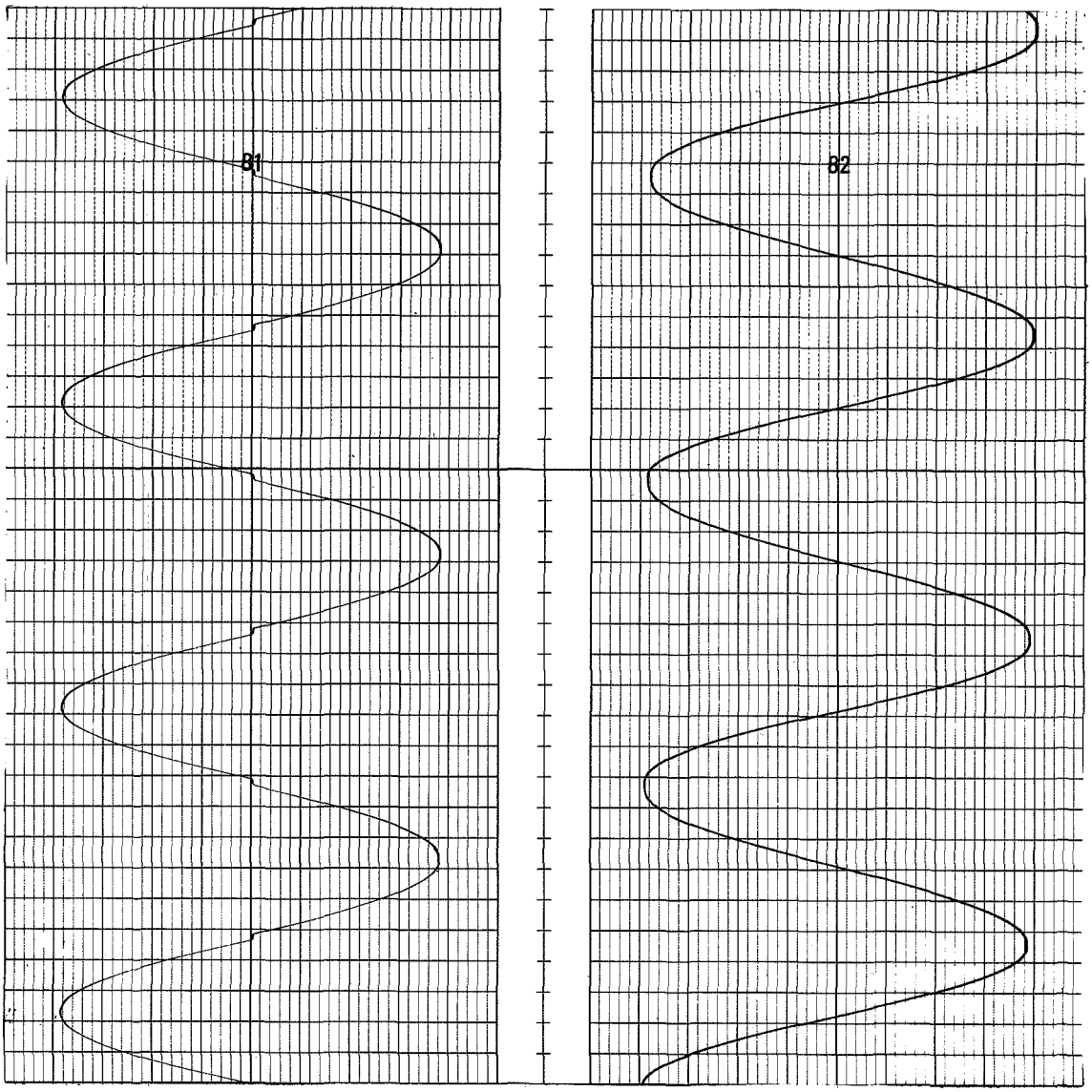

Figure 49. A simulation of nonlinear responses of the STAMP's tachometers and potentiometers.

APPENDIX A. PHYSICAL CHARACTERISTICS OF THE STAMP

Maximum Load:	3175 kg
Position Range:	
Roll	± 180 deg
Yaw	± 90 deg
Sidereal	± 45 deg
Position Accuracy:	
Roll - maximum error	- 3.2 arc s
Yaw - maximum error	- 2.9 arc s
Sidereal - maximum error	- 3.5 arc s
Command Signal Threshold:	0.01 deg/hr
Servosystem Drift Rate:	1.8 arc s
Rate Range:	
Rate trip relays are set at 15 deg/s	
Instrumentation:	
Tachometer resolution	0.036 arc s/s
Potentiometer resolution	3 arc s
Inductosyn resolution	0.333 arc s
Tachometer Output:	
Roll	154 mV/deg/s
Yaw	152 mV/deg/s
Sidereal	86 mV/deg/s

Potentiometer Output:	
Roll	50 mV/deg
Yaw	100 mV/deg
Sidereal	100 mV/deg
Hydraulic Supply Pressure	103.4 bars gage

APPENDIX B. FREQUENCY RESPONSES FOR THE ROLL AND SIDEREAL AXES

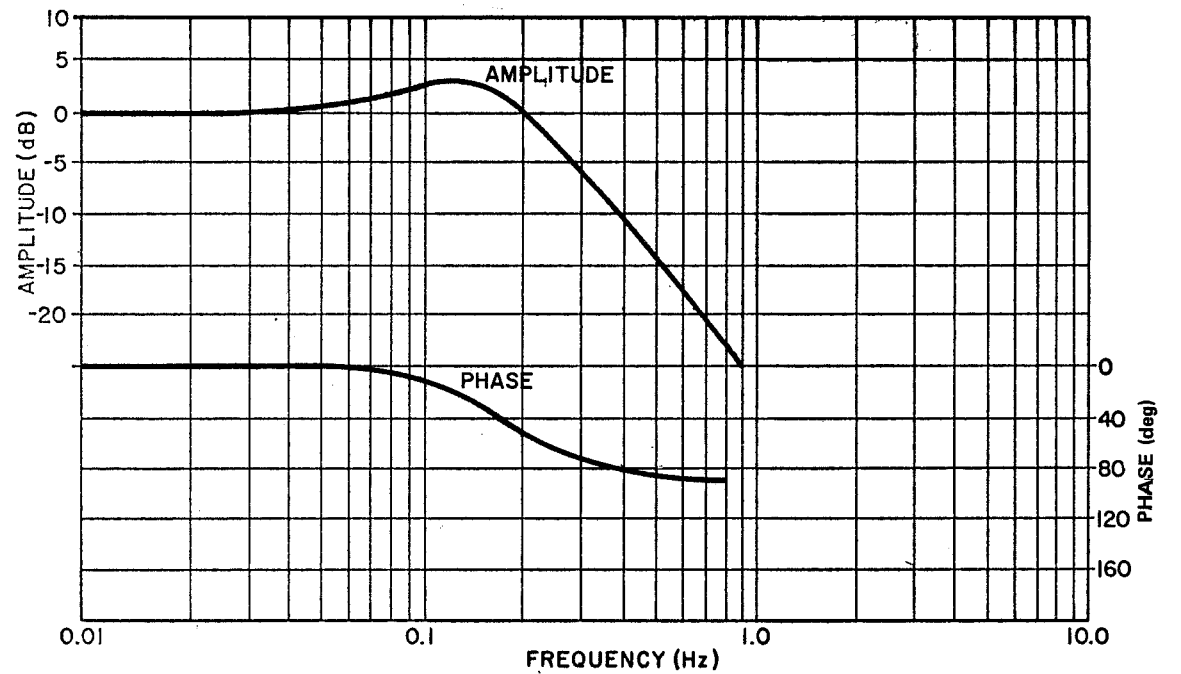

Figure B-1. Roll-axis frequency response for 0.03 deg/s input signal, analog-position mode, steel plate case.

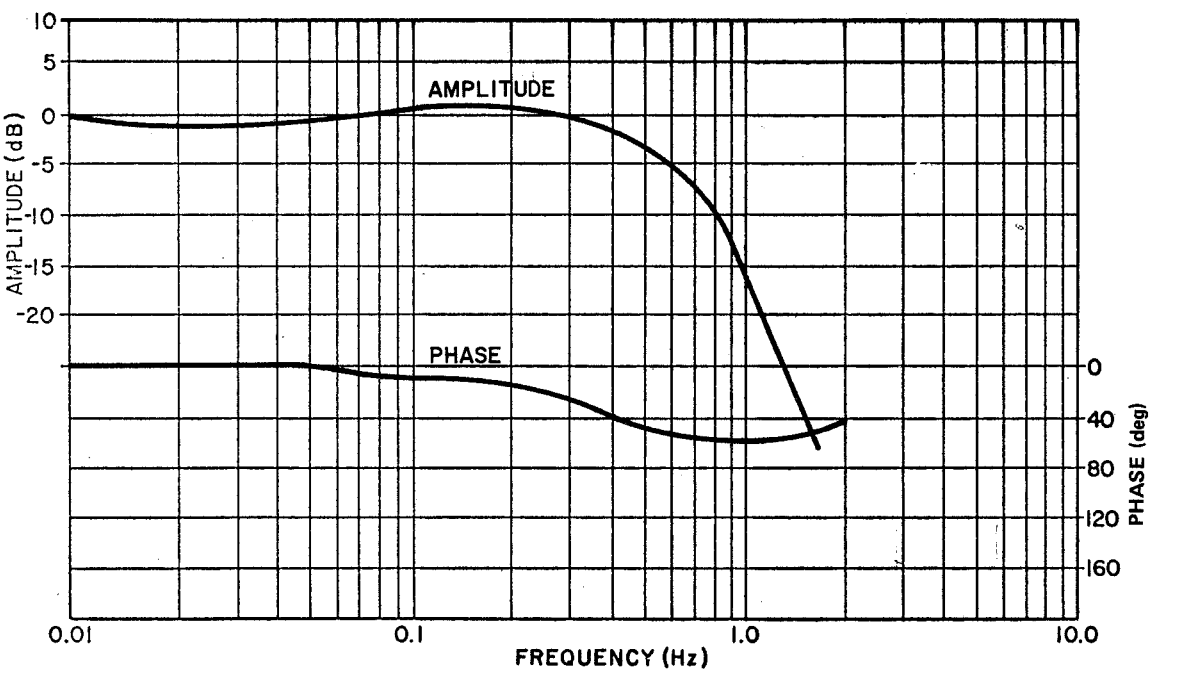

Figure B-2. Roll-axis frequency response for 0.1 deg/s input signal, analog-position mode, steel plate case.

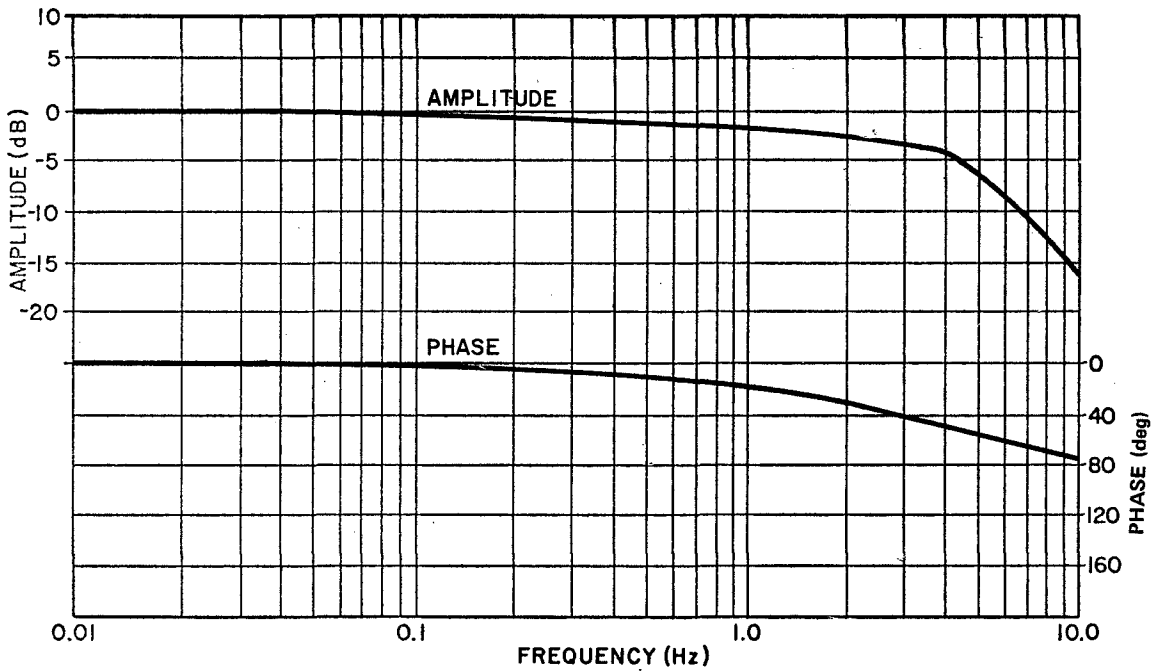

Figure B-3. Roll-axis frequency response for 0.5 deg/s input signal, analog-position mode, steel plate case.

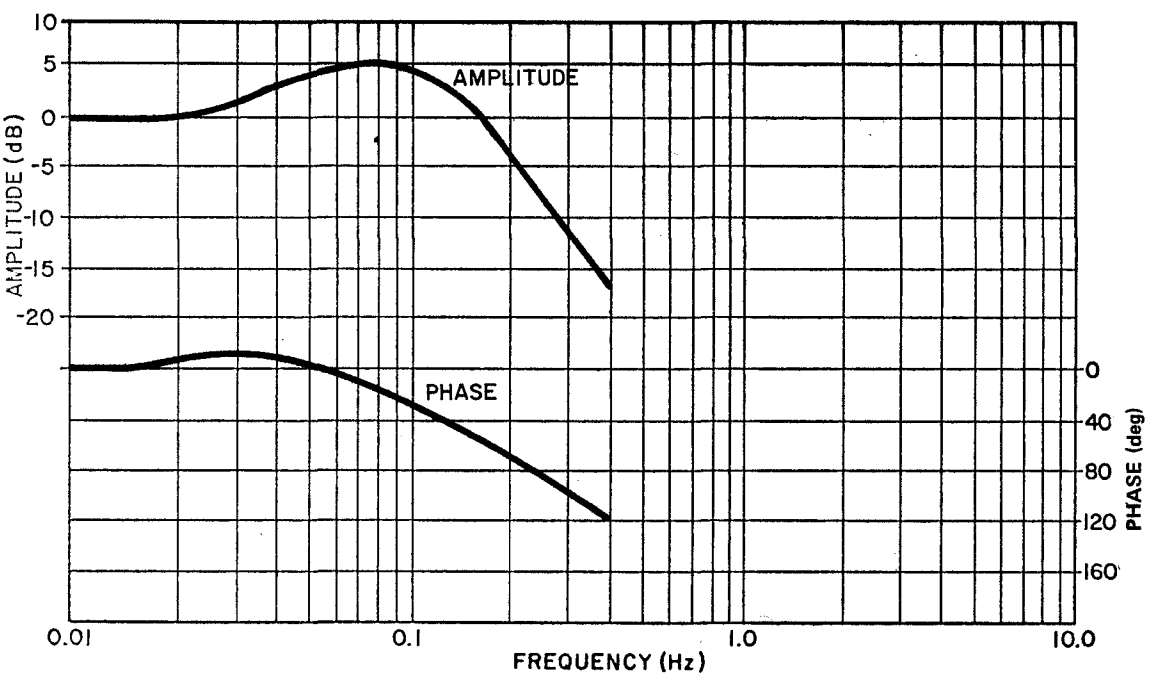

Figure B-4. Roll-axis frequency response for 0.01 deg/s input signal, analog-position mode, CMG case.

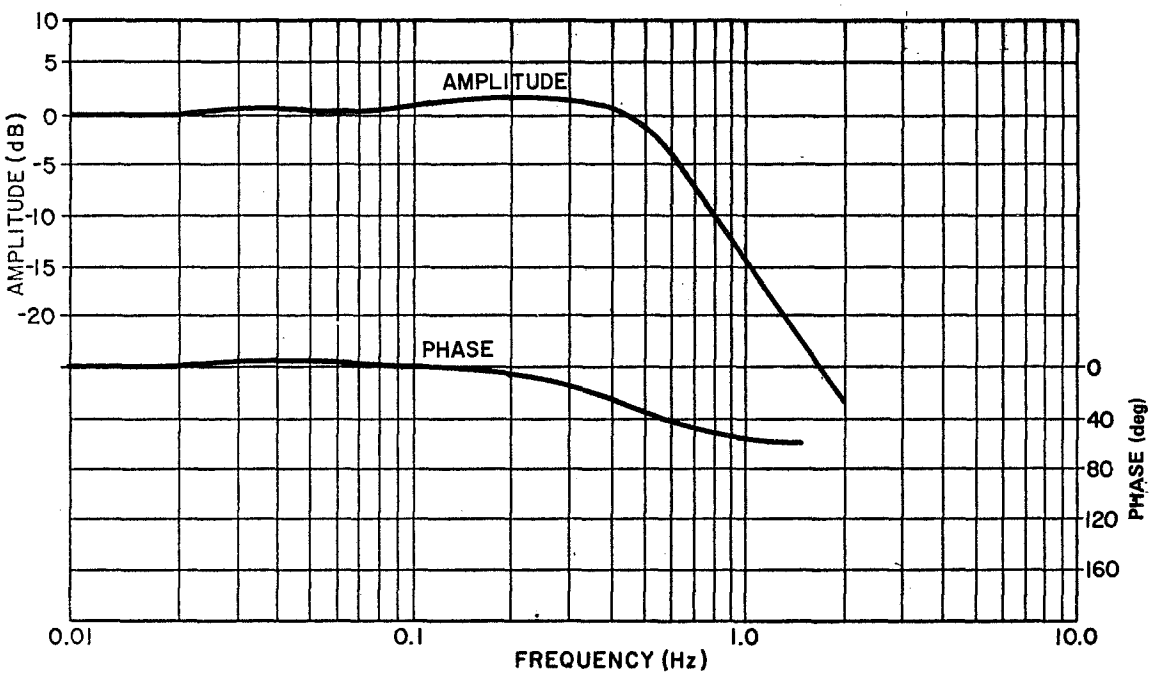

Figure B-5. Roll-axis frequency response for 0.1 deg/s input signal, analog-position mode, CMG case.

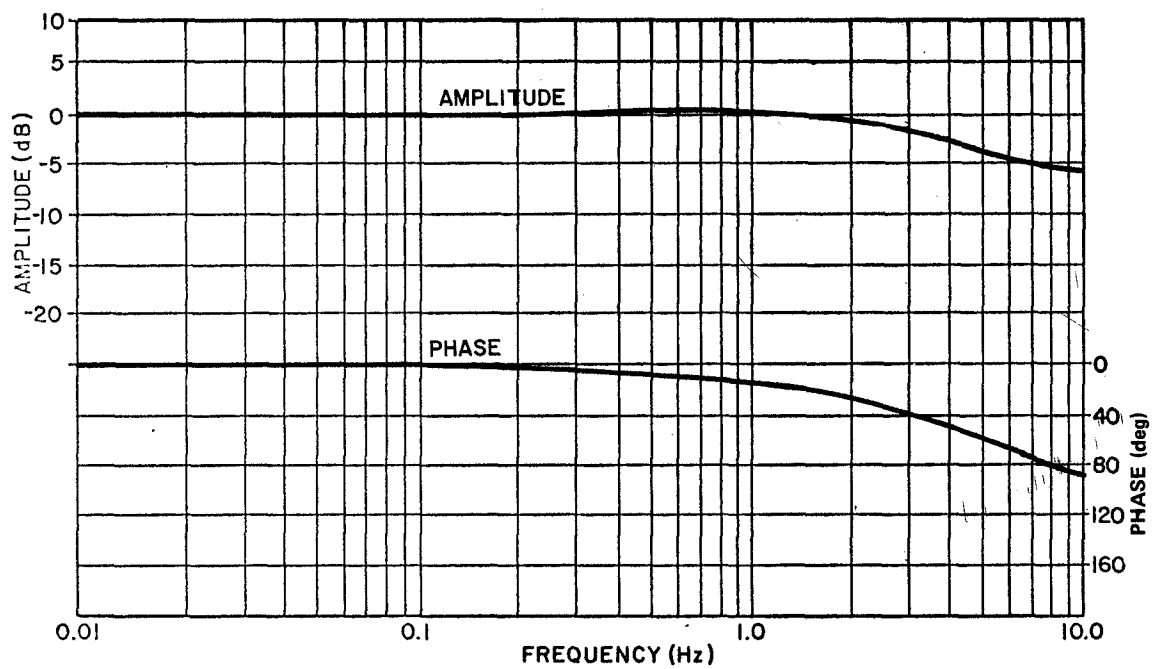

Figure B-6. Roll-axis frequency response for 0.5 deg/s input signal, analog-position mode, CMG case.

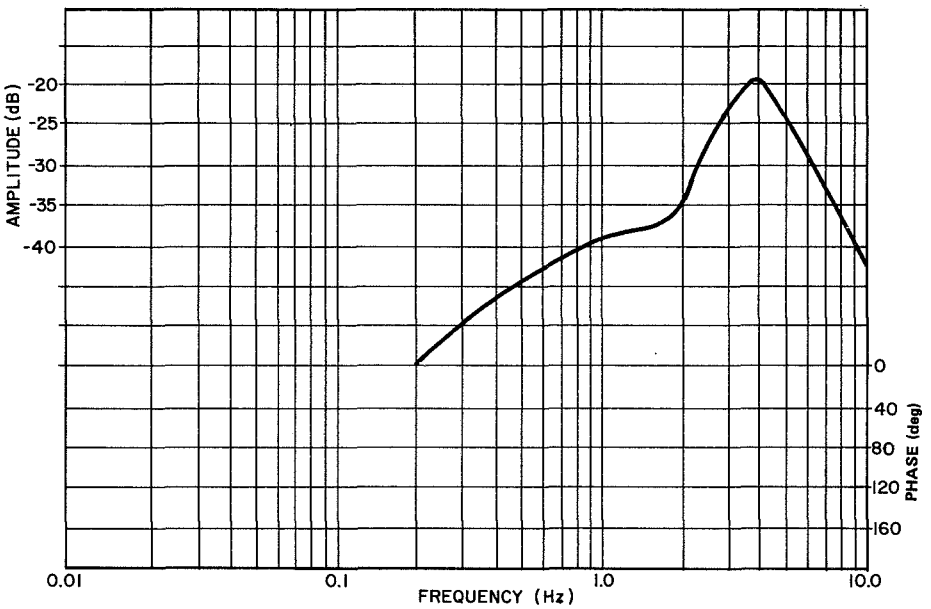

Figure B-7. Roll-yaw-axis coupling amplitude frequency response for 0.5 deg/s input signal, analog-position mode, CMG case.

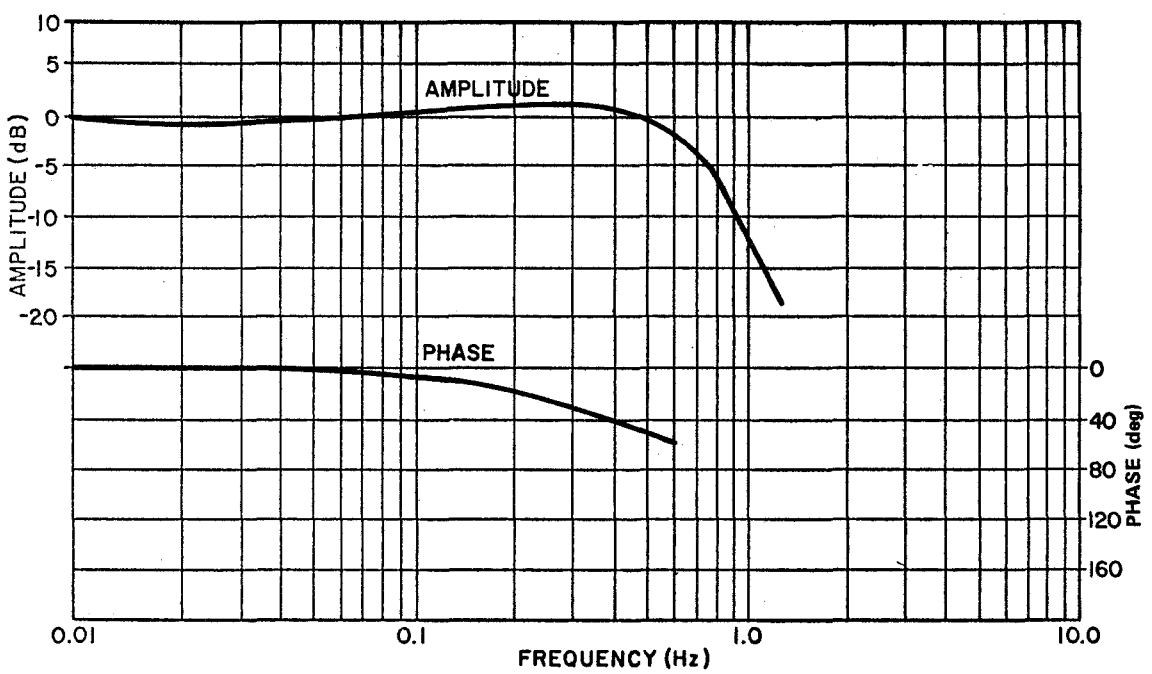

Figure B-8. Roll-axis frequency response for 0.01 deg/s input signal, digital mode, CMG case.

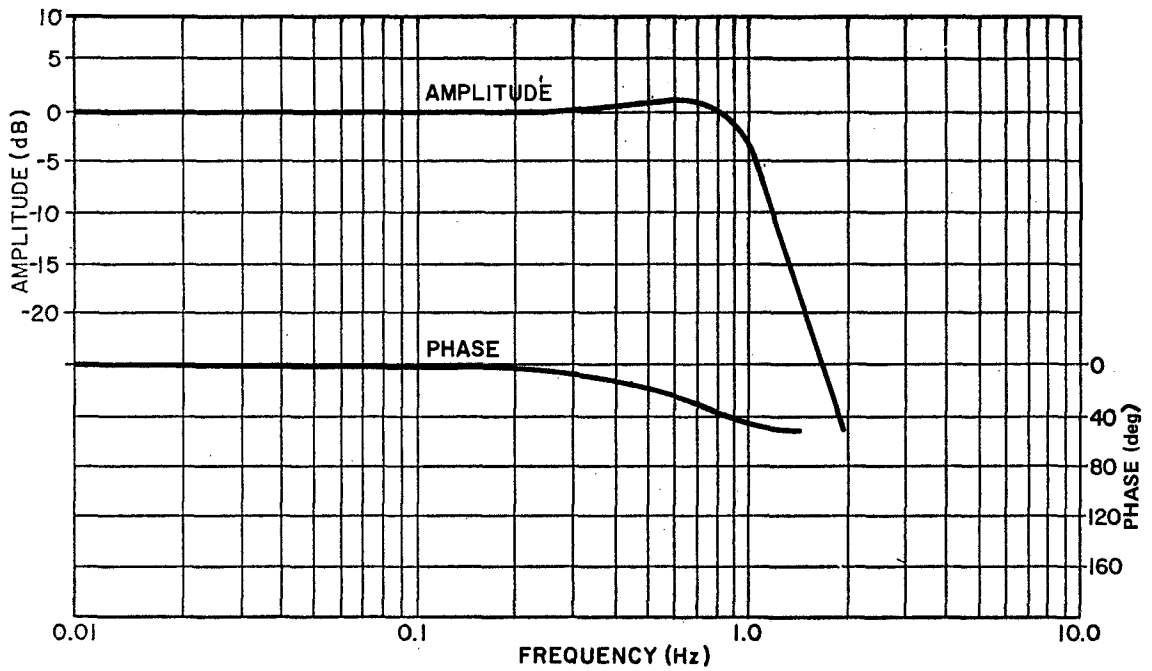

Figure B-9. Roll-axis frequency response for 0.1 deg/s input signal, digital mode, CMG case.

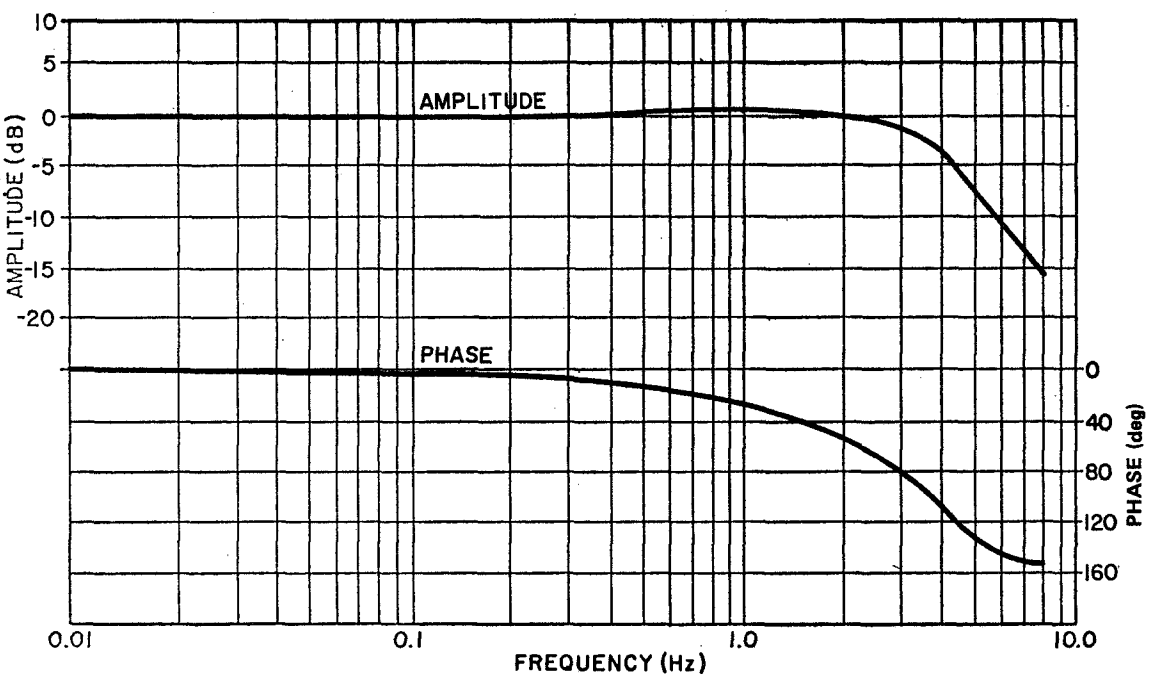

Figure B-10. Roll-axis frequency response for 0.5 deg/s input signal, digital mode, CMG case.

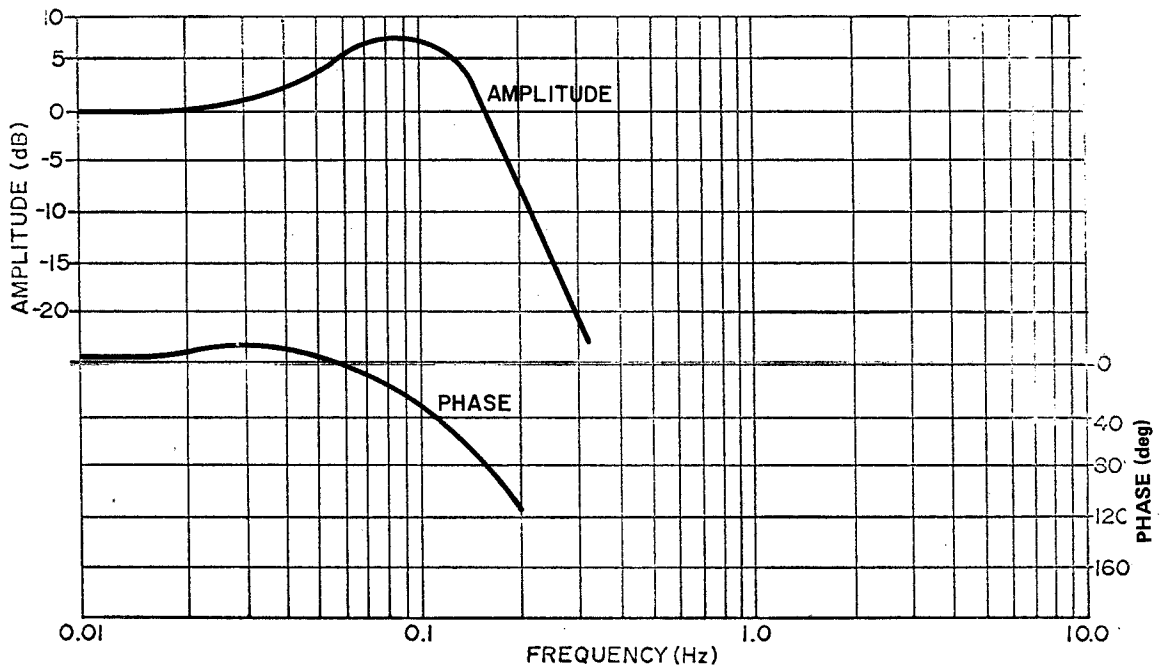

Figure B-11. Sidereal-axis frequency response for 0.01 deg/s input signal, analog-position mode, steel plate case.

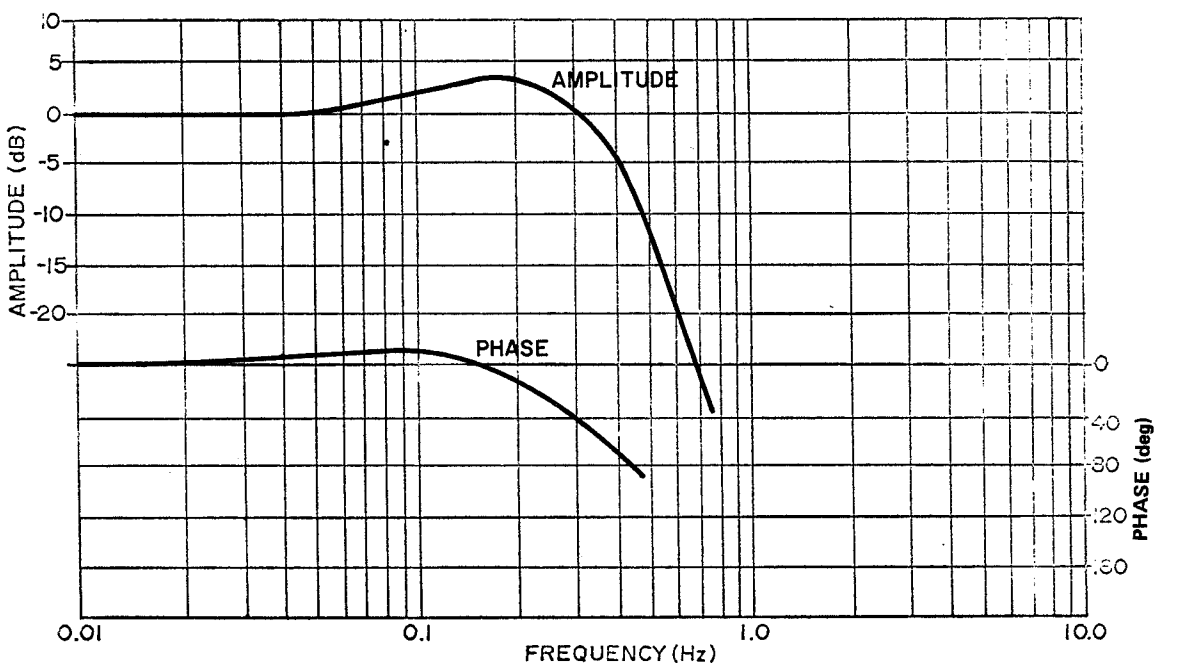

Figure B-12. Sidereal-axis frequency response for 0.05 deg/s input signal, analog-position mode, steel plate case.

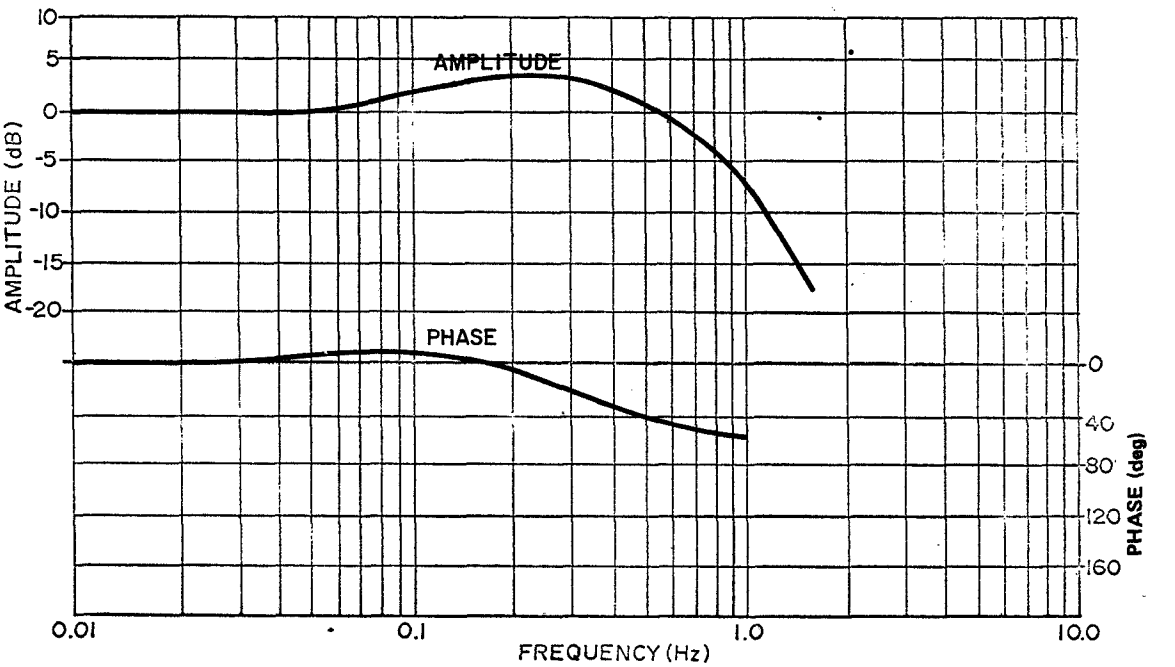

Figure B-13. Sidereal-axis frequency response for 0. 1 deg/s input signal, analog-position mode, steel plate case.

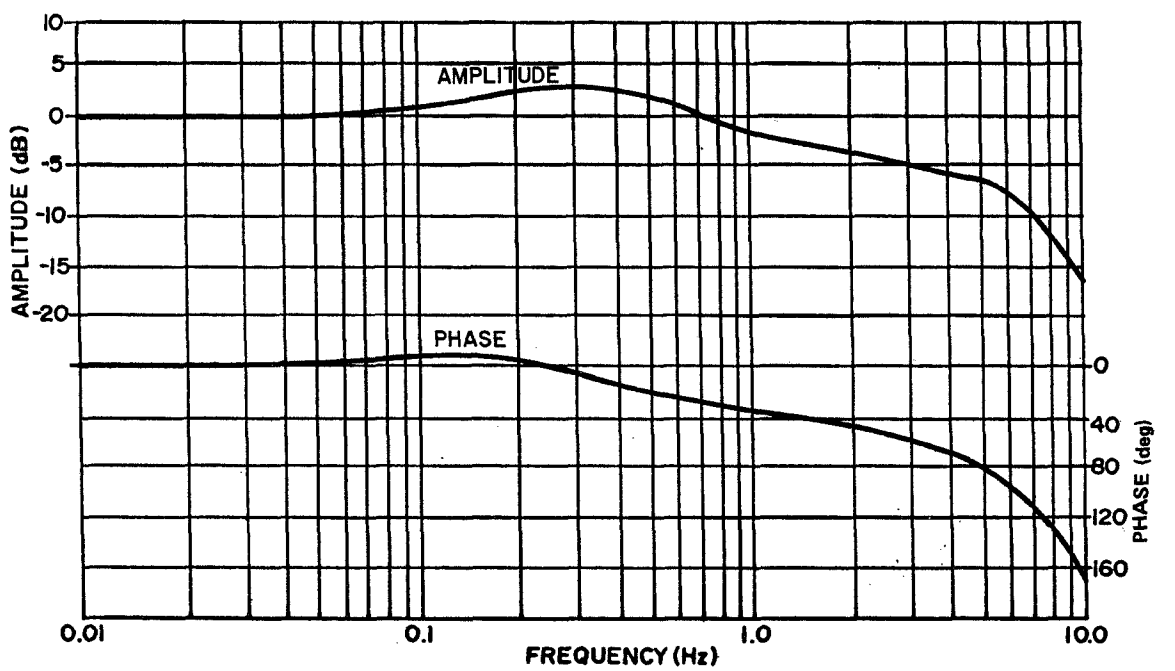

Figure B-14. Sidereal-axis frequency response for 0. 5 deg/s input signal, analog-position mode, steel plate case.

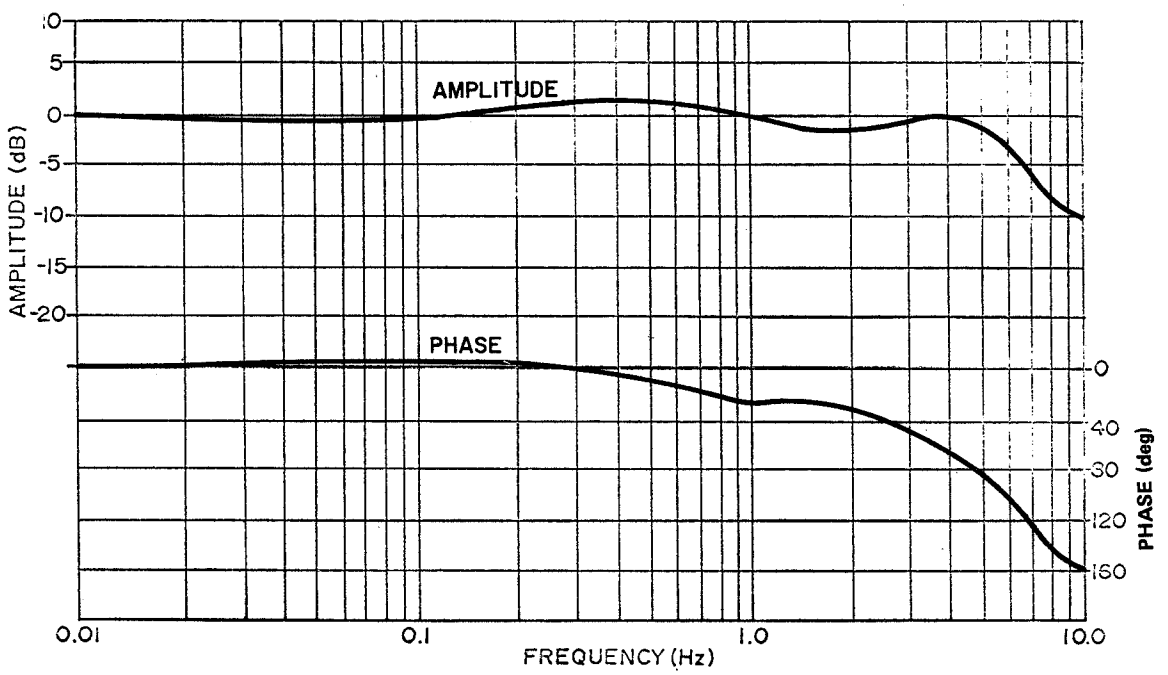

Figure B-15. Sidereal-axis frequency response for 1.0 deg/s input signal, analog-position mode, steel plate case.

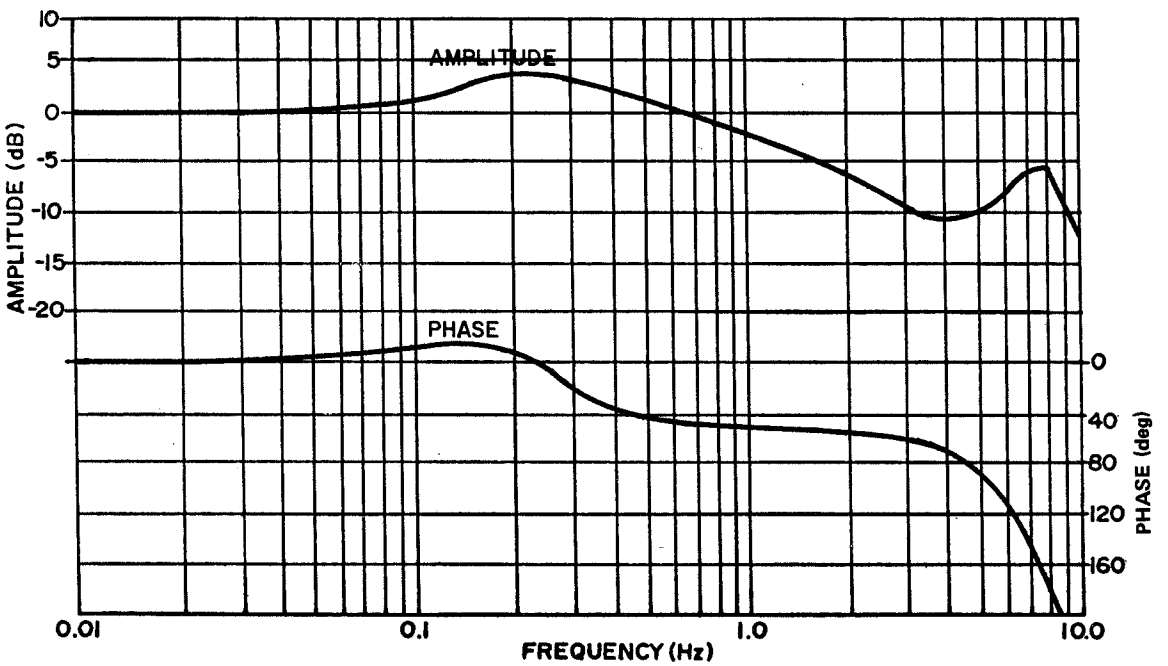

Figure B-16. Sidereal-axis frequency response for 0.05 deg/s input signal, analog-position mode, CMG case.

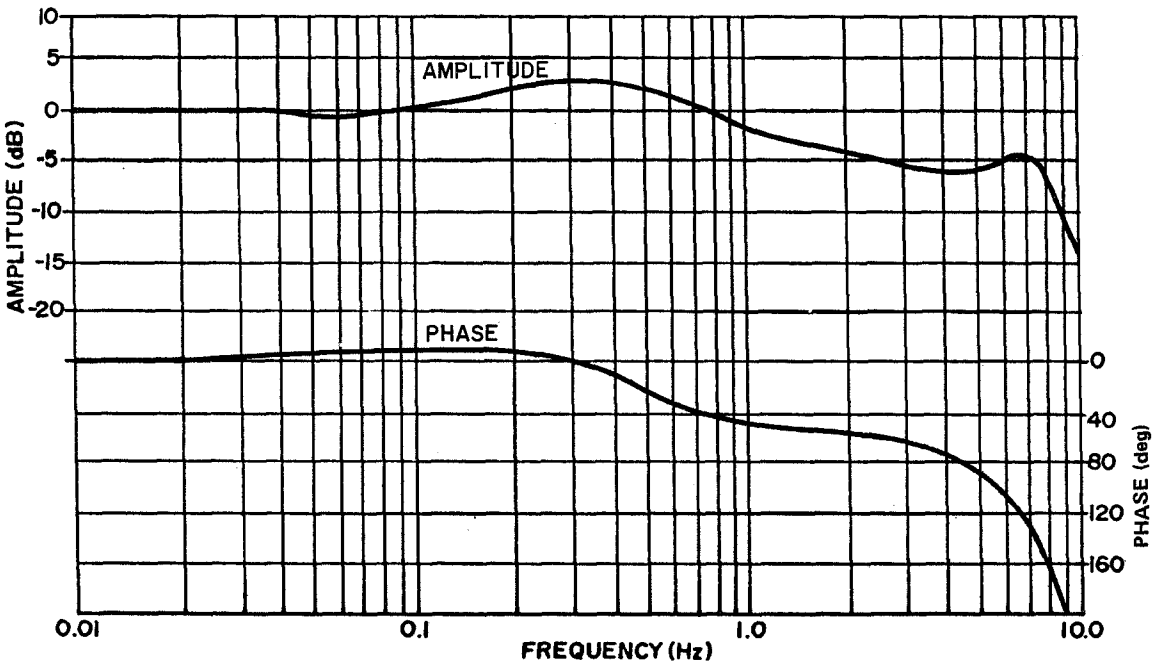

Figure B-17. Sidereal-axis frequency response for 0.1 deg/s input signal, analog-position mode, CMG case.

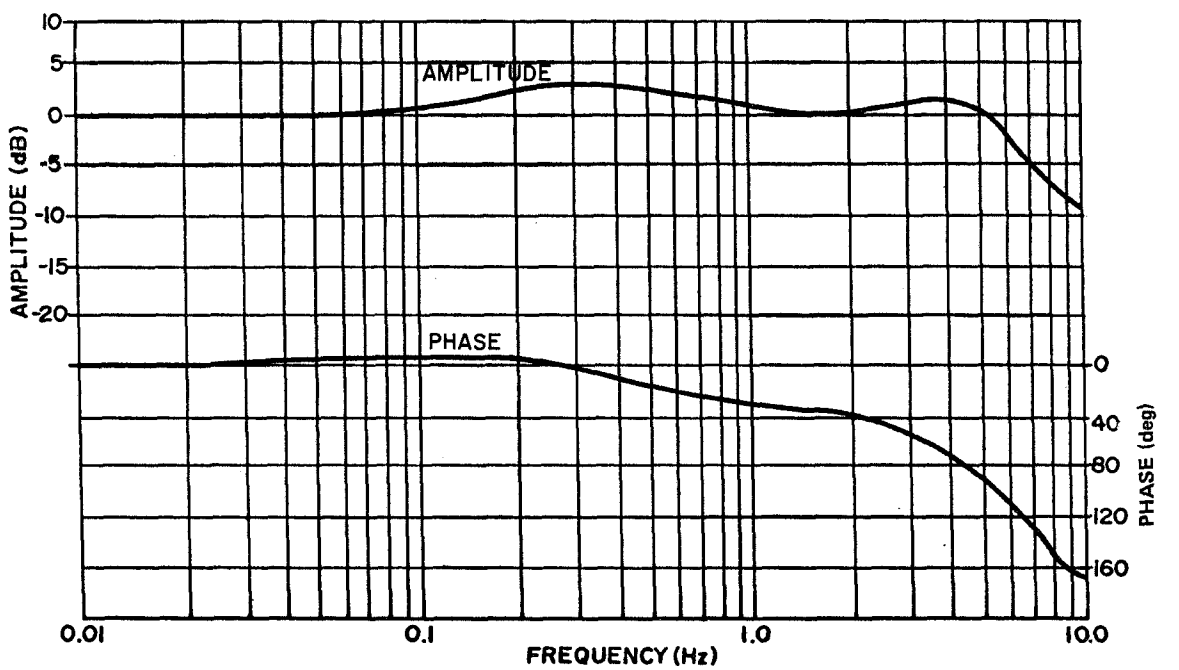

Figure B-18. Sidereal-axis frequency response for 0.5 deg/s input signal, analog-position mode, CMG case.

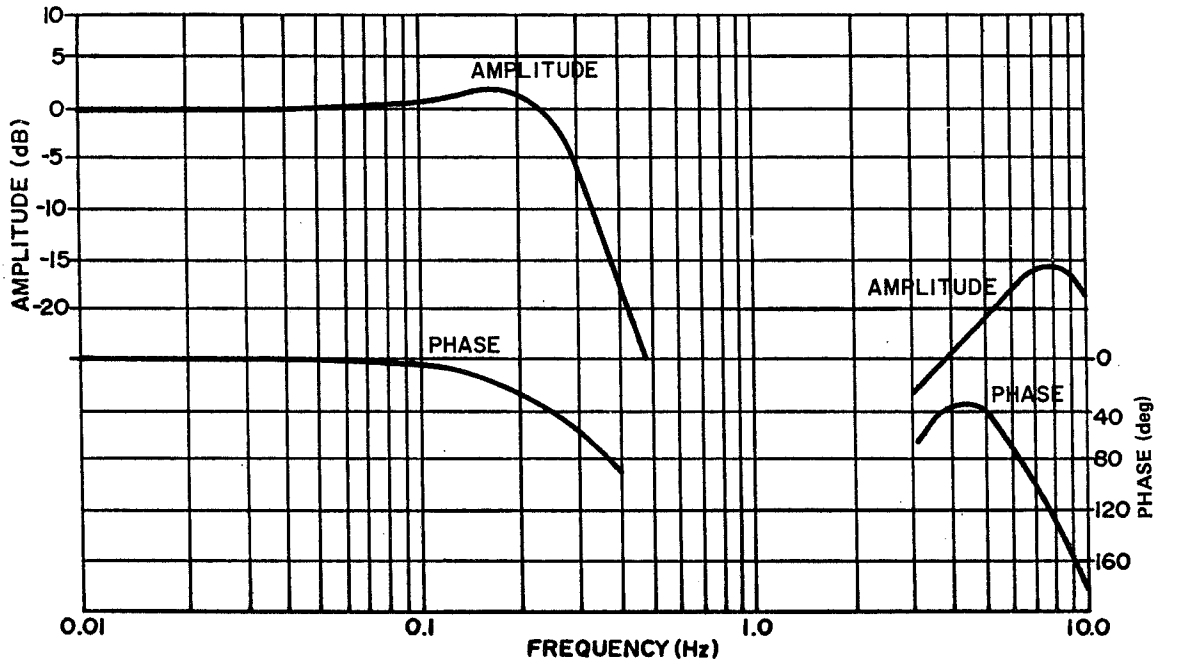

Figure B-19. Sidereal-axis frequency response for 0.05 deg/s input signal, digital mode, CMG case.

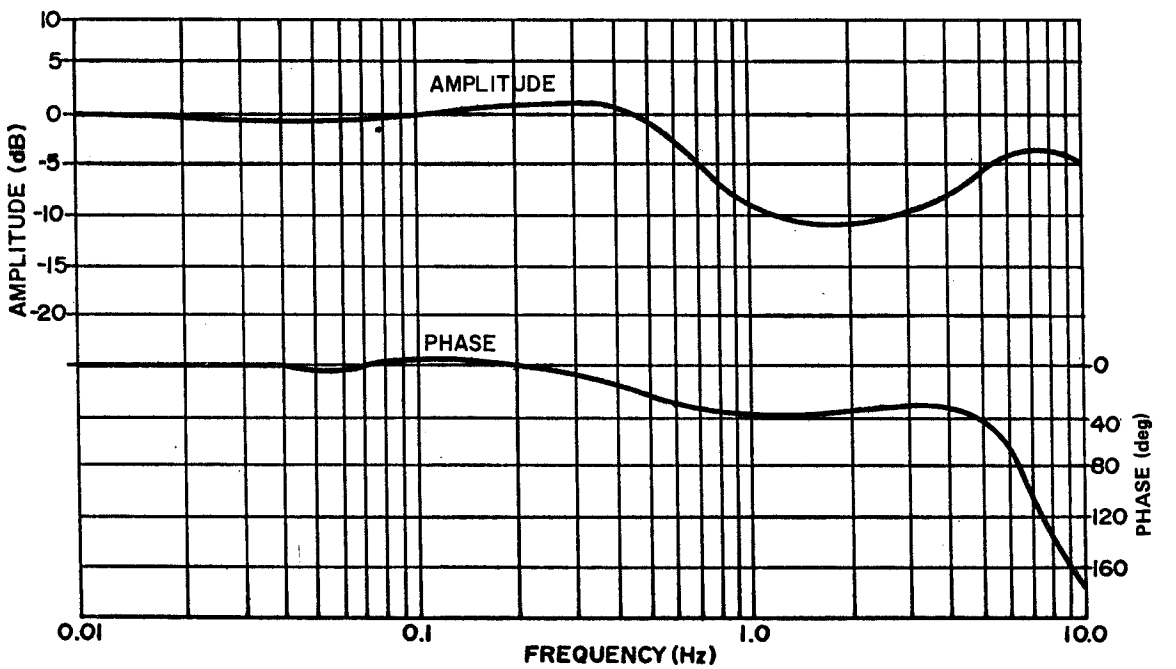

Figure B-20. Sidereal-axis frequency response for 0.1 deg/s input signal, digital mode, CMG case.

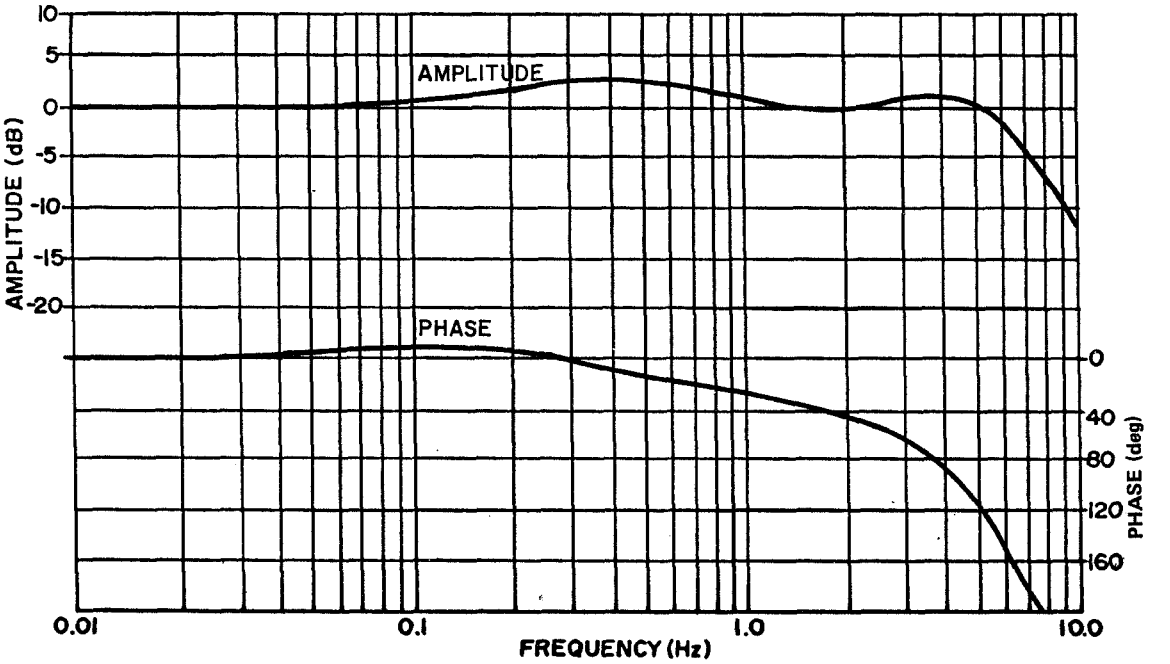

Figure B-21. Sidereal-axis frequency response for 0.5 deg/s input signal, digital mode, CMG case.

REFERENCES

1. Acceptance Test Procedure for the Dynamic Simulator. Contract No. NAS8-20688, F(8)-130-003-022-1182, Owens-Illinois, Fecker Systems Division, Pittsburgh, Pa., January 9, 1969, p. D-14.

2. Skylab A Guidance, Control and Navigation System Integration Test Plan. NASA - George C. Marshall Space Flight Center, S&E-ASTR-SG, 50M37942, August 3, 1970.

3. Rybak, S. Calvin: Apollo Applications Program (AAP) Payload Integration — Coupled Model of the ATM Motion Simulator. Martin-Marietta (The Bendix Corporation), Contract No. NAS8-2400, ED-2002-922, November 28, 1969.

4. Kuo, Benjamin C.: Automatic Control Systems. 2nd Edition, Prentice-Hall, Inc., 1967.

5. Dynamic Simulator for the Apollo Telescope Mount-Systems Analysis AE-2248. American Optical Company, Contract No. NAS8-20688, May 20, 1967.

6. Dominiak, Stanley W., Jr.; and Nakashima, Arthur K.: Apollo Applications Program (AAP) Payload Integration — Updated ATM Table Servo Stability Response Study. Martin-Marietta (The Bendix Corporation), Contract No. NAS8-24000, ED-2002-919-1, October 15, 1969.

7. Clark, D. C.: How to Select Rotary Electrohydraulic Servodrives. Hydraulics and Pneumatics, April 1970, pp. 194-203.

8. Lang, G. E.: CMG Control Subsystem Limit Cycle Study. Contract MC8-24000, The Bendix Corporation, Report No. BD-2244, September 14, 1970.

APPROVAL

TMX-64609

SKYLAB THREE-AXIS MOTION PLATFORM TEST RESULTS

By

Michael T. Borelli (MSFC)
Jack Templeton (Sperry Rand Corporation)

The information in this report has been reviewed for security classification. Review of any information concerning Department of Defense or Atomic Energy Commission programs has been made by the MSFC Security Classification Officer. This report, in its entirety, has been determined to be unclassified.

This document has also been reviewed and approved for technical accuracy.

Hans H. Hosenthien

H. H. HOSENTHIEN
Chief, Research and Development Analysis Office

W. F. Horton

for F. B. MOORE
Director, Astrionics Laboratory

DISTRIBUTION

INTERNAL

DIR

DEP-T

AD-S

A&TS-MS-H

A&TS-MS-IL (8)

A&TS-MS-IP (2)

S&E-CSE-DIR
Dr. Haeussermann

S&E-ASTR-DIR
Mr. Moore

S&E-ASTR-A
Mr. Hosenthien
Dr. Seltzer
Dr. Borelli (15)
Mr. Carroll
Mr. Kennel
Miss Flowers

S&E-ASTR-C
Mr. Swearingen
Mr. Lucus
Mr. Coppock
Mr. Lee
Mr. Vick (5)
Mr. Brown
Mr. Templeton (Sperry) (15)

S&E-ASTR-E
Mr. Aden

PM-PR-M

S&E-ASTR-G
Mr. Mandel
Dr. Doane
Mr. Kalange
Mr. Golley
Dr. Campbell
Mr. Cornelius

S&E-ASTR-I
Mr. Duggan

S&E-ASTR-M
Mr. Boehm

S&E-ASTR-R
Mr. Taylor

S&E-ASTR-S
Mr. Wojtalik
Mr. Brooks
Mr. Davis
Mr. Scott
Mr. Fisher
Mr. Sheldon

S&E-ASTR-ZX

A&TS-PAT
Mr. Wofford

A&TS-TU
Mr. Winslow (6)

EXTERNAL

Scientific and Technical Information
Facility (25)
P. O. Box 33
College Park, Maryland 20740
Attn: NASA Representative (S-AK/RKT)

DISTRIBUTION (Concluded)

EXTERNAL (Concluded)

Bendix Corporation
Navigation and Control Division (4)
Research Blvd.
Madison, Alabama 35758
Attn: Mr. E. Hahn

Bendix Research Laboratories
Denver Facility (5)
2796 S. Federal Blvd.
Denver, Colorado 80236
Attn: Mr. S. C. Rybak

MSFC—RSA, Ala